

DEVELOPMENT OF PAIRED ION ELECTROSPRAY IONIZATION MASS
SPECTROMETRY FOR ULTRASENSITIVE DETECTION OF ANIONS

by

CHENGDONG XU

Presented to the Faculty of the Graduate School of
The University of Texas at Arlington in Partial Fulfillment
of the Requirements
for the Degree of

DOCTOR OF PHILOSOPHY

THE UNIVERSITY OF TEXAS AT ARLINGTON

AUGUST 2014

Copyright © by Chengdong Xu 2014

All Rights Reserved



This dissertation is dedicated to those whom I love and those who love me.

Acknowledgements

I would like to express my sincere gratitude to my mentor, Professor Daniel W. Armstrong, for his constant guidance, support, and encouragement throughout my doctoral studies. I am indebted to him not only for sparking my interest in analytical chemistry but also for cultivating my personality and shaped my career path. I consider myself extremely fortunate to have the opportunity to conduct graduate research under his supervision. His knowledge, attitude, and life philosophy have a great influence on my life.

I am truly thankful to Professor Kevin A. Schug for his invaluable advice and direction during my graduate studies. It is fortunate to be educated by him in the field of analytical chemistry, particularly in mass spectrometry, which laid a solid foundation for my future research. I must express my appreciation to Professor Fred MacDonnell for his strong support in my graduate research. I enjoyed the collaborating project working with him and his student David Boston, which was really a pleasant experience.

I would like to thank my parents, father Jianjun Xu and mother Shuming Chen, for their selfless love and unconditional support during my life. I would like to thank my beloved Yuetao for her countless support to my research and career and to our family.

I would like to thank my group members: Chunlei, Edra, Eranda, Haixiao, John, Jonathan, Koko, Nilusha, Ping, Qing, Sirantha, Tharanga, Violet, Xiaotong, Yasith, Ying, Zach, and Choyce, Curran, Darshan, David, Eduardo, Lily, Howard, Momin, Ross and Dr. Alan Berthod. A special thank you should go to Prof. Armstrong's assistant Barbara Smith and the chemistry department staffs Brian, Chunk, Debbie, Jim and Jill for their kind help on providing laboratory supplies, research facilities and paperwork.

June 24th, 2014

Abstract

DEVELOPMENT OF PAIRED ION ELECTROSPRAY IONIZATION MASS SPECTROMETRY FOR ULTRASENSITIVE DETECTION OF ANIONS

Chengdong Xu, PhD

The University of Texas at Arlington, 2014

Supervising Professor: Daniel W. Armstrong

Mass spectrometry (MS) has emerged as an essential analytical technique over the last several decades. It is a widely applicable and powerful tool for determination and identification of different types of molecules. Electrospray ionization (ESI) is one of the most commonly used ionization sources for mass spectrometry. ESI-MS has advantages for the analysis of both small molecules and macromolecules due to its outstanding sensitivity, specificity, speed, and the capability for analyte structure elucidation. Currently, one challenging aspect in ESI-MS is the qualitative and quantitative determination of anionic species. This is due to the inherently poor detection sensitivity in the negative ion mode ESI-MS resulting from the prevalent electrical discharge (corona discharge). This dissertation discusses the development of a novel technique named paired ion electrospray ionization mass spectrometry (PIESI-MS) for the ultrasensitive determination of anions in the positive ion mode ESI-MS. PIEI-MS involves introducing low concentrations of structurally optimized ion-pairing reagents (IPRs) into the sample flow, thereby allowing the anions to be measured with extremely high sensitivity in the positive ion mode as the anion/IPR associated complexes. The reported LODs by PIEI-MS were usually from 2 to 3 orders of magnitude better than these of other known methods.

Specifically, this dissertation describes research in two areas:

1). Novel methodologies, based on HPLC-PIESI-MS, were developed and evaluated for the trace analysis of anionic molecules. The PIEESI-MS approach was found to be suitable for ultrasensitive determination of a variety of molecules, including small inorganic anions, medium sized organic anions, zwitterionic molecules, and metal cations. The absolute detection limits (LODs) of these analytes obtained using the PIEESI-MS approach were determined in both single ion monitoring mode (SIM) and selected reaction monitoring mode (SRM). LODs from sub-picogram to picogram were usually observed for most of the anions, which indicates 2 to 3 orders of magnitude improvement compared to most other reported methods. The accuracy, precision, linearity, and specificity were also evaluated as a part of method validation. SRM fragmentation pathways of the analyte/IPR complexes during the collision induced dissociation were examined.

2). Novel unsymmetrical dicationic ion-pairing reagents were rationally synthesized and their performance on detection of anions by PIEESI-MS were investigated. It was found that the unsymmetrical dications provided more sensitive detection by 1.5 to 12 times than their symmetrical dication analogues. The effective concentration range of the unsymmetrical dicationic ion-pairing reagents was optimized. A correlation was observed between the ESI response and the surface activity of the anion/IPR complex, which indicates that the analyte surface activity plays a vital role in the electrospray ionization process. The sensitivity enhancement mechanism in PIEESI-MS was further explored based on the concepts of the equilibrium partitioning model.

Table of Contents

Acknowledgements	iv
Abstract	v
List of Illustrations	xiii
List of Tables	xvii
Chapter 1 Introduction.....	1
1.1. Paired Ion Electrospray Mass Spectrometry (PIESI-MS).....	1
1.2. Methods for Detection of Anions	5
1.2.1. <i>Conductivity Detection</i>	6
1.2.2. <i>Ion Selective Electrodes</i>	6
1.2.3. <i>UV-Vis Detection</i>	7
1.2.4. <i>Amperometric Detection</i>	8
1.2.5. <i>Mass Spectrometry</i>	9
1.3. Research Objectives and Organization of the Dissertation.....	10
Chapter 2 High-performance Liquid Chromatography with Paired Ion Electrospray (PIESI) Tandem Mass Spectrometry for the Highly Sensitive Determination of Acidic Pesticides in Water	12
Abstract.....	12
2.1. Introduction	13
2.2. Experimental	15
2.2.1. <i>Materials</i>	15
2.2.2. <i>ESI-MS Analysis</i>	19
2.2.3. <i>Solid-Phase Extraction</i>	20
2.2.4. <i>Chromatography</i>	21

2.2.5. <i>Determination of Trace Pesticides in Stream and Pond Water</i>	
<i>Samples</i>	21
2.3. Results and Discussion	22
2.3.1. <i>Dicationic Ion Pairing Reagents and Tested Pesticides</i>	22
2.3.2. <i>Identification of Analyte/IPR Complex in the Full Scan Mode</i>	23
2.3.3. <i>LODs Obtained by PIESI-MS in the Single Ion Monitoring Mode</i>	24
2.3.4. <i>LODs Obtained by PIESI-MS in the Selected Reaction</i>	
<i>Monitoring Mode</i>	26
2.3.5. <i>Fragmentation Reactions during the Collision Induced</i>	
<i>Dissociation Process</i>	28
2.3.6. <i>Improvement of LODs Achieved by Using PIESI-MS</i>	29
2.3.7. <i>Method Validation</i>	31
2.3.8. <i>Solid-Phase Extraction Recovery Study</i>	33
2.3.9. <i>Chromatographic Separations of Nineteen Acidic Pesticides</i>	34
2.3.10. <i>Determination of the Concentrations of Pesticides in River</i>	
<i>and Pond Samples</i>	36
2.4. Conclusions	39
Chapter 3 Metal Cation Detection in the Positive Ion Mode ESI-MS Using a	
Tetracationic Salt as Gas-Phase Ion-Pairing Agent: Evaluation of the Effect	
of Chelating Agents on Detection sensitivity.....	40
Abstract.....	40
3.1. Introduction	41
3.2. Experimental.....	44
3.2.1. <i>Materials</i>	44
3.2.2. <i>ESI-MS Analysis</i>	48

3.2.3.	<i>Determination of Trace Lead (II) in CRM 3128e</i>	49
3.3.	Results and Discussion	49
3.3.1.	<i>Metal Chelating Reagents and Ion-Pairing Reagents</i>	49
3.3.2.	<i>LODs of Metal Cations Obtained in the Positive SIM Mode by Using Different Chelating Reagents</i>	50
3.3.3.	<i>LODs of Metal Cations Obtained in the Positive SRM Mode by Using Different Chelating Reagents</i>	53
3.3.4.	<i>SRM Fragmentation Pathway</i>	56
3.3.5.	<i>A Comparison of the Best LODs Obtained in the Positive Ion Mode and in the Negative Ion Mode</i>	58
3.3.6.	<i>Effect of Sample Solution pH on the Detection Sensitivity</i>	62
3.3.7.	<i>Quantitative Determination of Trace Lead (II) in CRM 3128e</i>	63
3.4.	Conclusions	67
Chapter 4 Sensitive Analysis of Metal Cations in Positive Ion Mode		
Electrospray Ionization Mass Spectrometry Using Commercial Chelating Agents and Cationic Ion-Pairing Reagents		
	Abstract.....	68
4.1.	Introduction	69
4.2.	Experimental	71
4.2.1.	<i>Chemicals</i>	71
4.2.2.	<i>ESI-MS Analyses</i>	72
4.3.	Results and Discussion	73
4.3.1.	<i>Metal Chelating Reagents and Ion-Pairing Reagents</i>	73
4.3.2.	<i>LODs of Metal Cations in the Positive SIM Mode with EDTA by Using Different Ion-Pairing Reagents</i>	74

4.3.3. LODs of Metal Cations in the Positive SIM Mode with EDDS by Using Different Ion-Pairing Reagents	77
4.3.4. A Comparison of the Best LODs Obtained in the Positive Ion Mode and in the Negative Ion Mode	78
4.3.5. SRM Fragmentation Pathway	83
4.4 Conclusions	85
Chapter 5 Use of Ion Pairing Reagents for Sensitive Detection and Separation of Phospholipids in the Positive Ion Mode LC-ESI-MS	87
Abstract.....	87
5.1. Introduction	88
5.2. Experimental.....	90
5.2.1. Chemicals.....	90
5.2.2. ESI-MS	90
5.2.3. Reversed-Phase Mode HPLC-ESI-MS	91
5.2.4. HILIC Mode HPLC-ESI-MS	91
5.3. Results and Discussion	91
5.3.1. Ion-Pairing Reagents and Analytes of Interest.....	91
5.3.2. Detection of Phospholipids Using IPRs in the Positive SIM Mode ESI-MS	94
5.3.3. Detection of Phospholipids Using IPRs in the Positive SRM Mode ESI-MS	98
5.3.4. HPLC-ESI-MS Analysis of Phospholipids	100
5.4. Conclusions	103
Chapter 6 Separation and Sensitive Determination of Sphingolipids at Low Femtomole Level by Using HPLC-PIESI-MS/MS	104

Abstract.....	104
6.1. Introduction	104
6.2. Experimental.....	106
6.2.1. Chemicals.....	106
6.2.2. <i>Instrumentation</i>	108
6.3. Results and Discussion	109
6.3.1. <i>LODs of Sphingolipids by PIESI-MS in the Single Ion Monitoring Mode</i>	109
6.3.2. <i>LODs of Sphingolipids by PIESI-MS in the Selected Reaction Monitoring Mode</i>	113
6.3.3. <i>Proposed SRM Fragmentation Pathways</i>	118
6.3.4. <i>Analysis of Sphingolipids by HPLC-PIESI-MS/MS</i>	120
6.4. Conclusions	121
Chapter 7 Mechanism and Sensitivity of Anion Detection Using Rationally Designed Unsymmetrical Dications in Paired Ion Electrospray Ionization Mass Spectrometry	
Abstract.....	122
7.1. Introduction	122
7.2. Experimental.....	126
7.2.1. <i>Dicationic Ion-Pairing Reagents</i>	126
7.2.2. <i>PIESI-MS Analyses</i>	128
7.2.3. <i>Surface Tension Measurements</i>	129
7.3. Results and Discussion	129
7.3.1. <i>Unsymmetrical Dicationic Ion-Pairing Reagents</i>	129

7.3.2. <i>A Comparison of the LODs Obtained by Using Unsymmetrical Dications and Symmetrical Dications</i>	130
7.3.3. <i>Surface Tension Measurements</i>	133
7.3.4. <i>Partitioning Behavior of the Species in the Aerosol Droplet</i>	137
7.3.5. <i>LODs Determined with the Use of Unsymmetrical Dications in the SRM Mode</i>	142
7.4. <i>Conclusions</i>	143
Chapter 8 General Summary	144
8.1. Part One (Chapters 2-6)	144
8.2. Part Two (Chapters 7)	145
Appendix A Publication Information and Contributing Authors	146
Appendix B Copyrights and Permissions.....	148
References.....	154
Biographical Information	163

List of Illustrations

Figure 1-1 Graph Showing the Growing Number of Research Publications in Mass Spectrometry, Based on Numbers of Publications per Year. Data Obtained from SciFinder Scholar Searching Results	2
Figure 1-2 Instrumental Configuration of HPLC-PIESI-MS.....	5
Figure 2-1 Positive Ion Mode Mass Spectrum of Dicationic Ion Pairing Reagent C ₅ (bpyr) ₂ and Cloprop Solution Obtained in Full Scan Mode (m/z 100 to m/z 1000).....	24
Figure 2-2 PIEESI-MS Signal-to-Noise Ratio Diagram of Dicamba.....	31
Figure 2-3 Percent Recoveries Obtained by SPE Four Pesticides Spiked Sample Solutions.	33
Figure 2-4 Chromatographic Separation and Detection of Nineteen Acidic Pesticides by Using HPLC-PIESI-MS.	35
Figure 2-5 HPLC-PIESI-MS Detection of Mecoprop in the Stream Water Sample (a), (b) and (c), and Mecoprop Standard (d) and Blank (e).	37
Figure 3-1 Structure of Tetracationic Ion-Pairing Reagent <i>1,1,1,6,6,11,11,16,16,16-decaphenyl-1,6,11,16-tetraphosphoniahexadecane (Tet)</i> Used in this Study.....	47
Figure 3-2 Mass spectrum of the Tetracationic Ion-Pairing Reagent (Tet) Obtained in Full Scan Mode Under Experimental Condition.....	50
Figure 3-3 Proposed Fragmentation Pathway for the Metal Cation-Chelating Agent-Ion-Pairing Reagent Ternary Complex.....	57
Figure 3-4 ESI-MS Signal-to-Noise Ratio Diagrams of Pb ²⁺ Using BETA. (a) 478 pg of Pb ²⁺ Injected, Analysis Performed in the Negative Ion Mode with BETA as Chelating Agent. (b) 478 pg of Pb ²⁺ Injected, Analysis Performed in Positive Ion Mode (SIM) with BETA and IPR. (c) 478 pg of Pb ²⁺ Injected, Analysis Performed in Positive Ion Mode (SRM) with BETA and IPR.....	61

Figure 3-5 The pH Dependencies of the ESI-MS Signal Intensities of Metal Chelate Complexes	62
Figure 3-6 The Effect of NH ₄ NO ₃ Concomitant (0–1 mM) on Signal Intensities of [²⁰⁸ Pb+EDTA+Tet] ²⁺ , [⁵² Cr+CyDTA+Tet] ³⁺ and [²⁰⁸ Pb+BETA+Tet] ²⁺	64
Figure 3-7 Calibration Curves for [²⁰⁸ Pb+EDTA+Tet] ²⁺ (Δ), [²⁰⁸ Pb+BETA+Tet] ²⁺ (x) and [¹¹⁴ Cd+EDTA+Tet] ²⁺ (◇) Using External Standard Calibration Method.	64
Figure 3-8 ESI S/N Ratio Diagram for the Direct Injection of [²⁰⁸ Pb+EDTA+Tet] ²⁺ in SIM Mode at <i>m/z</i> 779.3. Aliquots of 325, 750, 1500 and 3000 nM Injected in Triplicate	65
Figure 4-1 Structures of the Two Metal Chelating Agents Used in this Analysis.....	73
Figure 4-2 Structures of the Linear Tri- and Tetracationic Ion-Pairing Reagents Used in This Study	74
Figure 4-3 A Comparison of Limits of Detection of Ca ²⁺ Achieved in Negative and Positive Ion Mode ESI-MS. (A) and (B) Demonstrate an Injection of the [Ca ²⁺ +EDTA] ⁻ Complex Monitored in the SIM Negative Ion Mode at Two Different Concentrations. (C) and (D) Demonstrate the Results Achieved When the [Ca ²⁺ +EDTA] ⁻ Complex was Monitored in the SIM and SRM Positive Ion Mode with the Addition of the Ion-Pairing Reagent Tet 1	82
Figure 4-4 A Proposed Fragmentation Pathway for the Tandem Mass Spectrometric Analysis of Mn ²⁺ When Complexed with EDTA as a Chelating Agent and Tet 1 Tetracationic Ion-Pairing Reagent in Positive Ion Mode ESI-MS	84
Figure 5-1 Structures of the Dicationic Ion Pairing Reagents with Their Corresponding Abbreviations Used in This Study	92
Figure 5-2 Structures of the Linear Tricationic Ion Pairing Reagents with Their Corresponding Abbreviations.....	93
Figure 5-3 Structures of the Tetracationic Ion Pairing Reagents Used in This Study with Their Corresponding Abbreviations	94

Figure 5-4 Chromatographic Separation and Detection of the PC and PE Mixture and Their Homologues in the SIM Positive Mode ESI-MS. (A) Total Ion Chromatogram of This Mixture and (B) Extracted Ion Chromatogram in Which the Major Species of the Phospholipids are Detected with Tetracation Ion Pairing Reagent Tet 5.	101
Figure 5-5 Extracted Ion Chromatogram Displaying the LC Separation of PC, PG, and PE on a Silica Column in the Positive Ion Mode ESI-MS.	102
Figure 6-1 Structures and Abbreviations of the Dicationic Ion Pairing Reagents and Tetracationic Ion Pairing Reagents Used in this Study.	106
Figure 6-2 Structures and Abbreviations of the Sphingolipids.	107
Figure 6-3 Proposed CID Fragmentation Pathways of Complex [SM(d18:1/6:0) + Dicat II] ²⁺ m/z: 474.3.	115
Figure 6-4 A Comparison of the HPLC-MS Separation and Sensitivity of Three Sphingolipids in the (A) Regular Positive SIM Mode HPLC-MS without Using IPR ([SM(d18:1/2:0)] ⁺ m/z: 507.4; [SM(d18:1/6:0)] ⁺ m/z: 563.4; [PE-Cer(d17:1/12:0)] ⁺ m/z: 591.4), (B) Positive SIM Mode by HPLC-PIESI-MS Using the Dicat I ([SM(d18:1/2:0) + Dicat I] ²⁺ m/z: 415.4; [SM(d18:1/6:0) + Dicat I] ²⁺ m/z: 443.4; [PE-Cer(d17:1/12:0) + Dicat I] ²⁺ m/z: 457.4), and (C) Positive SRM Mode by HPLC-PIESI-MS Using the Dicat I ([SM(d18:1/2:0) + Dicat I] ²⁺ SRM m/z: 415.4 → 162.3; [SM(d18:1/6:0) + Dicat I] ²⁺ SRM m/z: 443.4 → 162.3; [PE-Cer(d17:1/12:0) + Dicat I] ²⁺ SRM m/z: 457.4 → 162.3)	119
Figure 7-1 PIESI Mass Spectra of Iodide by Using SDC I and UDC I. Concentration of I ⁻ Was 1 μM and the Molar ratio of Dication to I ⁻ Was 20:1. [SDC I + I] ⁺ m/z: 451.3; [UDC I + I] ⁺ m/z: 591.5. The Spectra Were Recorded Separately in the Single Ion Monitoring Mode with a Width of 50.	133
Figure 7-2 Surface Tension Measurements When Titrating SDC I and UDC I with SCN ⁻ . Concentration of SDC I and UDC I was 0.1 M. The Data Points at [SCN ⁻] = 0 M	

Represent Surface Tension of Neat Water (blank line), 0.1 M Aqueous Solution of SDC I (blue line) and 0.1 M Aqueous Solution of UDC I (red line), Respectively	134
Figure 7-3 Schematic Showing the Partitioning of an Analyte Anion Between the Surface of an Aerosol Droplet and the Bulk Interior. When the Concentration of the Dicationic Surfactant Is Low (“A” above), It Resides Mainly at the Surface of the Droplet as will Any Associated Anions. When the Concentration of Surface of the Dicationic Surfactant is High (“B” above), Monolayer can be Formed and All Additional Surfactant Resides in the Interior Bulk Solution. Thus the Anionic Analyte Has Increased Partitions to the Interior Bulk Solution	136
Figure 7-4 ESI-MS Response to the Dication/ SCN^- Complex Ion (in Black) and ESI-MS Response to the Protonated Methanol Ion (in Red) for Solutions Containing UDC I and SCN^- (UDC I : SCN^- = 10 : 1) as the Dication Concentration Increased from 1×10^{-6} to 5×10^{-4} M	139
Figure 7-5 ESI-MS Response to the ThrH^+ Ion as the Concentration of Threonine Solution Increased from 3×10^{-6} to 1×10^{-3} M. The Ion Intensity was Recorded by Monitoring the ThrH^+ Ion (m/z: 120.1) in the SIM Mode	140
Figure 7-6 (A) ESI-MS Response to the Dications for Equimolar Solution of SDC I and UDC I as the Concentration Increase from 2×10^{-7} to 2.5×10^{-3} M. The Ion Intensity Were Recorded by Simultaneously Monitoring the +2 Charged Dications ($[\text{SDC I}]^{2+}$ m/z: 162.2; $[\text{UDC I}]^{2+}$ m/z: 232.2) in SIM Mode. (B) ESI-MS Response to the Dication/ SCN^- Complex Ion for Solutions Containing 10^{-4} M of SDC I and UDC I as the Concentration of SCN^- Added Increases from 1×10^{-6} M to 2×10^{-4} M. The Ion Intensity Were Recorded by Simultaneously Monitoring the +1 Charged Dication/ SCN^- Complex Ion ($[\text{SDC I} + \text{SCN}]^+$ m/z: 382.3; $[\text{UDC I} + \text{SCN}]^+$ m/z: 522.5) in SIM Mode	141

List of Tables

Table 1-1 Ionization Methods for Mass Spectrometry and Their Suitable Analytes	3
Table 2-1 Names, Structures and Abbreviations of the Dicationic Ion Pairing Reagents Used in This Study.	16
Table 2-2 Name, Abbreviation, CAS Number, Exact Mass and Structure of Selected Acidic Pesticides.	17
Table 2-3 Limits of Detection of Pesticides Standard Solutions Obtained by PIESI-MS in the SIM and SRM Mode	27
Table 2-4 Proposed SRM Fragmentation Patterns of the Pesticide/IPR Complexes	28
Table 2-5 Comparison of Absolute Detection Limit of Acidic Pesticides Measured by This Method as Compared to Other LC-MS Methodologies Performed in the Negative Ion Mode.	30
Table 2-6 Limits of Detection and Linear Dynamic Ranges for Five Pesticide Samples. .	32
Table 2-7 Pesticides Concentrations Determined in Stream and Pond Water Samples. .	38
Table 3-1 Structures and Numbering of the Metal Chelating Agents Used in this Study. 44	
Table 3-2 Limits of Detection of Metal Cations Using Ion-Paring Reagent and Metal Chelating Agents by Single Ion Monitoring in Positive Ion Mode ESI-MS ^a	52
Table 3-3 Limits of Detection of Metal Cations Using Ion-Paring Reagent and Metal Chelating Agents by Selected Reaction Ion Monitoring in the Positive Ion Mode ESI-MS	54
Table 3-4 Mass-to-Charge Ratios of Precursor Ion and Product Ion for Each SRM Transition	55
Table 3-5 Limits of Detection of Metal Chelates in Negative Ion Mode ESI-MS.	59
Table 3-6 Comparison of Detection Limits Obtained with the Optimum Chelating Agents for Each Metal Ion in Positive Ion Mode versus Negative Ion Mode ESI-MS.....	60

Table 3-7 Relative Standard Deviation (RSD) and Percent Error of the NIST Standard Measurement	63
Table 3-8 Formation Constant ($\log K_f$) of Metal Chelates ^a	66
Table 3-9 SIM Mode LODs of the Metal Chelates and the IPR Complexes. Data Obtained from Table 3-2 of the Manuscript	66
Table 4-1 Limits of Detection (ng) and the Corresponding Charge of Each Metal Complex in SIM and SRM Mode Using EDTA as the Chelating Reagent	75
Table 4-2 Limits of Detection (ng) and the Corresponding Charge of Each Metal Complex in SIM and SRM Mode Using EDDS as the Chelating Reagent	76
Table 4-3 A Comparison of the Best LODs (pg) of the Metal Complexes Obtained in the Positive Ion Mode and in the Negative Ion Mode ESI-MS	79
Table 4-4 Limits of Detection (pg) of All Metals When Complexed with Each of the Chelating Agents in Both SIM and SRM Analysis Without the Presence of Cationic Ion-Pairing Reagents	80
Table 4-5 Comparison of Detection Limits ($\mu\text{g/L}$) for Five Metals Measured by Three Different Instruments and Methodologies	85
Table 5-1 LODs for Phospholipids by PIESI with Fifteen Different Ion Pairing Reagents	95
Table 5-2 LODs for Each Phospholipid Analyzed in the Negative Ion Mode ESI-MS	96
Table 6-1 Mass-to-Charge Ratio of Sphingolipids Monitored in the Positive SIM Mode Using PIESI-MS	110
Table 6-2 Mass-to-Charge Ratio Monitored During Collision Induced Dissociation (CID) in the Positive SRM Mode	111
Table 6-3 Limits of Detection of Sphingolipids Standard Solutions Obtained in the Positive SIM Mode Using PIESI-MS	112

Table 6-4 Limits of Detection of Sphingolipids Standard Solutions Obtained in the Positive SRM Mode Using PIESI-MS	114
Table 6-5 Comparison of Limits of Detection of Sphingolipids Standard Solutions Obtained by Using PIESI-MS and ESI-MS without Using IPR	116
Table 6-6 Comparison of Limits of Detection of Sphingolipid Standards Obtained by Using PIESI-MS and Formic Acid (FA) and Trifluoroacetic Acid (TFA) as Mobile Phase Additives	117
Table 7-1 Abbreviations and Structures of Dications and Anions Used in This Study ...	127
Table 7-2 Elemental Analysis Data of UDC I and UDC II.	128
Table 7-3 Comparison of Limits of Detection (LOD) of Anions Obtained with the Use of Unsymmetrical Dications (UDC I and UDC II) and Symmetrical Dications (SDC I and SDC II) in the SIM Mode by PIESI-MS.	132
Table 7-4 Comparison of Limits of Detection (LOD) of Anions Obtained with the Use of Unsymmetrical Dications (UDC I and UDC II) and Symmetrical Dications (SDC I and SDC II) in the SRM Mode by PIESI-MS	142

Chapter 1

Introduction

1.1. Paired Ion Electrospray Mass Spectrometry (PIESI-MS)

Mass spectrometry is an analytical technique that determines the mass of a molecule or an atom by measuring the mass-to-charge ratio (m/z) of their ions in the gas phase. The basic components of a mass spectrometry typically include a sample inlet, an ionization source, a mass analyzer, a detector, vacuum system, and data system. The ions of molecules or atoms are generated from an appropriate ion source, separated according to m/z in the mass analyzer, and qualitatively and quantitatively detected by their respective m/z and intensity.¹

As a powerful tool for sensitive detection and identification of a variety of molecules, mass spectrometry has enjoyed rapidly growth in the past several decades (Figure 1-1). A large portion of the rapid growth in mass spectrometry can be attributed to the revolution of development of the ionization sources. The ionization sources play a critical role in mass spectrometry since the molecules or atoms have to be measured after they were converted to ions. Prior to 1980s, the applications of mass spectrometry was only limited to small organic molecules because the ionization source used, such as electron ionization (EI) and chemical ionization (CI), were only suitable for volatile organics.² In recent decades, new ionization methods, such as fast atom/ion bombardment (FAB), electrospray ionization (ESI), and matrix-assisted laser desorption/ionization (MALDI), were developed by pioneering scientists including John B. Fenn, Koichi Tanaka, and Michael Barber (Table 1-1).³ This new generation of ionization techniques made mass spectrometry possible for the analysis of large and complex molecules of biological interest. This overcame previous limitations and greatly

broadened the analytes of interest and consequently catalyzed the growth of mass spectrometry.

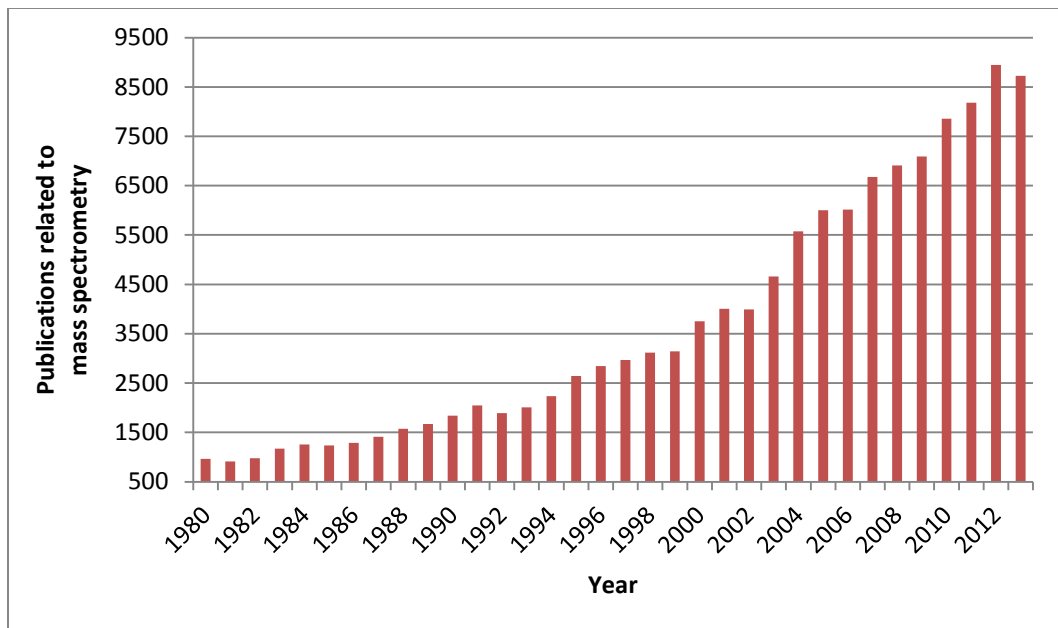


Figure 1-1 Graph Showing the Growing Number of Research Publications in Mass Spectrometry, Based on Numbers of Publications per Year. Data Obtained from SciFinder Scholar Searching Results

Recently, ambient ionization techniques have been developed allowing the analysis of samples at atmospheric pressure under ambient conditions. This included direct analysis in real time (DART), which was introduced by Laramée and Cody in 2005, and desorption electrospray ionization (DESI), which was invented by Cooks and coworkers in early 2004 (Table 1-1). The ambient ionization techniques further broaden the scope of mass spectrometry and have become an increasingly popular area of research.

Table 1-1 Ionization Methods for Mass Spectrometry and Their Suitable Analytes

Ionization Method	Abbreviation	Target Analyte	Inventor
Electron ionization	EI	Volatile and semi-volatile organics	Dempster ⁴
Chemical ionization	CI	Volatile and semi-volatile organics	Pioneered by Field ⁵
Plasma desorption ionization	DI	Non-volatile samples of medium to high molecular mass	Macfarlane ⁶
Matrix-assisted laser desorption/ionization	MALDI	Macromolecules	Koichi Tanaka ⁷
Surface-enhanced laser desorption/ionization	DELDI	Proteins	Hutchens ⁸
Desorption/ionization on silicon	DIOS	Macromolecules	Buriak and Siuzdak ⁹
Fast atom bombardment	FAB	Non-volatile organics and macromolecules	Barber and Bordoli ¹⁰
Secondary ion mass spectrometry	SIMS	Elements	Pioneered by Honig ¹¹
Inductively coupled plasma mass spectrometry	ICP-MS	Elements	Pioneered by Gray ¹²
Atmospheric Pressure Chemical Ionization	APCI	Non-volatile, non-polar/medium-polar organics and macromolecules	Pioneered by Horning ¹³
Electrospray ionization	ESI	Non-volatile, polar organics and macromolecules	Fenn ¹⁴
Direct Analysis in Real Time	DART	Volatile and non-volatile organics	Laramée and Cody ¹⁵
Desorption electrospray ionization	DESI	Volatile and non-volatile organics and macromolecules	Cooks ¹⁶
Paired ion electrospray ionization	PIESI	Anions	Armstrong ¹⁷⁻²²

The use of electrospray ionization source (ESI), which was introduced by Fenn et al.,¹⁴ has shown tremendously growth in the last several ages. Electrospray ionization mass spectrometry (ESI-MS) has the advantages such as outstanding speed, sensitivity, specificity and capability for the structure elucidation of analyte of interest. The power and broad applicability of ESI-MS has been demonstrated in the analysis of different classes of molecules ranging from macromolecule to small organics.²³ Currently, the majority of ESI-MS analyses are performed in the positive ion mode, where the analyte cation produced from protonation/adduct formation is measured, whereas the negative ion mode detection is less preferable.²⁴⁻²⁶ Anion detection performed in the negative ion mode is problematic primarily due to the low sensitivity and signal instability, which results from the predominant electrical discharge and the inherent background noise.^{27,28}

Paired ion electrospray ionization (PIESI) mass spectrometry was developed by Armstrong's group as a useful technique that provides ultrasensitive detection for anions.^{17-20,29} PIEESI-MS technique involves adding very low concentrations of multiple charged ion-pairing reagents (IPRs) into the sample stream, thereby allowing the the anionic molecules and some zwitterions to be measured with extremely high sensitivity in the positive ion mode ESI-MS as the anion/IPR associated complexes.²² With the use of optimal IPRs, sub-picogram (pg) limits of detection (LOD) can be obtained for small organic anions, and to low picogram for inorganic anions.^{17,20}

The typical instrumental configuration of PIEESI-MS is shown in Figure 1-2. A MS pump provides solvent flowing to the mass spectrometry and a Shimadzu LC-6A pump was used to introduce the dicationic ion-pairing reagent to the sample stream. The dicationic ion-pairing reagent aqueous solution was post-column added, resulting in the

formation of the IPR/analyte associated complexes in the mixing tee and their further detection in the ESI-MS.

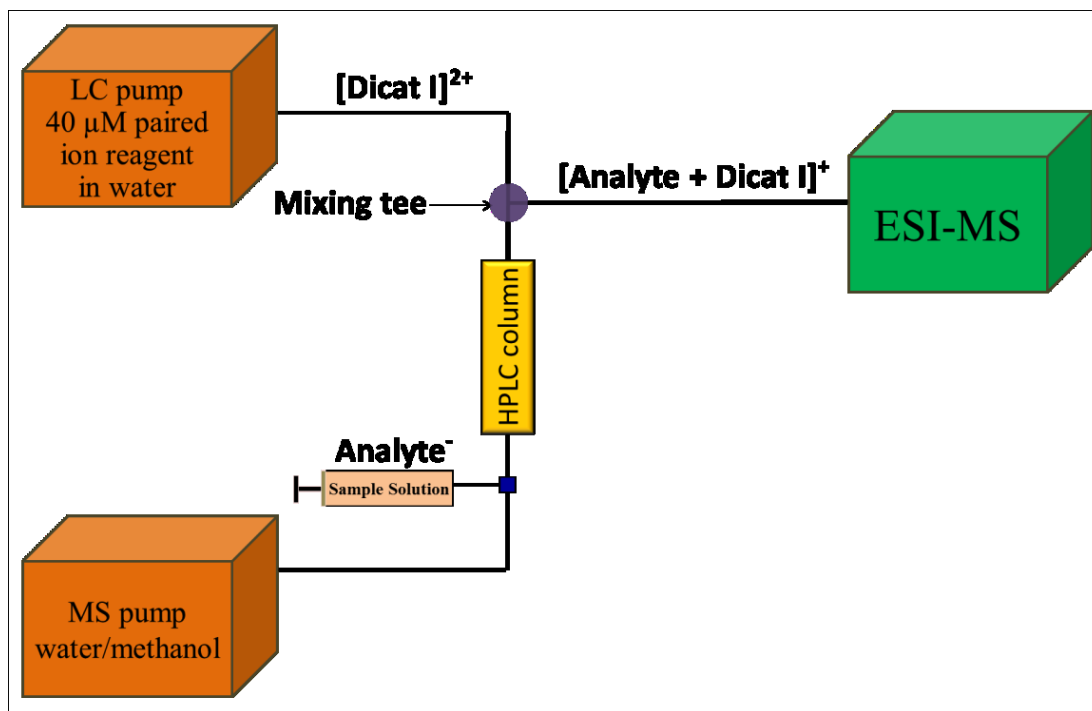


Figure 1-2 Instrumental Configuration of HPLC-PIESI-MS.

1.2. Methods for Detection of Anions

Anion detection continues to be of great importance and interest in many scientific and industrial areas, including food and agriculture chemistry, biochemistry environmental chemistry, pharmaceutical industry, beverage industry, etc. A sensitive detector is essential for the detection of anions, while most methodologies also involve separation and/or sample preparation techniques prior to analysis to minimize the matrix effects in “real world” samples. Currently, the most commonly used methods for anion

detection includes conductivity detection, ion-selective electrodes, UV-vis detection, amperometric detection, and mass spectrometry.

1.2.1. Conductivity Detection

A conductivity detector responds to the changes in conductivity as the eluent that contains ions of interest passes through the detector.³⁰ Conductivity detection can be coupled with a variety of separation methods, but most commonly, ion-exchange chromatography (IEC) is used.³¹ An ideal eluent for the conductivity detector would be a mobile phase with low conductivity. If a high-conductivity mobile phase is used, a suppressor will typically be applied after the ion-exchange column to eliminate the interference of the electrolytes in the mobile phase. Ion-exchange chromatography with conductivity detection is probably the most common method used for anion analysis. It has the advantage of universal detection of ions, low cost and robustness, however, it sometimes suffers from inadequate detection sensitivity, long system equilibration and poor method accuracy particularly when the IEC system is used for routine testing.³² Recently, contactless conductivity detection has been developed to improve the detection sensitivity and robustness.

1.2.2. Ion Selective Electrodes

Ion selective electrodes (ISE) are sensors with high selectivities for specific ions. The electrodes generate a potential difference responding to the changes in concentration of one or several types of ions. Compared to other anion detection techniques, ISEs have advantages such as low cost, portability, and ease of use, while the difficulties in quantitation are a challenge for the practical uses of this technique. In recent years, the state-of-the-art development of ISEs extended its anion detection capabilities to areas such as clinical chemistry,³³⁻³⁵ food chemistry,³⁶ environmental chemistry,³⁷ and the surfactant industry³⁸.

1.2.3. UV-Vis Detection

UV-vis absorbance spectroscopy is a well-developed technique, which measures the changes in absorbance to the UV radiation as the analyte solution pass through the detection cell. The compound absorbs the energy from UV/vis light for electron transition, which allows for promoting one electron from the non-bonding or bonding orbital into one of the empty anti-bonding orbitals. The amount of energy that the UV/vis light could provide is associated with its wavelength (λ). The relationship between the wavelength of the light and its energy is shown in Equation 1-1, where E is the energy of the light, h is the Planck constant, c is the speed of light, and λ is the wavelength of the light.

$$E = h \times \frac{c}{\lambda} \quad (1-1)$$

The quantitative relation between the absorbance and the concentration of analytes of interest is governed by the Beer–Lambert law (Equation 1-2), where A is the absorbance, ϵ is the molar absorptivity or extinction coefficient, c is the concentration of the analyte in the sample solution, and l is the pathlength of the UV cell.

$$A = \epsilon \times c \times l \quad (1-2)$$

Anion analysis can either be done by using “direct UV-Vis detection” or “indirect UV-Vis detection”. Organic anions with chromophores, such as those containing conjugated double bonds and aromatic rings, usually have strong UV absorbance due to $n - \pi^*$ or $\pi - \pi^*$ transitions. Some inorganic anions have broad UV absorption bands if they contain lone pairs of electrons. These anions can be directly detected by UV-vis spectroscopy with an eluent with no or weak UV-vis absorption. However, these can be significant interference and a decrease in sensitivity if the eluent has strong absorption in the same wavelength region as the analyte. Indirect UV-vis detection is a more universal method which is applicable to a widely variety of anions including those without suitable chromophores. This technique utilizes an eluent containing background ions with high

UV-vis absorption. Detection is achieved when the analyte displaces the background ions in the eluent, resulting in a quantifiable decrease in the background signal.³⁹ With the use of different types of background absorbing species, such as chromate, aromatic carboxylates, and aromatic sulfonates; numerous inorganic anions that lack of a chromophore (nitrate, phosphate, halides, acetate, ascorbate, citrate, gluconate) have been successfully analyzed.³⁹

1.2.4. Amperometric Detection

Amperometric detection is based on the measurement of electric current resulting from the oxidation/reduction reaction of an analyte occurring at a working electrode. Some common materials for the electrode can be silver, platinum, or glassy carbon. Amperometric detection is usually hyphenated to separation methods such as HPLC and IC, and it used as complementary tool to the conductivity detection and UV-vis detection. This method has shown to have advantages in terms of sensitivity and selectivity for specific types of anions, such as nitrite, arsenite, thiosulfate, cyanide, and sulfite.⁴⁰ It was noted that amperometric detection has the limitation that it is generally only sensitive for anions that are electrochemically active. Nevertheless, considerable effort has been expended in the development of materials allowing for the detection of electrochemically inactive anions. For example, Wang et al. developed chemically modified electrode based on a polyaniline conducting polymer as a detector for flow-injection analysis and ion chromatography.⁴¹ It was found that some electrochemically inactive anions (perchlorate, sulfate, nitrate, and acetate) can be sensitively and reproducibly detected by this approach with linearity over three orders of magnitude.⁴¹ Barisci et al. reported the use of chloride-containing polypyrrole electrode for the determination of electroinactive anions, such as fluoride, chloride, nitrate, phosphate and sulfate.⁴² These ions were detected after the separation by IC using a low conductivity

mobile phase. They observed that using different potential waveforms and current sampling protocols resulted in changes in the selectivity of the anions.⁴²

1.2.5. Mass Spectrometry

The mass spectrometry is often the detector of choice for anion analysis. Compared to other spectrophotometric and electrochemical approaches for anion detection, mass spectrometry has the unique advantages such as superior sensitivity, specificity, speed, and reproducibility as well as the capability of providing structural information and the oxidation state of the anions of interest. With the rapid development of ionization sources and mass analyzers in recent years, the application of mass spectrometry has been significantly broadened. This technique is currently widely applicable to increasing numbers of users in industry and academic.

Inductively coupled plasma mass spectrometry (ICP-MS) has been used as a technique for detection of anions since the 1990s. ICP-MS utilizes inductively coupled plasma as the ionization source and a mass analyzer to separate and quantify the ions. The high-temperature plasma is usually supplied by electromagnetic induction, which effectively eliminates the chemical interferences generated during ionization, thereby allowing more sensitive detection of atomic/molecular species. Divjak et al. has reported the determination of inorganic anions (sulfide, sulfite, sulfate, and thiosulfate, halogen and oxyhalogen anions, phosphate, selenite, selenite, and arsenate) using ICP-MS coupled with ion chromatographic separation.^{43,44} LODs ranged from ng/L to µg/L levels were obtained with the use of this method.^{43,44} ICP-MS has advantages such as high detection selectivity, high speed and outstanding linearity. However, some disadvantages, such as isobaric interferences, high maintenance costs, and no speciation information, are limitations of this technique.

Electrospray ionization mass spectrometry (ESI-MS), which was introduced by Fenn et al., has merged as an important technique over the last decade.^{14,23,45-47} As a “soft ionization” technique, it provides sensitivity, high speed, and robust analysis for a broad range of small and large molecules. The electrospray ionization process involves four steps: (1) charge separation at the tip of spray capillary, followed by (2) dispersal of charged droplets into a fine aerosol, (3) solvent evaporation from the charged droplet, and (4) ion evaporation from the small charged droplets.⁴⁸ Recently, there has been increasing interest in using ESI-MS for the detection and quantification of anions. ESI-MS has several unique advantages compared to other types of mass spectrometry such as ICP-MS. First, the sensitivity of ESI-MS, along with its speed, linearity and specificity, make it a powerful tool for anion detection. Secondly, ESI-MS directly provides the molecular weight, oxidation states, and speciation information of the anions because ionization is done at room temperature and thus the structure information is preserved during the analysis.^{23,27,49,50}

1.3. Research Objectives and Organization of the Dissertation

This dissertation is focused on the development of paired ion electrospray ionization mass spectrometry (PIESI-MS) for the ultrasensitive determination of anions. The first portion of the dissertation (Chapters 2-6) focuses on PIEESI-MS method development and practical applications in the trace analysis of anionic molecules. Chapter 2 describes the development of HPLC-PIESI-MS for the ultrasensitive determination of pesticides. It was found that HPLC-PIESI-MS method provides extremely low detection limits for acidic pesticides and excellent performance in terms of precision, accuracy, specificity and linearity. Chapter 3 and Chapter 4 describe the application of HPLC-PIESI-MS on the ultrasensitive determination of metal cations, which demonstrates the possibility of using PIEESI-MS for the detection chelated cationic

molecules. The effect of both the ion-pairing reagents and the metal chelating reagents on the detection limits was evaluated. The pH effect on the detection sensitivity of metal cations was evaluated as well. These studies provide useful information for the practical application of the PIESI-MS method. Chapter 5 and Chapter 6 describe the use of HPLC-PIESI-MS for the ultrasensitive determination of lipids (phospholipids and sphingolipids), which demonstrates the capability of PIESI-MS for ultrasensitive determination of medium sized, zwitterionic charge state molecules. The hyphenation of PIESI-MS and separation techniques such as HPLC was evaluated.

The second portion of the dissertation (Chapter 7) discusses the development of unsymmetrical ion-pairing reagents for PIESI analysis and the sensitivity enhancement mechanism of PIESI-MS. Two unsymmetrical ion-pairing reagents were designed and synthesized and their performance on anion detection by PIESI-MS was evaluated. A direct correlation between the ESI signal and the analyte surface activity was found. This sheds light on the mechanism and further emphasizes the role that surface activity plays in the electrospray ionization process. Finally, a general summary is presented in Chapter 8.

Chapter 2

High-performance Liquid Chromatography with Paired Ion Electrospray (PIESI) Tandem Mass Spectrometry for the Highly Sensitive Determination of Acidic Pesticides in Water

Abstract

A novel method based on the paired ion electrospray (PIESI) mass spectrometry has been developed for determination of acidic pesticides at ultratrace levels. The proposed approach provides greatly enhanced sensitivity for acidic pesticides and overcomes the drawbacks of the less sensitive negative ion mode ESI-MS. The limits of detection (LOD) of 19 acidic pesticides were evaluated with four types of dicationic ion-pairing reagent (IPR) in both single ion monitoring (SIM) and selected reaction monitoring (SRM) mode. The LOD of 19 pesticides obtained with the use of the optimal dicationic ion-pairing reagent ranged from 0.6 pg to 19 pg, indicating the superior sensitivity provided by this method. The transition pathways for different pesticide-IPR complexes during the collision induced dissociation (CID) were identified. To evaluate and eliminate any matrix effects and further decrease the detection limits, off-line solid-phase extraction (SPE) was performed for DI water and a river water matrix spiked with 2000 ng L⁻¹ and 20 ng L⁻¹ pesticides standards respectively, which showed an average percent recovery of 93 %. The chromatographic separation of the acidic pesticides was conducted by high-performance liquid chromatography (HPLC) using a C18 column (250 mm × 2.1 mm) in the reversed phase mode using linear gradient elution. The optimized HPLC-PIESI-MS/MS method was utilized for determination of acidic pesticide at ng L⁻¹ level in stream/pond water samples. This experimental approach is 1 to 3 orders of magnitude more sensitive for these analytes than other reported methods performed in the negative ion mode.

2.1. Introduction

During the last few decades the occurrence of pesticides in water has become a major concern in environmental, agriculture and food science due to the toxicological risks of contaminated water.⁵¹⁻⁵⁷ Public awareness of possible health hazards of pesticides has led to strict criteria regarding drinking water quality. The pesticides tolerance level in drinking water in the European Union (EU) was established at $0.1 \mu\text{g L}^{-1}$ for an individual pesticide or $0.5 \mu\text{g L}^{-1}$ for the sum of all pesticide residues in one sample.^{53,54} In the United States, the Environmental Protection Agency (EPA) has regulated tolerance limits for each pesticide based on the potential risks to human health caused by that pesticide, and the pesticide maximum contaminant level (MCL) in drinking water was set to be ranged from $0.2 \mu\text{g L}^{-1}$ to $700 \mu\text{g L}^{-1}$.^{55,56}

The often low concentrations of pesticides in water samples requires the development of analytical approaches that allow for the detection and quantification of pesticides with high sensitivity. Due to a *wide* variety of chemical and physical properties of the pesticides, there is probably no single universal method that could be optimal for analyzing all types of pesticides present in water.⁵⁸ At present, most of the analytical approaches for detection of pesticides in water are established based on gas chromatography coupled with electron impact mass spectrometry (GC-MS).⁵⁹⁻⁶⁵ It has the advantages of fast analysis speed, decent detection limits for most pesticides, a large linear dynamic range and it is not seriously compromised by matrix effects.^{66,67} However, there are still several significant constraints that prevent GC-MS from becoming a more broadly applicable method for pesticide detection. One of the major analytical limitations is that the acidic and thermolabile pesticides, which account for 15-20% of the present-day pesticides, are not GC-amenable.^{51,58} Acidic pesticides cannot be directly analyzed

by GC-MS since they process “active” hydrogen(s), and thus are relatively polar and often have very high boiling points. Although derivatization makes GC-MS suitable for analysis of some acidic pesticides, the derivatization reaction increases the overall analysis time and introduces more variance to the analysis results due to the fact that the yield is usually sensitive to the reaction conditions.^{68,69} Alternatively, liquid chromatography coupled with mass spectrometry (LC-MS) has come to the forefront as a routine analytical approach and it has been utilized for the analysis of acidic pesticides without prior derivatization, using: a particle beam (PB) interface,⁷⁰ atmospheric pressure chemical ionization (APCI) interface,^{51,71,72} and electrospray ionization (ESI) interfaces⁷³⁻⁷⁶. With these approaches it often is possible to achieve 0.15 to 50 ng limits of detection (LODs). ESI-MS has been investigated to be a potentially promising method for analyzing acidic pesticides, but the LODs provided in the negative ion mode are more moderate and sometimes inadequate for trace analysis.^{17,77} When operating in the negative ion mode with standard chromatographic solvents (primarily water, methanol and acetonitrile), the corona discharge is more prevalent, which leads to an unstable Taylor cone and ultimately provokes signal instability and poor limits of detection.^{78,79}

Recently, we have developed an innovative approach based on paired ion electrospray (PIESI) mass spectrometry for ultratrace analysis of anions in positive ion mode ESI-MS.^{17,18,77,80-82} PIESI mass spectrometry involves the introduction of very low concentrations of a structurally optimized ion-pairing reagent (IPR) into the sample stream. The anion can then be measured in the positive ion mode ESI-MS as the IPR/anion associated complex with much lower limits of detection (often by several orders of magnitude). The reason for the great signal enhancement has been shown to be the result of several factors. First, detection by this approach is carried out in the more sensitive positive ion mode. Secondly, the anionic analytes are brought to a much higher

mass range (as the complex), where there is inherently less chemical noise.^{19,83} Furthermore, the IPR/anion binary complex was shown to have greater surface activity than the native anion, resulting in improved ionization efficiency and further enhanced sensitivity.^{21,84-87} The purpose of this study was to evaluate the feasibility of adapting this approach to the sensitive detection and quantitation of acidic pesticides. Nineteen acidic pesticides of different types (phenoxy acid, halogenated aliphatic acid and other aromatic acids) were detected using the four best dicationic ion-pairing reagents originally synthesized in our laboratories.^{17,77,88} The limits of detection of each pesticide were evaluated in both the single ion monitoring (SIM) and selected reaction monitoring (SRM) by PIESI mass spectrometry. The method was also characterized in term of linearity and method detection limits (MDLs). If needed, solid-phase extraction (SPE) can be employed for concentration of large volumes of sample with the purpose of further improving the already low LODs. In these cases, the recoveries were considered as well. The SRM transition pathways for four types of pesticides/dicaionic IPR binary complexes were identified. Moreover, an HPLC method was developed and coupled with PIESI mass spectrometry for simultaneously separation and identification of selected pesticides. The developed HPLC-PIESI-MS/MS methodology was utilized for determination of acidic pesticide concentrations in stream/pond water samples at the low parts per trillion levels.

2.2. Experimental

2.2.1. Materials

Four types of dicationic ion pairing reagent solutions: 1,9-nonanediyl-bis(3-methylimidazolium) difluoride solution, 1,5-pentanediy-bis(3-benzylimidazolium) difluoride solution, 1,5-pentanediy-bis(1-butylpyrrolidinium) difluoride solution, and 1,3-

propanediyl-bis(tripropylphosphonium) difluoride solution were developed in our laboratory, and were commercially available from Sigma-Aldrich (St. Louis, MO). The names, structures and abbreviations of the ion pairing reagents (IPR) used in this study are given in Table 2-1. All 19 pesticides were purchased as analytical standard (purity >99%) either from Sigma-Aldrich (St. Louis, MO) or from Tokyo Chemical Industry Co., Ltd. (Portland, OR). Their structures, CAS registry numbers and exact masses are given in Table 2-2. Solvents used for the ESI-MS analysis and sample preparation were of HPLC-grade and were purchased from Honeywell Burdick and Jackson (Morristown, NJ). The SPE cartridge used in this analysis was Discovery DSC-18 (6mL Tubes, 1 g Sorbent per Cartridge, 50 μm Particle Size, 70 \AA Pore size) obtained from Supelco, Sigma-Aldrich Co. (Bellefonte, PA). ACS grade formic acid (88%) was obtained from J. T. Baker. Inc.. 20 mL High-density polyethylene (HDPE) vials were purchased from Wheaton (Millville, NJ). The individual standard stock solution was prepared daily in HDPE vials and further diluted to desired concentration for analysis with methanol/water (50:50, v/v) mixture.

Table 2-1 Names, Structures and Abbreviations of the Dicationic Ion Pairing Reagents Used in This Study.

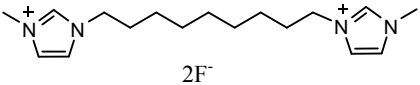
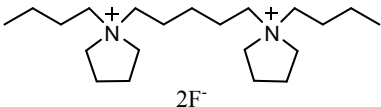
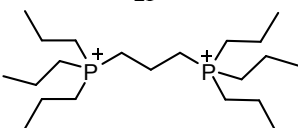
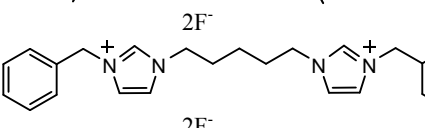
Names	Structures	Abbreviations
1,9-Nonanediyl-bis(3-methylimidazolium) difluoride		C ₉ (mim) ₂
1,5-Pentanediy-bis(1-butylpyrrolidinium) difluoride		C ₅ (bpyr) ₂
1,3-Propanediyl-bis(tripropylphosphonium) difluoride		C ₃ (triprp) ₂
1,5-Pentanediy-bis(3-benzylimidazolium) difluoride		C ₅ (benzim) ₂

Table 2-2 Name, Abbreviation, CAS Number, Exact Mass and Structure of Selected Acidic Pesticides.

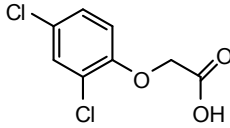
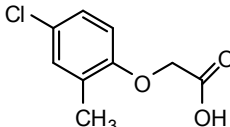
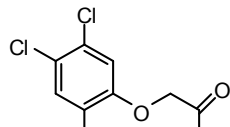
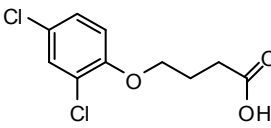
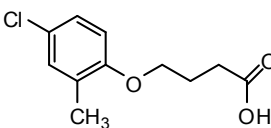
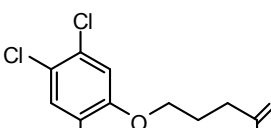
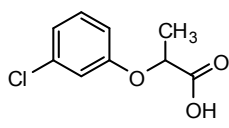
Compound Name (Abbreviation)	CAS No.	Exact Mass	Structure
2,4-dichlorophenoxyacetic acid (2,4-D)	94-75-7	219.97	
4-chloro-o-tolyloxyacetic acid (MCPA)	94-74-6	200.02	
2,4,5-trichlorophenoxyacetic acid (2,4,5-T)	93-76-5	253.93	
4-(2,4-dichlorophenoxy)butyric acid (2,4-DB)	94-82-6	248.00	
4-(4-chloro-o-tolyloxy)butyric acid (MCPB)	94-81-5	228.06	
4-(2,4,5-trichlorophenoxy)butyric acid (2,4,5-TB)	93-80-1	281.96	
2-(3-chlorophenoxy)propionic acid (cloprop)	101-10-0	200.02	

Table 2-2—Continued

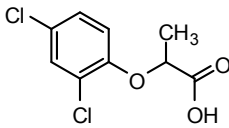
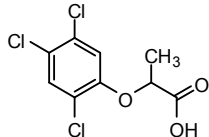
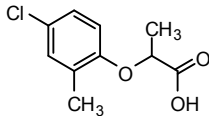
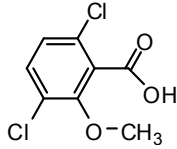
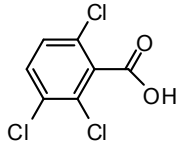
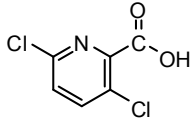
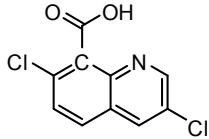
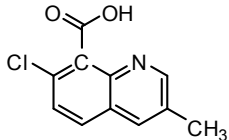
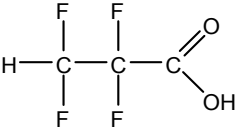
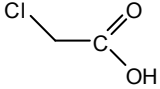
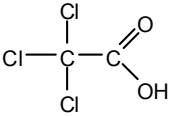
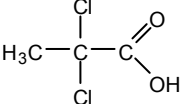
2-(2,4-dichlorophenoxy)propionic acid (dichlorprop)	120-36-5	233.99	
2-(2,4,5-trichlorophenoxy)propionic acid (fenoprop)	93-72-1	267.95	
2-(4-chloro-o-tolyloxy)propionic acid (mecoprop)	93-65-2	214.04	
3,6-dichloro-2-methoxybenzoic acid (dicamba)	1918-00-9	219.97	
2,3,6-trichlorobenzoic acid (2,3,6-TBA)	50-31-7	223.92	
3,6-dichloro-2-pyridinecarboxylic acid (Clopyralid)	1702-17-6	190.95	
3,7-dichloro-8-quinolinecarboxylic acid (Quinclorac)	84087-01-4	240.97	
7-chloro-3-methyl-8-quinolinecarboxylic acid (Quinmerac)	90717-03-6	221.02	

Table 2-2—Continued

2,2,3,3-tetrafluoropropanoic acid (flupropanate)	756-09-2	146.00	
2-chloroacetic acid (MCA)	79-11-8	93.98	
2,2,2-trichloroacetic acid (TCA)	76-03-9	161.90	
2,2-Dichloropropionic acid (dalapon)	75-99-0	141.96	

2.2.2. ESI-MS Analysis

The mass spectrometer used in this study was A Finnigan LXQ (Thermo Fisher Scientific, San Jose, CA). The paired ion electrospray was performed in the positive ion mode and the MS condition was set as follows: spray voltage, 3kV; capillary voltage, 11V; capillary temperature, 350°C; sheath gas flow, 37 arbitrary units (AU); and the auxiliary gas flow, 6 AU. Normalized collision energy in the selected reaction monitoring (SRM) acquisition mode was set at 30, the Q value was set at 0.25 and the activation time was set at 30 ms. Mass-to-charge ratio width was set as 5 for in both SIM and SRM experiment. A Surveyor MS pump (Thermo Fisher Scientific, San Jose, CA) provided a 300 μ L/min (67% MeOH/33% H₂O) carrier flow, and a Shimadzu LC-6A pump (Shimadzu, Columbia, MD) applied the 40 μ M dicationic ion-pairing reagent solution in water at rate of 100 μ L/min. The introduction of dicationic solution into the LC flow was accomplished

via a Y-type mixing tee, resulting in a total flow rate of 400 $\mu\text{L}/\text{min}$ and an overall solvent composition of 50% MeOH/50% H_2O with 10 μM dicationic ion-pairing reagent. The sample was injected into the system through a six-port injection valve. The injection volume was set at 5 μL for LOD determination and 25 μL for stream/pond water samples analysis using full loop injection mode. The schematic diagram of instrumental configuration is shown in Figure 1-2. The detection limits for the instrumental LOD were determined by series dilution of standard solution with methanol/water (50:50, v/v) mixture until a signal-to-noise ratio of 3 was noted in 5 replicate injections of each sample. The signal-to-noise ratio was calculated based on a Genesis Peak Detection Algorithm provided by the Xcalibur 2.0 software.

2.2.3. Solid-Phase Extraction

To conduct the solid-phase extraction (SPE), a Discovery DSC-18 cartridge was firstly washed with 5 mL of methanol/acetone (50:50, v/v) mixture to remove the contaminants from its manufacture process, and sequentially conditioned with 10 mL of HPLC grade water. The 200 mL aqueous sample was acidified with formic acid to pH 2, and then loaded onto the cartridge at a flow rate of approximately 3 mL/min. After extraction, the cartridge was dried by blowing with enough nitrogen to remove the interstitial liquid. Elution was finally performed with 2 mL of methanol at a flow rate of 1 mL/min. The resulting effluent was put in a single 20 mL HDPE vial, and the sample blown to approximately 0.1 mL with a stream of dry argon. The sample is then reconstituted to a volume of 1.5 mL with methanol/water (50:50, v/v) mixture. It should be noted anion exchange cartridge was also evaluated for concentration of analyte, however, it shows relative lower recoveries compared to reverse phase cartridge and therefore was not used in this study. The SPE reproducibility was examined by using sample solutions spiked with 100 ng/L of 2,4-D standard. Eight extractions in two different

days were performed by using the developed method. The relative standard deviation (RSD) calculated for eight determinations was 7 %. For the recovery studies, the 200 mL of DI water or river water was spiked with each pesticide at a level of 2000 ng L⁻¹ or 20 ng L⁻¹, and then was extracted by using SPE following the procedure described above. The recoveries of pesticides were calculated by integrating the peak area for each analyte after SPE and comparing those results with those acquired from standard solutions.

2.2.4. Chromatography

The HPLC-PIESI-MS experiment was carried out under the PIESI-MS condition described above with slightly modification on the instrumental setup. The sample was injected into the column by a Thermo Fisher Surveyor autosampler (Thermo Fisher Scientific, San Jose, CA) with 25µL injection volume. The separation was performed on an Ascentis™ C18 column (250 mm × 2.1 mm) which is purchased from Supelco, Sigma-Aldrich Co. (Bellefonte, PA). The mobile phase was composed of 5 mM formic acid in water (elute A) and 5 mM formic acid in methanol (elute B). 40 µM of dicationic ion-pairing reagent aqueous solution was post-column added at 100 µL/min through a Y-type mixing tee located between the column and the mass spectrometer. The flow rate through the column was 400 µL/min. The LC flow directly went into the MS without post-column flow splitting. The column was equilibrated with 95 % of mobile phase A and 5 % of mobile phase B for 30 min, then a linear gradient solvent program was performed starting with an initial mobile phase composition of 95 % mobile phase A and decrease to and 5 % mobile phase A in 20 min. Data collection and peak integration was done by Xcalibur 2.0 software.

2.2.5. Determination of Trace Pesticides in Stream and Pond Water Samples

The method developed herein has been applied to determine the pesticide concentrations in stream/pond water samples. The stream and pond water samples were

taken at the end of February from Rush Creek in the Shady Valley golf club (Arlington, Texas, USA), and from Village Creek and one pond at the Lake Arlington golf course (Arlington, Texas, USA). Water samples were collected in 1-L amber glass bottles with solid-top caps with fluoropolymer resin liner and stored at 4°C in the dark. Before analysis, water samples were allowed to reach to room temperature and then were forced through a cellulose fiber paper by vacuum filtration. Thereafter, SPE and of HPLC-PIESI-MS analysis were carried out by using the procedure described above. The existence of pesticides in water samples was identified by monitoring the individual mass in SIM mode and further assured in SRM mode by using the most intense transition for each pesticide (see Table 2-3) with identical retention time and isotope ratio compared to those determined for standard solution. 2,4,5-T was used as the internal standard (IS) since it was found to be absent in all three river/pond water samples. All samples were extracted and analyzed in triplicate. The quantification of the pesticides was accomplished in the SRM mode by using internal calibration ($R^2 > 0.99$). The six-point calibration curve was produced by plotting the ratio of peak area of analyte to peak area of the IS versus the concentration of injected standard solution.

2.3. Results and Discussion

2.3.1. Dicationic Ion Pairing Reagents and Tested Pesticides

Empirical observations in previous reports indicate that the effectiveness of the dicationic pairing agents was greatly affected by their structure and geometry, including their charged moiety and alkyl linkage chain length.^{18,77,81} The four dicationic ion-pairing reagents (IPR) used in this study were chosen as they afforded the best performance when used for other inorganic and organic anions in previous studies.^{17,77} Their names and chemical structures are provided in Table 2-1. The dications utilize charged moieties

including imidazolium ($C_9(\text{mim})_2$ and $C_5(\text{benzim})_2$), pyrrolidinium ($C_5(\text{bpyr})_2$) and phosphonium ($C_3(\text{triprp})_2$). The alkyl linkage chain length separating the dications differs from C_3 to C_9 . The alkyl linkage chain between the two charged moieties gives additional flexibility to the dicationic ion-pairing reagents. Consequently compared to some of the rigid divalent cationic pairing agents (as in Ref. 28), these dications have relatively flexible geometries which enable them to bend around and more tightly associate with some anions. The list of the target pesticides along with their CAS registry numbers, exact masses and structures are given in Table 2-2. The nineteen pesticides selected for this work represent the most commonly used acidic pesticides in agriculture, and they are divided into three groups: phenoxy acid pesticides (2,4-D, MCPA, 2,4,5-T, 2,4-DB, MCPB, 2,4,5-TB, cloprop, dichlorprop, fenoprop and mecoprop), halogenated aliphatic acid pesticides (flupropanate, MCA, TCA and dalapon) and other aromatic acidic pesticides (dicamba, 2,3,6-TBA, clopyralid, quinclorac and quinmerac). It is noted that with the exception of halogenated aliphatic acids (flupropanate, MCA, TCA and dalapon), all the other pesticides contain at least one aromatic ring and thus could undergo π - π interactions with the aromatic dicationic IPR such as $C_9(\text{mim})_2$ and $C_5(\text{benzim})_2$. Also, all the pesticides reported in this work have a carboxylic acid group, which in ionized form, provides the anion that is analyzed.

2.3.2. Identification of Analyte/IPR Complex in the Full Scan Mode

Figure 2-1 shows a positive ion mass spectrum of the binary complex obtained in full scan mode by directly infusing the mixture of 20 μM dication $C_5(\text{bpyr})_2$ and 20 μM cloprop solution into the ESI-MS. An intense peak can be seen for the divalent cation of $C_5(\text{bpyr})_2$ ($[C_5(\text{bpyr})_2]^{2+}$ m/z 162.17). In addition, a singly charged binary complex ion ($[\text{cloprop} + C_5(\text{bpyr})_2]^+$ m/z 523.42) is observed. The enlarged spectrum shows the isotope distribution of the complex ion peak. The peak height ratio of m/z 523.42 and m/z

525.42 corresponds to $^{35}\text{Cl}/^{37}\text{Cl}$ isotope ratio which is approximately 3 to 1 and therefore further confirms the makeup of the complex ion. The yield for the complexation in this case cannot be accurately calculated based on the ion counts for each species, since the two ion species $[\text{cloprop} + \text{C}_5(\text{bpyr})_2]^+$ and $[\text{C}_5(\text{bpyr})_2]^{2+}$ may have different ionization efficiencies and detector responses. However, under the experimental condition where the dicationic IPR injected is in large excess over the analyte, the analyte is anticipated to be fully converted to the analyte/IPR complex.

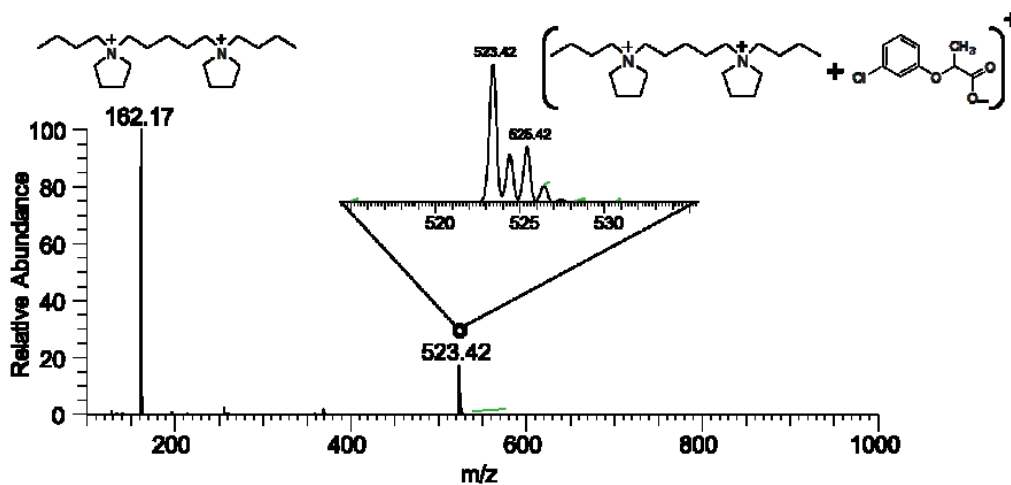


Figure 2-1 Positive Ion Mode Mass Spectrum of Dicationic Ion Pairing Reagent $\text{C}_5(\text{bpyr})_2$ and Cloprop Solution Obtained in Full Scan Mode (m/z 100 to m/z 1000).

2.3.3. LODs Obtained by PIESI-MS in the Single Ion Monitoring Mode

The absolute limits of detection for a total of 19 acidic pesticides obtained with four types of dications in positive ion mode by single ion monitoring and selected reaction monitoring are listed in Table 2. The monoisotopic mass was used to calculate the mass to charge ratio of the complex, which will result in the most abundant isotope being

selected. The best detection limit for each pesticide is indicated by the bold type (Table 2). Overall, all 19 acidic pesticides were successfully detected by this method and a wide range of LODs (from nanogram (ng) to picogram (pg) level) were obtained. The LOD for the same pesticides varies significantly when using different dicationic ion-pairing reagent, indicating that the IPR plays a critical role on the detection sensitivity. For example, the LOD (SIM) was 36 ng for 2,4-DB with the use of IPR $C_9(\text{mim})_2$, while it was 37 pg by using $C_5(\text{bpyr})_2$, which is approximately a 1000 fold improvement. Similarly, the LOD for mecoprop was found to be 300 pg by SIM with $C_9(\text{mim})_2$, but the use of $C_3(\text{triprp})_2$ results in a LOD approximately 80 times better (3.8 pg). IPR $C_5(\text{bpyr})_2$ shows better detection limits when detecting phenoxy acid pesticides in the SIM mode while $C_5(\text{benzim})_2$ seems to be superior for aromatic acidic pesticides and $C_3(\text{triprp})_2$ was found to be a better IPR for detection of halogenated aliphatic acid pesticides. Interestingly, $C_9(\text{mim})_2$ which was considered to be one of the better ion-pairing reagents in previous studies did not provide high detection sensitivity for these acidic pesticides, particularly when analyzing phenoxybutyric herbicides such as 2,4-DB, MCPB and 2,4,5-TB. On the other hand, it was observed that the LODs of related analytes can be quite different even when there are slight changes in their chemical structures. Dicamba and 2,3,6-TBA have same chemical structure except that the dicamba has an electron-donating group (methoxyl group) at the 2-position of the benzene ring rather than an electron-withdrawing group (chlorine substituent) for 2,3,6-TBA. However, it was shown that the LOD of dicamba was approximately one order of magnitude better as compared to 2,3,6-TBA by SIM with four types of IPR. Another noteworthy feature is that the LODs for the analytes with higher pKa values (2,4-DB (pKa=4.8), MCPB (pKa=4.8) and 2,4,5-TB (pKa=4.5)) were significantly higher in comparison with their analogs which have lower pKa values (2,4-D (pKa=2.6), MCPA (pKa=3.1), and 2,4,5-T (pKa=2.1)) when using IPR

$C_9(\text{mim})_2$, $C_3(\text{triprp})_2$ and $C_5(\text{benzim})_2$. Attempts to form more analyte ion by adjusting the sample solution pH to basic with sodium hydroxide and ammonium hydroxide did not further improve the detection limits. In fact the LODs were indistinguishable when using the neutral sample solution as opposed to adjusting the pH to slightly higher values (7 to 9). Furthermore, the results were rather worse when the pH was above 10. The decrease of detection sensitivity probably due to the fact that adding the sodium hydroxide and ammonium hydroxide into the sample solution generated sodium/ammonium salts which leads to either ion suppression in the ESI interface or inhibition of the IPR/analyte complex formation due to the high ionic strength in the solution.

2.3.4. LODs Obtained by PIESI-MS in the Selected Reaction Monitoring Mode

SRM usually provides lower LODs than SIM as it enhances analytical specificity and reduces the noise in the mass region being analyzed. As shown in Table 2-3, the LODs for most pesticides were improved by typically 2 to 10 fold as compared to those results obtained by SIM. The IPR $C_5(\text{bpyr})_2$ which shows best LOD improvement was found to be the most effective IPR for detecting these acidic pesticides in the SRM mode. All LODs acquired for the studied acidic pesticides are below 19 pg. The LODs of quinclorac (0.60 pg), flupropanate (0.088 pg) and dalapon (0.75 pg) reach sub-pg level with the use of IPR $C_5(\text{bpyr})_2$, $C_5(\text{benzim})_2$ and $C_5(\text{bpyr})_2$ respectively. Nevertheless, it was also observed that not all LODs measured by SRM were greatly improved as compared to SIM. For example, the LOD of dicamba was 10 pg with $C_9(\text{mim})_2$ by SIM but increased to 40 pg when detected by SRM, representing an unusual LOD change from SIM to SRM. The decreased sensitivity in SRM may be because the product ion generated from the collision induced dissociation (CID) is unstable, and therefore less detectable.

Table 2-3 Limits of Detection of Pesticides Standard Solutions Obtained by PIESI-MS in the SIM and SRM Mode

Sample	C ₃ (triprp) ₂				C ₅ (benzim) ₂				C ₅ (bpyr) ₂				C ₉ (mim) ₂			
	SIM		SRM		SIM		SRM		SIM		SRM		SIM		SRM	
	LOD (pg)	m/z ^a	LOD (pg)	m/z ^b	LOD (pg)	m/z ^a	LOD (pg)	m/z ^b	LOD (pg)	m/z ^a	LOD (pg)	m/z ^b	LOD (pg)	m/z ^a	LOD (pg)	m/z ^b
2,4-D	10	581.3	8.0	187.2	16	605.2	8.0	385.3	45	543.3	7.0	416.2	75	509.2	200	289.3
MCPA	15	561.3	15	187.2	10	585.3	10	385.3	3.6	523.4	1.1	396.3	35	489.3	35	289.3
2,4,5-T	16	615.3	24	187.2	25	639.2	3.7	385.3	25	577.3	3.7	450.2	120	543.2	90	289.3
2,4-DB	700	609.3	700	187.2	2000	633.3	2000	385.3	37	571.4	6.7	444.3	36000	537.3	11000	289.3
MCPB	1100	589.4	720	187.2	1300	613.3	1200	385.3	30	551.4	9.0	424.3	25000	517.3	25000	289.3
2,4,5-TB	1800	643.3	6000	187.2	5300	667.2	2500	385.3	32	605.3	6.0	478.3	35000	571.2	10000	289.3
cloprop	10	561.3	10	187.2	7.0	585.3	3.5	385.3	9.0	523.4	2.7	396.3	140	489.3	96	289.3
dichlorprop	20	595.3	12	187.2	10	619.2	4.0	385.3	30	557.3	4.5	430.3	100	523.2	55	289.3
fenoprop	20	629.3	20	187.2	30	653.2	10	385.3	20	591.3	4.0	464.3	80	557.2	25	289.3
mecoprop	3.8	575.4	2.8	187.2	15	599.3	4.7	385.3	30	537.4	12	410.3	300	503.3	140	289.3
dicamba	6.5	581.3	6.5	187.2	6.0	605.2	2.6	385.3	15	543.3	3.0	416.3	10	509.2	40	289.3
2,3,6-TBA	60	585.2	60	187.2	17	609.2	3.8	385.3	110	547.3	6.3	420.2	200	513.2	600	289.3
Clopyralid	4.5	552.3	4.5	187.2	5.0	576.2	5.0	385.3	20	514.3	1.5	387.2	16	480.2	11	289.3
Quinclorac	7.5	602.3	7.5	187.2	10	626.2	3.0	385.3	6.0	564.3	0.60	437.2	90	530.2	60	289.3
Quinmerac	7.0	582.3	5.2	187.2	3.5	606.3	3.5	385.3	15	544.4	2.8	417.3	20	510.3	100	289.3
flupropanate	3.5	507.3	1.1	187.2	3.1	531.3	0.088	385.3	5.0	469.4	5.0	342.2	4.2	435.3	4.2	289.3
MCA	10	455.3	35	187.2	17	479.2	15	385.3	6.0	417.3	3.0	290.2	15	383.2	1900	289.3
TCA	1.5	523.2	2.0	187.2	15	547.1	7.5	385.3	160	485.2	19	359.3	6400	451.2	2000	289.3
dalapon	5.0	503.3	5.0	187.2	15	527.2	2.9	385.3	10	465.3	0.75	359.3	19	431.2	20	289.3

^a Indicates the mass-to-charge ratio of the complex monitored in the SIM mode.

^b Indicates the mass-to-charge ratio of the SRM fragment monitored in the SRM mode.

2.3.5. Fragmentation Reactions during the Collision Induced Dissociation Process

The proposed fragmentation pathways for each types of IPR-analyte complex were determined and are briefly summarized in Table 2-4. The most common cleavage in CID was of the C_α-N bond (in C₅(bpyr)₂ and C₅(benzim)₂) and the C_α- C_β bond (in C₃(tripp)₂) to form the daughter ions and another radical ion. Also, the two imidazole dicationic ion-pairing reagents were able to form charge-reduced species [M-H]⁺ by the loss of the C₂ hydrogen on one imidazole ring. Unlike the diverse fragmentation patterns observed previously, the fragmentation pathway of the IPR-analyte complexes were found to be consistent for each particular IPR in this study (Table 2-3 and Table 2-4).

Table 2-4 Proposed SRM Fragmentation Patterns of the Pesticide/IPR Complexes

Structure of IPR part of precursor ion	Structure of product ion	m/z of product ion
		187.6 ^a
		361.3
		385.2 ^a
		227.2
		196.2
		197.2 + Analyte Mass ^{a,b}
		289.3 [*]

^a Indicates the most abundant fragment ion generated in the CID.

^b With the exception for TCA and dalapon. The daughter ion of both TCA and dalapon has a m/z 359.3 and could be the complex ion [C₅(bpyr)₂+Cl]⁺ (m/z = 359.3).

Interestingly, the anionic analyte molecule was found to dissociate from the dication after CID when pairing with $C_9(\text{mim})_2$, $C_3(\text{triprp})_2$ and $C_5(\text{benzim})_2$, resulting in a positively charged dication moiety as the SRM fragment ion. Whereas most of the $C_5(\text{bpyr})_2$ -anion complex remains intact after the fragmentation. The daughter ion of $C_5(\text{bpyr})_2$ -analyte complex is composed of a dication moiety $C^{13}H^{26}N^+$ ($m/z = 196.2$) and a protonated anion molecule. In all cases except for $C_5(\text{bpyr})_2$ -TCA complex and $C_5(\text{bpyr})_2$ -dalapon complex, which generate the predominant daughter ion in CID at m/z 359.3 and it was deduced to be $[C_5(\text{bpyr})_2\text{-Cl}]^+$ ion ($m/z = 359.3$).

2.3.6. Improvement of LODs Achieved by Using PIESI-MS

Table 2-5 compares the absolute detection limit (pg) of the acidic pesticides obtained by *PIESI-MS* in the SRM mode using IPR $C_5(\text{bpyr})_2$ with other LC-MS methodologies reported in the literature. Notably, the *PIESI-MS* method with the use of dicationic ion-pairing reagents is more sensitive by one to three orders of magnitude compared to most reported methodologies performed in the negative ion mode. It should be noted that this study focused on the sensitivity enhancement of the instrumental method (i.e., the mass spectrometer). Thus, Table 2-5 compares the absolute LODs, which are expressed in mass units and represents the sensitivity of mass spectrometry (without considering the LOD improvement achieved by any sample enrichment techniques or large-volume injection techniques). Such preconcentration or large volume injection techniques can be used prior to any instrumental measurement to lower the LOD for analytes in any matrix. However, they have no effect on the inherent sensitivity of an instrument which is the main focus of this study.

Table 2-5 Comparison of Absolute Detection Limit of Acidic Pesticides Measured by This Method as Compared to Other LC-MS Methodologies Performed in the Negative Ion Mode.

Ionization mode, scan mode	Absolute LOD ^{a,b} (pg)	References
PB	1000 - 40000	[17]
APCI-NI, SIM	2500 - 50000	[1]
APCI-NI, SIM	500 - 5000	[18]
APCI-NI, SIM	1000 - 8000	[19]
ESI-NI, SIM	500 - 1500	[21]
ESI-NI, SIM	150 - 1600	[23]
ESI-NI, SRM	200 - 1200	[22]
ESI-PI, SRM [‡]	0.6 - 19	Present method ^c

^a Since not all the references reported the LODs in the same units, all LODs have been converted to mass units for comparisons. Therefore the LODs present are absolute detection limits. For the methods using SPE to concentrate samples for analysis, the LODs have been corrected by the SPE concentration factors.

^b In some references the LODs were reported for all acidic/basic/neutral pesticides analyzed. In these cases only the LODs for acidic pesticides that belong to the same categories as in this study are considered.

^c The LOD range reported is based on LODs of 19 pesticides obtained using dicationic $C_5(bpyr)_2$ by PIESI-MS in the SRM mode.

Figure 2-2 shows an example of the signal-to-noise enhancement when the dicationic ion-pairing reagent $C_5(bpyr)_2$ was used for the detection of dicamba. An injection of 200 ng mL⁻¹ of dicamba solution showed no signal when detected in the negative ion mode at m/z 219.0, whereas significant response (S/N = 64) for the same

concentration of dicamba was observed when it was detected as an $C_5(\text{bpyr})_2/\text{dicamba}$ complex at m/z 543.3 in the SIM mode by PIESI-MS. Detection performed by SRM resulted in a further improved signal ($S/N = 345$), which was more than 5 times stronger compared to that by SIM.

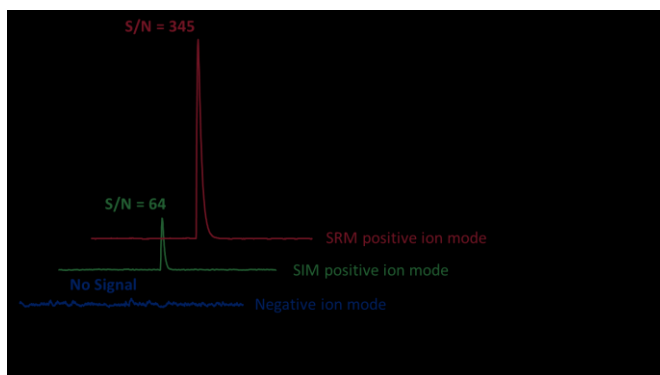


Figure 2-2 PIESI-MS Signal-to-Noise Ratio Diagram of Dicamba

2.3.7. Method Validation

Table 2-6 shows the method validation data of five selected pesticides in terms of LOD, MDL and linearity. The LODs were determined in the SRM mode by PIESI-MS with dication $C_5(\text{bpyr})_2$ (data was obtained from Table 2-3), and the mass-to-charge ratios of the SRM transition are given in Table 2-6. The method detection limit (MDL) was calculated with the consideration of the SPE concentration factor (133 times in this study) and the sample loop size (5 μL). It should be noted that since the MDL is dependent on the volume of sample solution concentrated by SPE and also on the volume of sample solution injected into the system, it can be further improved by concentrating a larger volume of sample on SPE or by using a larger sample injection loop. The linearity was evaluated by calculating the correlation coefficients of the linear regression ($R^2 > 0.99$). A linear response in a concentration range of 2 to 3 orders of magnitude was demonstrated

by calibration graphs of five selected pesticides. It is noted that either the LOD or linear dynamic range can be instrumentally dependent. Compared to quadrupole ion trap (QIT) the linear ion trap (LIT) has the advantages of larger ion storage capacity and higher trapping efficiency⁸⁹, and thus usually provides better sensitivity than QIT. However, ion trap mass analyzer suffers from a low dynamic range for quantification which can be improved by using a triple quadrupole (QqQ) mass analyzer. The triple quadrupole instruments offer better performance for target compound quantitation than ion trap instruments and therefore could further improve the detection limits reported here. Additionally, optimization of the instrumental parameters for each particular IPR/analyte complex may results in an improved LOD. Increasing the spray voltage and decreasing the capillary temperature was previously found to have big impact the detection sensitivity⁸⁰.

Table 2-6 Limits of Detection and Linear Dynamic Ranges for Five Pesticide Samples.

Compound	Quantification mass in SIM (m/z)	SRM transition (m/z)	LOD ^a (pg)	MDL ^a (ng/L)	Linear dynamic range ^b (pg)	R ²
dicamba	543.32	543.32→416.3	3.0	5.0	50 - 30000	0.994
quinclorac	564.32	564.32→437.2	0.6	0.9	20 - 40000	0.996
2,4-D	543.32	543.32→416.3	7.0	11	150 - 100000	0.996
2,4,5-T	577.28	577.28→450.2	3.7	6.0	75 - 50000	0.995
MCPA	523.37	523.37→396.3	1.1	1.6	12.5 - 100000	0.998

^a The LOD/MDL were obtained in SRM mode with dicaionic ion pairing reagent C₅(bpyr)₂.

^b The linear range was evaluated in SIM mode with dicaionic ion pairing reagent

C₅(bpyr)₂.

2.3.8. Solid-Phase Extraction Recovery Study

Method efficacy was evaluated by means of a SPE recovery study (Figure 2-3). A reversed phase cartridge, Discovery DSC-18, was selected because of its good recoveries and efficacy, as well as large breakthrough volumes. The SPE recovery studies were performed with the fortification of DI water and a river water at two different level concentrations (2000 ng L⁻¹ and 20 ng L⁻¹). Four selected analytes were detected after SPE with the percentage recovery ranging from 91% to 93% for DI water matrix and 95% to 102% for a river water matrix at 2000 ng L⁻¹ spiked concentration, and from 83% to 112% for DI water matrix and 81% to 98% for a river water matrix at 2000 ng L⁻¹ spiked concentration, indicating a good recovery for pesticides at ultratrace levels.

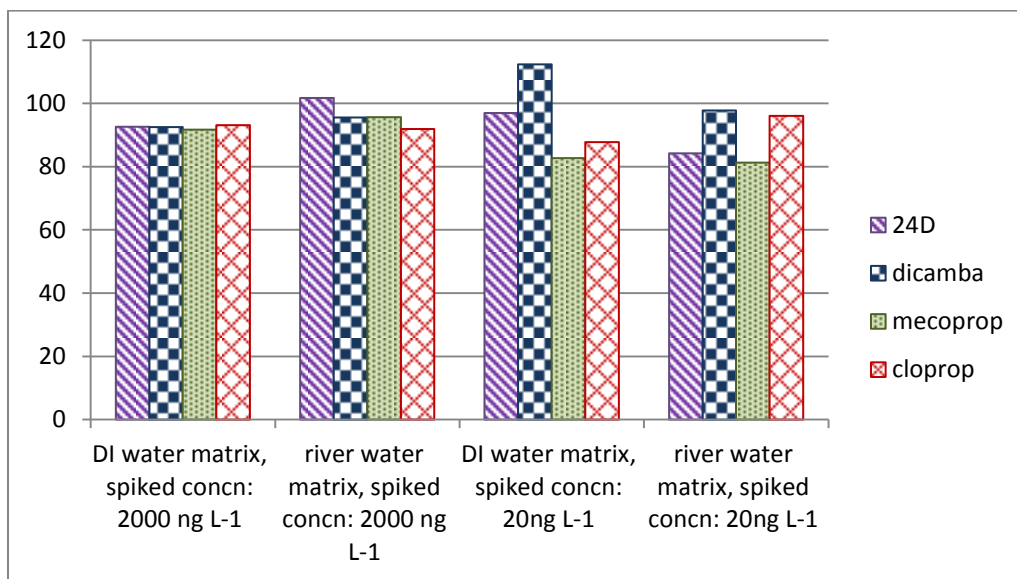


Figure 2-3 Percent Recoveries Obtained by SPE Four Pesticides Spiked Sample Solutions.

2.3.9. Chromatographic Separations of Nineteen Acidic Pesticides

Chromatography is an indispensable methodology to separate mixtures and provides a solution for elimination of matrix effects which may cause ionization suppression or enhancement resulting in imprecision and inaccuracy in quantitative analysis. Figure 2-4 shows the simultaneous chromatographic separation and detection of nineteen acidic pesticides by using LC-PIESI-MS. The separation was obtained in the reverse phase mode using an Ascentis™ C18 column with a linear gradient program (see Experimental Section). The PIEESI-MS detection was performed with dication $C_5(\text{bpyr})_2$ by using full scan mode for the entire run and individual m/z for each pesticides were chosen to generate the extracted ion chromatogram (EIC). All the pesticides were separated within 20 min under the chromatographic conditions and the retention time of each pesticide was confirmed by the corresponding chromatograms of pesticide standards monitored by both MS and UV-Vis detector. Since EIC allows the mass spectrometer to be highly selective for a particular m/z , the pesticides that have different m/z can be identified without baseline resolution. Yet some analytes which are isomers of one another, such as dicamba and 2,4-D (m/z 543.3) or cloprop and MCPA (m/z 523.4), have the same m/z and therefore require adequate chromatographic resolution. With the optimized mobile phase condition, baseline separation ($R_s > 1.5$) was obtained for dicamba ($R_t = 10.10$ min) and 2,4-D ($R_t = 12.54$ min), and for cloprop ($R_t = 11.91$ min) and MCPA ($R_t = 12.74$ min), demonstrating an unambiguous identification of pesticide isomers by the this method. Multiple peaks were observed in some of the extracted ion chromatogram due to the overlapping of analyte isotope distributions. For example, the $C_5(\text{bpyr})_2$ dication complex of quinmerac was formed at m/z 544.37, which overlaps the isotopes of dicamba and 2,4-D, resulting in three peaks showing in the EIC at m/z 544.37.



Figure 2-4 Chromatographic Separation and Detection of Nineteen Acidic Pesticides by
Using HPLC-PIESI-MS.

2.3.10. Determination of the Concentrations of Pesticides in River and Pond Samples

The developed method was used to determine the pesticide concentrations in stream and pond water samples. Golf courses are sometimes heavily treated with pesticides therefore the water in the streams and one pond at two local golf courses were used as representative water samples for analysis. It should be noted that the samples were taken in February which was before the typical spring application of pesticides. The surface water usually contains humic materials, dissolved organic matter (DOM) and salt as the characteristic matrix components.^{90,91} Some of these components in the sample matrix are polar and ionisable and may affect the response of ESI-MS causing either signal suppression or enhancement. For this reason, the SPE and HPLC has been used remove the disturbing components in the matrix prior to ESI process with the purpose of eliminating the matrix effect, and the internal standard calibration was used for correction of the loss or gain of the ESI-MS signal caused by sample matrix. The SPE recovery study, as a way of evaluating the matrix effect, showed that the average recovery is similar for the DI water matrix as for the river water matrix indicating the matrix effect was minimized for the water samples used in this study. An example of HPLC-PIESI-MS detection of mecoprop in the stream water sample is shown in Figure 2-5. All samples were extracted and analyzed in triplicate and the quantitation results are shown in Table 2-7. Among the four pesticides monitored in this study, 2,4-D, mecoprop and cloprop were detected in all three stream/pond water samples while dicamba was found only in one location. The 2,4-D was found to have the highest concentrations in these sampling areas with a range from 71 ng L⁻¹ to 240 ng L⁻¹, which is approximately 3 to 6 times higher than the rest of pesticides analyzed. The pesticide concentrations in Village Creek was shown to be essentially lower than that in the pond (~2 to 3 fold), despite the fact that both water samples were taken from the same course.

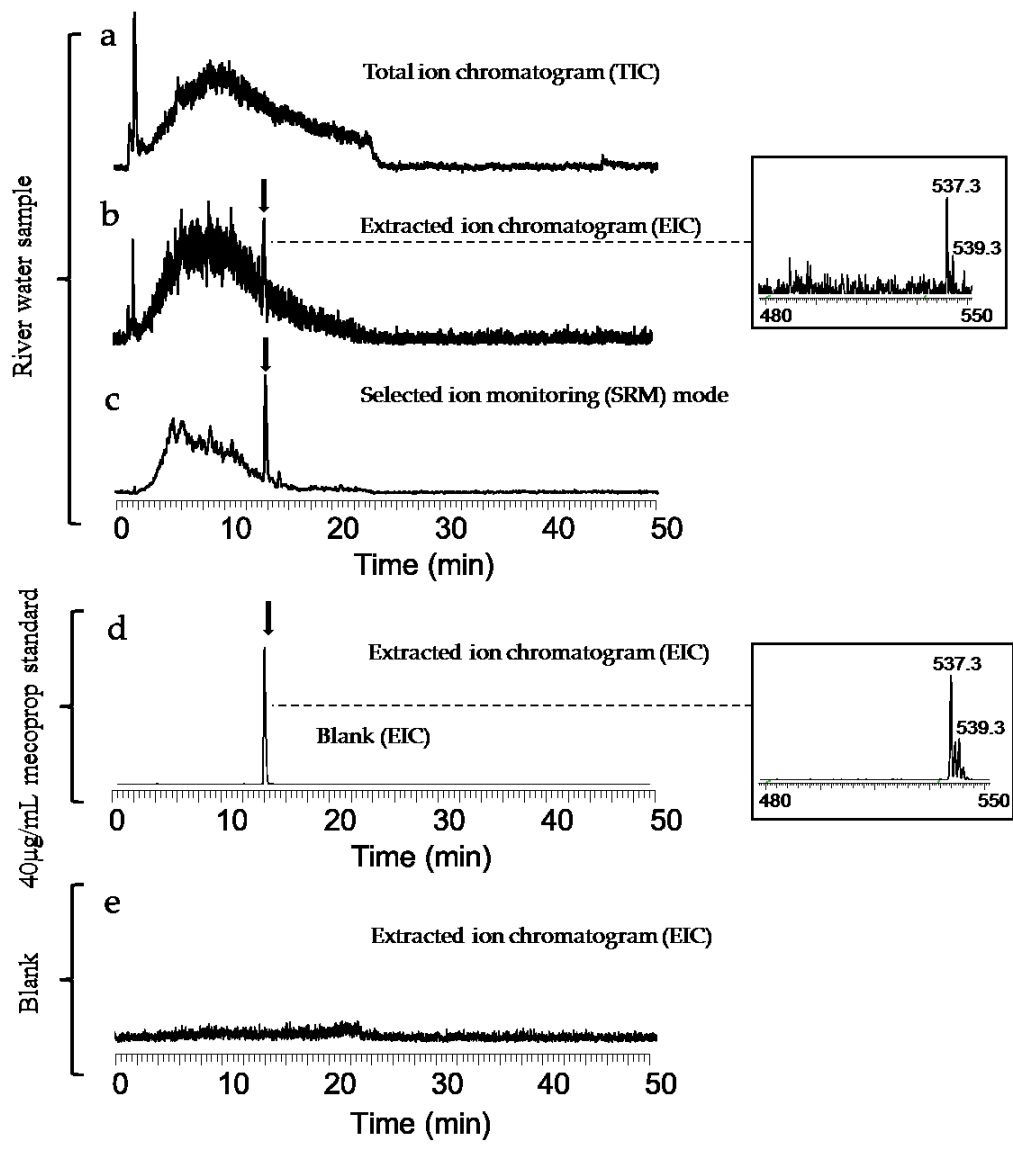


Figure 2-5 HPLC-PIESI-MS Detection of Mecoprop in the Stream Water Sample (a), (b) and (c), and Mecoprop Standard (d) and Blank (e).

Table 2-7 Pesticides Concentrations Determined in Stream and Pond Water Samples.

Pesticide name	Pesticide concentration, ng L ⁻¹ (mean ± standard deviation, n = 3)		
	Rush Creek ^a	Village Creek ^b	Pond ^b
24D	180 ± 10	71 ± 2	240 ± 40
Dicamba	35 ± 6	— ^c	— ^c
mecoprop	58 ± 5	17 ± 1	45 ± 9
Cloprop	54 ± 3	18 ± 3	37 ± 1

^a Sample was taken from Shady Valley golf club.

^b Sample was taken from Lake Arlington golf course.

^c Pesticide concentration in the sample is below 1.5 ng L⁻¹ (LOD of dicamba) and was not determined. All the other pesticides were not detected in the stream/pond samples obtained in these three locations.

This could be because the storage water (pond) has a slower rate of fluid turnover compared to the flowing water (stream) where the pollutants are more diluted. Although the overall pesticide levels are highly seasonal, since meteorological events and agricultural activities significantly affect the pesticide amount in water ⁷⁵, it was shown that the concentration for all acidic pesticides monitored were lower than 300 ng L⁻¹ in this study indicating relatively low pesticide concentrations at these locations and at the selected sampling time.

2.4. Conclusions

The method developed based on paired ion electrospray (PIESI) mass spectrometry was shown to be highly sensitive and efficient for the determination of acidic pesticides at ultratrace levels. The LODs for nineteen acidic pesticides were evaluated with four different types of dicationic ion-pairing reagents in both SIM and SRM modes of PIESI mass spectrometry. This study illustrates that the nature of both the IPR and the anionic analyte plays an important role on the observed detection limits. The best LODs with the optimal IPR were ranged from 0.6 pg to 19 pg, which was shown to be one to three orders of magnitude more sensitive (in terms of absolute LODs) than other reported methodologies performed in the negative ion mode. The SRM transition pathways of dication/analyte binary complex during the CID process have been investigated. The SPE recovery studies were carried out with the use of DI water and a river water matrix spiked with both high level (2000 ng L⁻¹) and low level (20 ng L⁻¹) pesticide concentrations, showing good recoveries in the range of 81 % to 112 %. This method is readily compatible with liquid chromatography, and by using the developed HPLC-PIESI-MS/MS method, nineteen selected pesticides can be simultaneously separated within 20 mins under the optimized condition. Low parts per trillion levels of pesticides in river/pond water samples were easily determined via the present method. This technique should be broadly applicable to other groups of acidic pesticides, such as imidazolinone pesticides, and could also allow for a broader investigation of previously undetectable acidic pesticides in surface waters or groundwaters.

Chapter 3

Metal Cation Detection in the Positive Ion Mode ESI-MS Using a Tetracationic Salt as Gas-Phase Ion-Pairing Agent: Evaluation of the Effect of Chelating Agents on Detection sensitivity

Abstract

The detection of metal cations continues to be essential in many scientific and industrial areas of interest. The most common ESI-MS approach involves chelating the metal ions and detecting the organometallic complex in the negative ion mode. However, it is well known the negative ion mode ESI-MS is generally less sensitive than the positive ion mode. To achieve for greater sensitivity, it is necessary to examine the feasibility of detecting the chelated detection metal cations in positive ion mode ESI-MS. Since the highly solvated native metal cations have relatively low ionization efficiency in ESI-MS, and can be difficult to detect in the positive ion mode, a tetracationic ion-pairing agent was added to form a complex with the negatively charged metal chelate. The use of the ion pairing agent leads to generate an overall positively charged complex, which can be detected at higher m/z in the positive ion mode by electrospray ionization linear quadrupole ion trap mass spectrometry. Thirteen chelating agents with diverse structures were evaluated in this study. The nature of the chelating agent played as important a role as was previously determined for cationic pairing agent. The detection limits of six metal cations reached sub-picogram levels and significant improvements were observed when compared to negative ion mode detection where the metal-chelates were monitored without adding the ion-pairing reagent (IPR). Also, selective reaction monitoring (SRM) analyses were performed on the ternary complexes, which improved detection limits by one to three orders of magnitude. With this method the metal cations are able to be

analyzed in the positive ion mode ESI-MS with the advantage of speed, sensitivity and selectivity. The optimum solution pH for this type of analysis is 5-7. Tandem MS further increases the sensitivity. Speciation is straightforward making this a broadly useful approach for the analysis of metal ions.

3.1. Introduction

Metal cation detection is of great interest to environmental and biological sciences, and currently remains as one of the important tasks in analytical chemistry.⁹²⁻⁹⁴ The most commonly used technique for metal ion analysis is ion chromatography coupled with conductivity detection. This technique has been successfully employed to the separation and detection of metal cations, and has been applied as a multi-elemental technique in various analytical purposes.^{95,96} Another methodology widely used for metal cation detection is atomic absorption spectroscopy (AAS). As a highly selective method, AAS is suitable to analyze a wide range of elements, particularly metals in solution or in solid samples.⁹⁷ Nevertheless, these techniques for metal cation detection sometimes suffer from inadequate sensitivity, especially when analyzing trace amounts in environmental and biological samples and/or where severe matrix effects are present.^{50,92,98} Inductively coupled plasma mass spectrometry (ICP-MS) is an ideal technique for metal cation detection because it allows for multi-elemental analyses with high sensitivity and provides reasonable precision and accuracy, as well as a large linear dynamic range.⁹⁹⁻¹⁰⁴ Though ICP-MS has proven to be a powerful and durable method for metal cation detection, the development of new methodologies are continuously evaluated due to their potential merit regarding general scientific interest or practical uses. Recently, there has been interest in using electrospray ionization mass spectrometry (ESI-MS) for metal cation detection because ESI-MS has several unique

advantages. First, the sensitivity of ESI-MS, along with its speed and low sample consumption, makes it a powerful tool for detecting cations.^{105,106} Secondly, compared to ICP-MS in which the ions are produced in the high temperature plasma, the ionization of ESI-MS is performed in room temperature, which enables it to directly provide the molecular weight and speciation information of the metal cations.^{17,50,107} Recently several reports indicated that ESI-MS is a viable approach for metal cation detection when the cations have been bound to ligands or complexed with an appropriate chelating agent.^{49,50,108-110} Mollah et al. reported a method to identify metal cations and metal complexes in negative ion mode ESI-MS by adding hydrochloric or nitric acid to the aqueous metal solutions.⁴⁹ Hotta et al. determined trace metals in natural samples in ESI-MS negative ion mode by using EDTA and other structurally similar chelating agents.⁵⁰

Although using chelating reagents as additives in ESI-MS provides a rapid and simple way to analyze metal cations, the sensitivity obtained in the negative ion mode ESI-MS is not always adequate. Corona discharge is more prevalent in the negative ion mode, which results in an unstable Taylor cone and higher background noise leading to poorer limits of detection (LOD).^{17,29} Furthermore, arcing is more likely to occur due to corona discharge, and can lead to a loss in ESI current.^{78,79} Thus it can be anticipated that LODs can be improved if detection was performed in the positive ion mode ESI-MS. However, native metal cations can be difficult to detect in the positive ion mode ESI-MS. The large solvation energy of native metal cations considerably reduces the ionization efficiency in ESI-MS.^{111,112} Also, the mass-to-charge ratio (m/z) of some multiply charged metal cations may fall below the low mass cut-off (LMCO) of ion trap mass analyzers or cause it to reside in a low mass region where there is inherently more chemical noise.

Recently, we developed a new electrospray ionization mass spectrometry approach for sensitive detection of singly, doubly and triply charged anions in positive

mode ESI-MS.^{17,18,29,77,80,81,113,114} This method involves the addition of low concentrations of dicationic, tricationic or tetracationic ion-pairing reagents. The ion-pairing reagents associate with anions in solution, forming an overall positively charged complex, which can be detected in the positive ion mode ESI-MS with much lower detection limits (often several orders of magnitude). In this study, we use an ion-pairing reagent (IPR) to complex with negative charged metal chelates. This higher mass complex can then be detected in the positive ion mode ESI-MS. In a previous report, the efficacy of a broad range of pairing agents was studied.⁸² However, the role and effect of different chelating agents was not considered. Since the nature of the chelating agent could have a significant effect on detection sensitivity, the current study was undertaken. Thirteen chelating reagents were evaluated for the detection of six metal cations when associated with a tetracationic ion-pairing reagent. The effect of sample solution pH on detection sensitivity was examined in this study. Several advantages of this method may include: (a) detection is performed in the more sensitive positive ion mode; (b) the metal cations are brought to a higher mass range, and out of the low mass range which is dominated by background noise; (c) complexing the native metal cation with chelating agents and an ion-pairing reagent lowers its solvation energy, which facilitates the generation of gas phase ions and leads to sensitivity enhancements; (d) the ternary complex is expected to have greater surface activity than the metal or metal chelate, resulting in improved ionization efficiency and further improved sensitivity;^{21,84-86,115} and (e) this method is capable of simultaneous multi-element measurements.

3.2. Experimental

3.2.1. Materials

Solvents used for the analysis and sample preparation were of HPLC-grade and were purchased from Honeywell Burdick and Jackson (Morristown, NJ). Tin chloride, ruthenium chloride, calcium chloride, lead chloride, cadmium chloride and chromium chloride were obtained from Sigma-Aldrich (St. Louis, MO). All chelating agents were obtained as the sodium/ammonium salt or as free acid from Sigma-Aldrich (St. Louis, MO). The names and structures of the thirteen metal chelating agents used in this study are listed in Table 3-1. They include EDTA and its analogs (I, II, III, IV, V, VI, VII, VIII), azo compounds (X, XI, XII), and others (IX, XIII).

Table 3-1 Structures and Numbering of the Metal Chelating Agents Used in this Study.

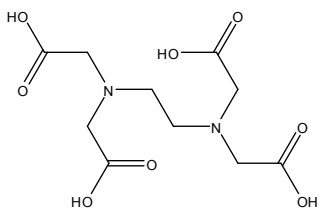
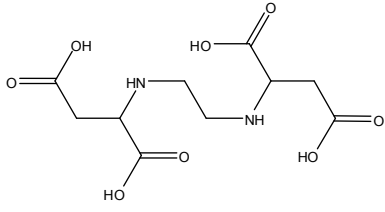
Number	Name	Structure
I	Ethylenediamine- N,N,N',N'-tetraacetic acid (EDTA)	
II	Ethylenediamine-N,N'- disuccinic acid (EDDsA)	

Table 3-1—Continued

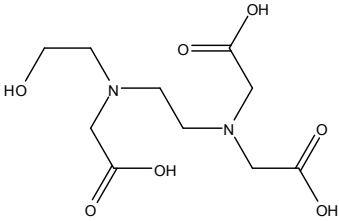
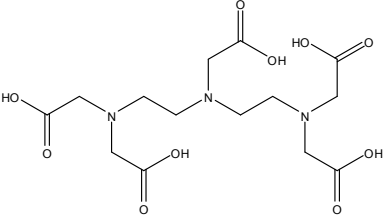
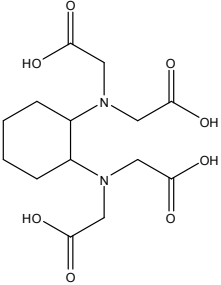
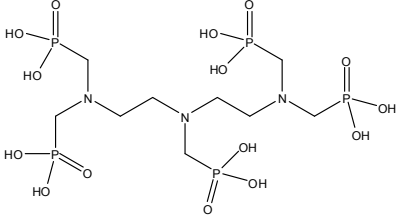
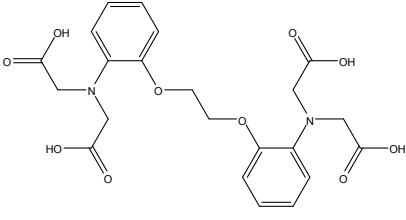
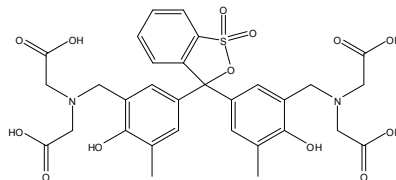
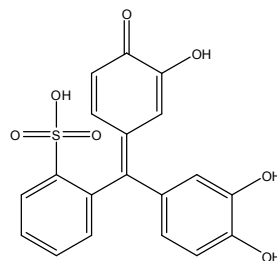
III	<p style="text-align: center;">N-(2- hydroxyethyl)ethylenediamin e-N,N,N'-triacetic acid (HEDTA)</p>	
IV	<p style="text-align: center;">Diethylenetriaminepenta acetic acid (DTPA)</p>	
V	<p style="text-align: center;">1,2- Diaminocyclohexanetetraacet ic acid (CyDTA)</p>	
VI	<p style="text-align: center;">Diethylenetriaminepenta methylenephosphonic acid (DTPMPA)</p>	
VII	<p style="text-align: center;">1,2-Bis(2- aminophenoxy)ethane- N,N,N',N'-tetraacetic acid (BETA)</p>	

Table 3-1—Continued

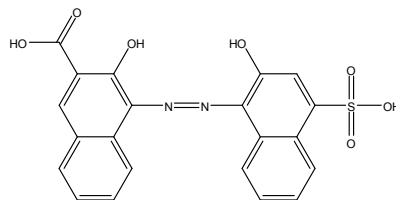
VII
I 3,3'-Bis[N,N-
bis(carboxymethyl)aminomet
hyl]-o-cresolsulfonephthalein
(Xylenol Orange)



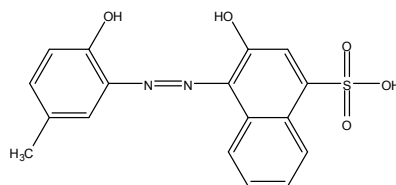
IX
3,3',4'-
Trihydroxyfuchson-2''-
sulfonic acid (Pyrocatechol
Violet)



X
Hydroxy-1-(2-hydroxy-
4-sulfo-1-naphthylazo)-3-
naphthoic acid
(Calconcarboxylic acid)



XI
1-(1-Hydroxy-4-methyl-
2-phenylazo)-2-naphthol-4-
sulfonic acid (Calmagite)



XII
1-(1-Hydroxy-2-
naphthylazo)-6-nitro-2-
naphthol-4-sulfonic acid
(Eriochrome black T)

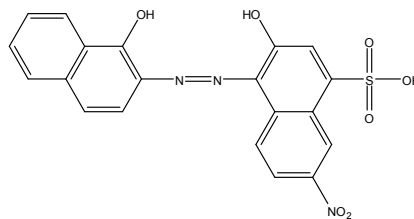
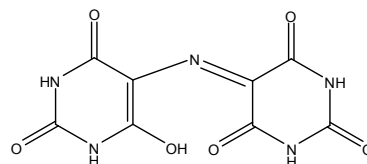


Table 3-1—Continued

XII
I 5,5'-Nitrilodibarbituric acid (Murexide)



The initial metal standard solutions were prepared daily by mixing a given amount of metal solution and chelating reagent solution, which lead to a final concentration of 10 μM of metal cation and 1mM of chelating reagent, in which the molar ratio of metal cation and chelating agent is 1 to 100. This large excess of chelating agent ensures complete complex formation and would allow for multiple metals to be present in the sample without competitive binding disrupting certain species association equilibria. This solution was then diluted sequentially to obtain desired concentrations for each metal species. The tetracationic ion-pairing reagent 1,1,1,6,6,11,11,16,16,16-decaphenyl-1,6,11,16-tetraphosphoniahexadecane (**Tet**) was synthesized in its bromide form as reported in previous studies^{17,18,29,77,80,114} and was subsequently ion exchanged to its fluoride form. Figure 3-1 gives the structure and abbreviation of the tetracationic ion-pairing reagent used in this study.

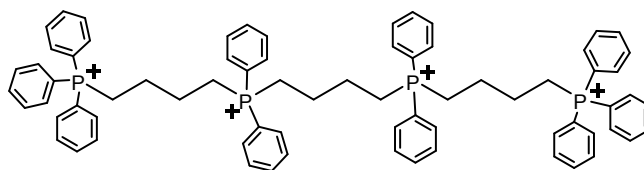


Figure 3-1 Structure of Tetracationic Ion-Pairing Reagent 1,1,1,6,6,11,11,16,16,16-decaphenyl-1,6,11,16-tetraphosphoniahexadecane (**Tet**) Used in this Study

3.2.2. ESI-MS Analysis

A Thermo LXQ linear ion trap mass spectrometer (Thermo Fisher Scientific, San Jose, CA) was used for all reported analyses. The ESI-MS was operated under the following source-dependent parameters: spray voltage, 3kV; capillary voltage, 11V; desolvation temperature, 350°C; sheath gas flow, 37 arbitrary units (AU); and the auxiliary gas flow, 6 AU. For the selective reaction monitoring (SRM) experiments, the collision induced dissociation (CID) was carried out with a normalized collision energy of 30, a Q value of 0.25 and an activation time of 30 ms. A Surveyor MS pump (Thermo Fisher Scientific, San Jose, CA) with a vacuum degasser provided a 300 $\mu\text{L}/\text{min}$ (67% MeOH/33% H_2O) carrier flow. A Shimadzu LC-6A pump (Shimadzu, Columbia, MD) was used to introduce the 40 μM of ion-pairing reagent solution into the LC flow from a Y-type mixing tee at rate of 100 $\mu\text{L}/\text{min}$. This set-up results in a total flow rate of 400 $\mu\text{L}/\text{min}$ and an overall solvent composition of 50% MeOH/50% H_2O with 10 μM ion-pairing reagent. The sample solutions were injected using a six-port injection valve located between the Y-type mixing tee and the Surveyor MS pump. The sample solution was mixed with the ion-pairing reagent solution in the Y-type mixing tee, where the positively charged complexes formed, and were carried into the ESI-MS. The instrumental setup is shown in Figure 1-2. A 5 μL injection loop was used for the direct injection which is expected to give the largest source for possible experimental error ($\pm 5\%$). Detection limits were determined when 5 replicate injections at a given concentration resulted in a signal-to-noise ratio of 3, which was calculated based on Genesis Peak Detection Algorithm. Data analysis was performed in the Xcalibur 2.0 software.

3.2.3. Determination of Trace Lead (II) in CRM 3128e

The method developed herein has been validated by analyzing a certified reference material (CRM). The certified reference material (lead standard (CRM 3128e)) was obtained from National Institute of Standards and Technology (USA). CRM 3128e originally contains 48.24 mM lead (II) and 1.6 M HNO₃. In order to make the concentration of measured sample fall into the linear range of the calibration curve, a 10000 times dilution was made to the standard. Consequently, a sample with 482.4 nM lead (II) and 0.016 mM HNO₃ was obtained. The diluted sample was immediately mixed with the appropriate amount of EDTA and was adjusted to pH 6 for subsequent analysis. The same configuration used in ESI-MS analysis was used for determination of lead (II) in the CRM. To make the calibration curve, a series of lead (II)-EDTA solutions were prepared by mixing the lead nitrate stock solution with the appropriate amount of EDTA stock solution. Aliquots of 325, 750, 1500 and 3000 nM were injected into the LC-ESI-MS system in triplicate and detected in selected ion monitoring (SIM) mode at m/z 779.3. The calibration curve was produced by plotting the peak area of signal from injected sample versus the amount of metal added.

3.3. Results and Discussion

3.3.1. Metal Chelating Reagents and Ion-Pairing Reagents

There is a wide variety of metal ion chelating agents (Table 3-1), each of which has distinct properties, advantages and disadvantages. Chelating agents I, II, III, IV, VI and VII have flexible structures, while other chelating agents contain aromatic rings, such as V, VIII, IX, X, XI, XII and XIII, and have relatively rigid structures. The structure of the tetracationic ion-pairing reagent (**Tet**) is shown in Figure 3-1. **Tet** is a phosphonium based tetracationic salt with three C4 alkyl linkage chains, two diphenylphosphonium groups

and two triphenylphosphonium moieties. Previous studies have shown that **Tet** is an outstanding ion-pairing reagent which resulted in very low LODs for a variety of anionic analytes. Compared to other dicationic and tricationic ion-pairing reagents, this tetracation has a flexible structure which enables it to bend around and tightly associate with anions.^{18,29,81}



Figure 3-2 Mass spectrum of the Tetracationic Ion-Pairing Reagent (**Tet**) Obtained in Full Scan Mode Under Experimental Condition.

3.3.2. LODs of Metal Cations Obtained in the Positive SIM Mode by Using Different Chelating Reagents

Table 3-2 lists the LODs for six metal cations, when individually complexed with each of the chelating agents and **Tet**, and subsequently detected in the positive single ion monitoring mode. It should be noted that many of the metal/chelating reagent/IPR ternary complexes do not exist in only one charge state, which may be due to the fact that these ternary complexes can either lose or adduct protons in the gas phase.^{29,50} Therefore, all the possible m/z of the complexes were calculated and the LODs were obtained by

monitoring the m/z which gave the highest signal. Figure 3-2 shows the mass spectrum of **Tet** obtained in full scan, which shows the in-source deprotonation of the tetracationic ion-pairing reagent. In terms of overall sensitivity, picogram (pg) level LODs for each of these six metals can be obtained in the SIM mode using many of the chelating agents. Meanwhile, a wide range (from ng to pg) of LODs can be observed for each metal, indicating that different chelating agents have varying efficacies for each metal. For example, the LOD for Pb^{2+} using XIII is 2.5 ng, while the LOD using VII is 2.6 pg, representing a 1000 fold improvement. It was found that EDTA analogs generally gave lower LODs than other types of chelating agents. The best LODs for five out of six metals (Ru^{3+} , Ca^{2+} , Pb^{2+} , Cd^{2+} and Cr^{3+}) were achieved by EDTA analogs (II, I, VII, VI, V respectively). However, this was not the case for Sn^{2+} . It is very interesting that the lowest LOD for Sn^{2+} was obtained by using XI, which is an azo compound with a relatively rigid structure. Based on our previous studies, the use of rigid ion-pairing agents usually produces poor LODs.^[23, 30] If this trend also held true for chelating agents, the rigid structure of XI should have a negative effect on its detection sensitivity. However, this is clearly not the case for the Sn^{2+} chelate. It is likely that XI has the ability to undergo π - π interactions with the tetracationic ion-pairing reagent, which may contribute to this low LOD.^[23] Understandably, chelating agent XIII, which has neither structural flexibility nor additional π - π interactions resulted in poor LODs for most metals (Ru^{3+} , Ca^{2+} , Pb^{2+} , Cd^{2+} and Cr^{3+}). Although EDTA analogs generally provide better LODs, they do not seem to be greatly superior to other kinds of chelating agents. Azo compounds (X, XI, XII), IX and XIII also yielded low LODs in certain cases and proved to be complementary to the EDTA analogue complexes.

Table 3-2 Limits of Detection of Metal Cations Using Ion-Pairing Reagent and Metal

Chelating Agents by Single Ion Monitoring in Positive Ion Mode ESI-MS^a

¹²⁰ Sn ²⁺			¹⁰² Ru ³⁺			⁴⁰ Ca ²⁺		
Chelating agent	LOD (ng)	Base peak	Chelating agent	LOD (ng)	Base peak	Chelating agent	LOD (ng)	Base peak
XI	3.60 × 10⁻³	768.3 (+2)	II	6.12 × 10⁻³	726.3 (+2)	I	4.00 × 10⁻⁴	695.3 (+2)
I	1.50 × 10⁻²	735.3 (+2)	I	7.65 × 10⁻³	1451.5 (+1)	V	1.40 × 10⁻³	722.3 (+2)
XIII	1.80 × 10 ⁻²	722.7 (+2)	VIII	1.53 × 10 ⁻²	1831.6 (+1)	XI	1.50 × 10 ⁻³	728.3 (+2)
IV	2.52 × 10 ⁻²	785.8 (+2)	V	2.30 × 10 ⁻²	753.3 (+2)	IV	2.00 × 10 ⁻³	1490.6 (+1)
III	2.70 × 10 ⁻²	728.3 (+2)	IV	5.10 × 10 ⁻²	518.2 (+3)	IX	2.00 × 10 ⁻³	742.2 (+2)
VII	3.00 × 10 ⁻²	827.3 (+2)	X	6.12 × 10 ⁻²	799.2 (+2)	VIII	4.00 × 10 ⁻³	885.3 (+2)
XII	3.00 × 10 ⁻²	808.7 (+2)	VII	7.65 × 10 ⁻²	1635.6 (+1)	II	6.00 × 10 ⁻³	463.9 (+3)
X	4.50 × 10 ⁻²	1615.5 (+1)	XII	1.28 × 10 ⁻¹	799.7 (+2)	III	6.60 × 10 ⁻³	459.2 (+3)
IX	6.00 × 10 ⁻²	782.2 (+2)	VI	2.10 × 10 ⁻¹	866.7 (+2)	XIII	8.00 × 10 ⁻³	1364.5 (+1)
V	6.60 × 10 ⁻²	1523.6 (+1)	IX	2.55 × 10 ⁻¹	387.1 (+4)	VII	1.00 × 10 ⁻²	525.2 (+3)
II	7.20 × 10 ⁻²	735.3 (+2)	III	3.83 × 10 ⁻¹	719.3 (+2)	VI	2.00 × 10 ⁻²	418.4 (+4)
VIII	1.20 × 10 ⁻¹	925.3 (+2)	XIII	5.10 × 10 ⁻¹	713.7 (+2)	X	8.00 × 10 ⁻²	768.2 (+2)
VI	1.50 × 10 ⁻¹	350.9 (+5)	XI	5.87 × 10 ⁻¹	1517.5 (+1)	XII	2.00 × 10 ⁻¹	512.8 (+3)
²⁰⁸ Pb ²⁺			¹¹⁴ Cd ²⁺			⁵² Cr ³⁺		
Chelating agent	LOD (ng)	Base peak	Chelating agent	LOD (ng)	Base peak	Chelating agent	LOD (ng)	Base peak
VII	2.60 × 10⁻³	871.3 (+2)	VI	1.43 × 10⁻³	872.7 (+2)	V	1.82 × 10⁻³	485.5 (+3)
VIII	3.64 × 10⁻³	969.3 (+2)	VII	5.70 × 10⁻³	824.3 (+2)	VIII	2.08 × 10⁻³	890.8 (+2)
IV	8.84 × 10 ⁻³	829.8 (+2)	XII	6.84 × 10 ⁻³	805.7 (+2)	IV	4.16 × 10 ⁻³	751.3 (+2)
II	1.04 × 10 ⁻²	1557.5 (+1)	IV	7.13 × 10 ⁻³	1564.6 (+1)	II	2.60 × 10 ⁻²	467.5 (+3)
V	1.87 × 10 ⁻²	806.3 (+2)	XI	1.71 × 10 ⁻²	765.3 (+2)	VII	3.25 × 10 ⁻²	528.9 (+3)
III	6.76 × 10 ⁻²	772.3 (+2)	X	2.39 × 10 ⁻²	805.2 (+2)	VI	5.20 × 10 ⁻²	841.2 (+2)
VI	7.59 × 10 ⁻²	613.5 (+3)	IX	5.70 × 10 ⁻²	779.2 (+2)	XI	1.43 × 10 ⁻¹	367.4 (+4)
XI	8.32 × 10 ⁻²	1623.5 (+1)	III	6.27 × 10 ⁻²	725.3 (+2)	III	1.56 × 10 ⁻¹	347.4 (+4)
X	1.04 × 10 ⁻¹	852.2 (+2)	VIII	6.56 × 10 ⁻²	615.2 (+3)	I	2.60 × 10 ⁻¹	467.5 (+3)
IX	1.04 × 10 ⁻¹	826.2 (+2)	V	1.05 × 10 ⁻¹	506.5 (+3)	X	6.50 × 10 ⁻¹	310.1 (+5)
XII	1.30 × 10 ⁻¹	568.8 (+3)	II	1.14 × 10 ⁻¹	1463.5 (+1)	XII	7.80 × 10 ⁻¹	310.3 (+5)
I	3.22 × 10 ⁻¹	779.3 (+2)	XIII	1.82 × 10 ⁻¹	719.7 (+2)	XIII	1.04 × 10 ⁰	459.2 (+3)
XIII	2.50 × 10 ⁰	766.7 (+2)	I	2.02 × 10 ⁻¹	732.3 (+2)	IX	1.51 × 10 ⁰	299.7 (+5)

^aThe bold entries highlight the two lowest limits of detection for each metal.

3.3.3. LODs of Metal Cations Obtained in the Positive SRM Mode by Using Different Chelating Reagents

Another aspect of this study was to show that SRM can be carried out on metal/chelating reagent/IPR ternary complexes. Table 3-3 lists the LODs for the six metal cations in the positive SRM mode. The SRM m/z column in Table 3-3 shows the most abundant fragment of the complex which was monitored in SRM mode. The mass-to-charge ratios of precursor ion and daughter ion for each monitored SRM transition are listed in Table 3-4. Using SRM improves specificity in analysis and reduces the noise in the region being analyzed, thus the LODs can be further improved.¹¹⁶ The best LODs for Sn^{2+} , Ru^{3+} , Ca^{2+} , Pb^{2+} , Cd^{2+} and Cr^{3+} achieved by SRM were 840 fg, 765 fg, 50 fg, 94 fg, 340 fg and 910 fg respectively. It was found that most LODs in the SRM mode were approximately one order of magnitude lower than those found with SIM. However, it should be noted that not all LODs were improved by SRM. For certain metals, the SRM transition could not be monitored when complexed with some chelating agents, or the LODs were similar to these found in the SIM mode. Although the reason for the differences in LOD improvement during SRM transition seems to be complicated, it is clear that choosing the right chelating agent is important for obtaining better detection limits for each metal in both SIM and SRM modes.

Table 3-3 Limits of Detection of Metal Cations Using Ion-Paring Reagent and Metal Chelating Agents by Selected Reaction Ion Monitoring in the Positive Ion Mode ESI-MS

$^{120}\text{Sn}^{2+}$			$^{102}\text{Ru}^{3+}$			$^{40}\text{Ca}^{2+}$		
Chelating agent	LOD (ng)	SRM m/z	Chelating agent	LOD (ng)	SRM m/z	Chelating agent	LOD (ng)	SRM m/z
XI	8.40×10^{-4}	518.3	II	7.65×10^{-4}	696.3	IX	5.00×10^{-5}	723.8
V	2.40×10^{-3}	1446.6	I	1.20×10^{-3}	1414.3	I	6.00×10^{-5}	564.3
IV	3.60×10^{-3}	756.8	V	3.06×10^{-3}	723.4	II	1.50×10^{-4}	354.3
I	4.50×10^{-3}	724.8	VIII	5.10×10^{-3}	1781.2	IV	4.00×10^{-4}	1490.6
XIII	6.00×10^{-3}	581.4	IX	7.65×10^{-3}	277.0	V	6.00×10^{-4}	591.8
XII	9.00×10^{-3}	503.3	III	1.02×10^{-2}	688.8	XI	1.00×10^{-3}	709.8
II	1.16×10^{-2}	603.7	XIII	2.55×10^{-2}	579.3	VIII	1.60×10^{-3}	863.4
X	1.20×10^{-2}	1519.9	VII	3.06×10^{-2}	1573.5	VII	2.00×10^{-3}	448.2
III	1.35×10^{-2}	503.3	IV	5.10×10^{-2}	530.3	III	2.00×10^{-3}	279.2
VIII	4.80×10^{-2}	858.3	XII	1.02×10^{-1}	761.3	X	3.00×10^{-3}	524.2
VII	6.00×10^{-2}	483.2	VI	1.06×10^{-1}	829.9	VI	6.00×10^{-3}	399.8
IX	3.60×10^{-1}	317.3	XI	2.04×10^{-1}	1157.1	XIII	7.00×10^{-3}	1327.3
VI	— ^a	— ^a	X	— ^a	— ^a	XII	2.00×10^{-1}	257.1
$^{208}\text{Pb}^{2+}$			$^{114}\text{Cd}^{2+}$			$^{52}\text{Cr}^{3+}$		
Chelating agent	LOD (ng)	SRM m/z	Chelating agent	LOD (ng)	SRM m/z	Chelating agent	LOD (ng)	SRM m/z
VII	9.36×10^{-5}	740.2	IV	3.40×10^{-4}	1301.5	V	9.10×10^{-4}	279.2
V	3.85×10^{-4}	503.3	VII	4.28×10^{-4}	692.8	VIII	1.18×10^{-3}	812.4
VIII	5.41×10^{-4}	800.3	VI	1.43×10^{-3}	530.8	VII	1.48×10^{-3}	279.7
IV	3.64×10^{-3}	807.9	XII	2.39×10^{-3}	782.8	IV	3.12×10^{-3}	740.4
III	4.16×10^{-3}	640.8	IX	3.14×10^{-3}	723.3	II	2.00×10^{-2}	354.9
II	5.72×10^{-3}	1485.4	VIII	3.42×10^{-3}	530.3	I	4.81×10^{-2}	453.0
IX	1.56×10^{-2}	632.8	I	5.70×10^{-3}	600.8	VI	5.20×10^{-2}	680.3
VI	6.76×10^{-2}	579.3	X	1.14×10^{-2}	771.3	III	6.24×10^{-2}	329.2
XI	8.32×10^{-2}	1446.3	III	2.00×10^{-2}	593.8	XI	1.30×10^{-1}	354.6
I	1.46×10^{-1}	503.3	V	2.63×10^{-2}	279.2	XIII	3.38×10^{-1}	381.2
XII	1.87×10^{-1}	549.3	II	7.13×10^{-2}	1363.5	X	— ^a	— ^a
X	2.60×10^{-1}	746.8	XI	1.14×10^{-1}	671.0	XII	— ^a	— ^a
XIII	3.17×10^{-1}	744.8	XIII	1.82×10^{-1}	663.8	IX	— ^a	— ^a

^aIndicate the SRM transition could not be monitored. The bold entries highlight the twolowest limits of detection for each metal.

Table 3-4 Mass-to-Charge Ratios of Precursor Ion and Product Ion for Each SRM

Transition					
$^{120}\text{Sn}^{2+}$			$^{102}\text{Ru}^{3+}$		
Chelating agent	Precursor ion (m/z)	Daughter ion (m/z)	Chelating agent	Precursor ion (m/z)	Daughter ion (m/z)
I	735.3	→ 724.8	I	1451.5	→ 1414.3
II	735.3	→ 603.7	II	726.3	→ 696.3
III	728.3	→ 503.3	III	719.3	→ 688.8
IV	785.8	→ 756.8	IV	518.2	→ 530.3
IX	782.2	→ 317.3	IX	387.1	→ 277.0
V	1523.6	→ 1446.6	V	753.3	→ 723.4
VI	—	—	VI	866.7	→ 829.9
VII	827.3	→ 483.2	VII	1635.6	→ 1573.5
VIII	925.3	→ 858.3	VIII	1831.6	→ 1781.2
X	1615.5	→ 1519.9	X	—	—
XI	768.3	→ 518.3	XI	1517.5	→ 1157.1
XII	808.7	→ 503.3	XII	799.7	→ 761.3
XIII	722.7	→ 581.4	XIII	713.7	→ 579.3
$^{40}\text{Ca}^{2+}$			$^{208}\text{Pb}^{2+}$		
Chelating agent	Precursor ion (m/z)	Daughter ion (m/z)	Chelating agent	Precursor ion (m/z)	Daughter ion (m/z)
I	695.3	→ 564.3	I	779.3	→ 503.3
II	463.9	→ 354.3	II	1557.5	→ 1485.4
III	459.2	→ 279.2	III	772.3	→ 640.8
IV	1490.6	→ 1490.6	IV	829.8	→ 807.9
IX	742.2	→ 723.8	IX	826.2	→ 632.8
V	722.3	→ 591.8	V	806.3	→ 503.3
VI	418.4	→ 399.8	VI	613.5	→ 579.3
VII	525.2	→ 448.2	VII	871.3	→ 740.3
VIII	885.3	→ 863.4	VIII	969.3	→ 800.3
X	768.2	→ 524.2	X	852.2	→ 746.8
XI	728.3	→ 709.8	XI	1623.5	→ 1446.3
XII	512.8	→ 257.1	XII	568.8	→ 549.3
XIII	1364.5	→ 1327.3	XIII	766.7	→ 744.8

Table 3-4—Continued

$^{114}\text{Cd}^{2+}$			$^{52}\text{Cr}^{3+}$		
Chelating agent	Precursor ion (m/z)	Daughter ion (m/z)	Chelating agent	Precursor ion (m/z)	Daughter ion (m/z)
I	732.3	→ 600.8	I	467.5	→ 453.0
II	1463.5	→ 1363.5	II	467.5	→ 354.9
III	725.3	→ 593.8	III	347.4	→ 329.2
IV	1564.6	→ 1301.5	IV	751.3	→ 740.4
IX	779.2	→ 723.3	IX	—	—
V	506.5	→ 279.2	V	485.5	→ 279.2
VI	872.7	→ 530.8	VI	841.2	→ 680.3
VII	824.3	→ 692.8	VII	528.9	→ 279.7
VIII	615.2	→ 530.3	VIII	890.8	→ 812.4
X	805.2	→ 771.3	X	—	—
XI	765.3	→ 671.0	XI	367.4	→ 354.6
XII	805.7	→ 782.8	XII	—	—
XIII	719.7	→ 663.8	XIII	459.2	→ 381.2

3.3.4. SRM Fragmentation Pathway

Figure 3-3 shows a proposed SRM transition pathway for the complex of Pb^{2+} , **Tet**, and chelating agent VII (1,2-bis(2-aminophenoxy)ethane-N,N',N'-tetraacetic acid, BETA). It was determined that this fragment pathway was common in these SRM analyses, but it is not the only transition. The parent complex $[\text{Pb}^{\text{II}}\text{-BETA-Tet}]^{2+}$ (m/z 871.3) was formed when the metal chelate $[\text{Pb}^{\text{II}}\text{-BETA}]^{2-}$ associates with Tet^{4+} , and was subsequently fragmented during CID, generating the secondary ion $[\text{Pb}^{\text{II}}\text{-HBETA-C}_{54}\text{H}_{58}\text{P}_3]$. The formation of the secondary ion at m/z 740.2 suggests the parent complex has undergone a loss of PPh_3 (m/z 262.1) and the charge state of the daughter ion further confirms this transition pathway. It was found that during this SRM transition the covalent bond at one of the terminal cationic moieties in **Tet** was broken while the complex, including the coordination bond between metal ion and chelating agent, remained intact. This pattern of gas phase dissociation is consistent with that of our previous observations.¹⁸

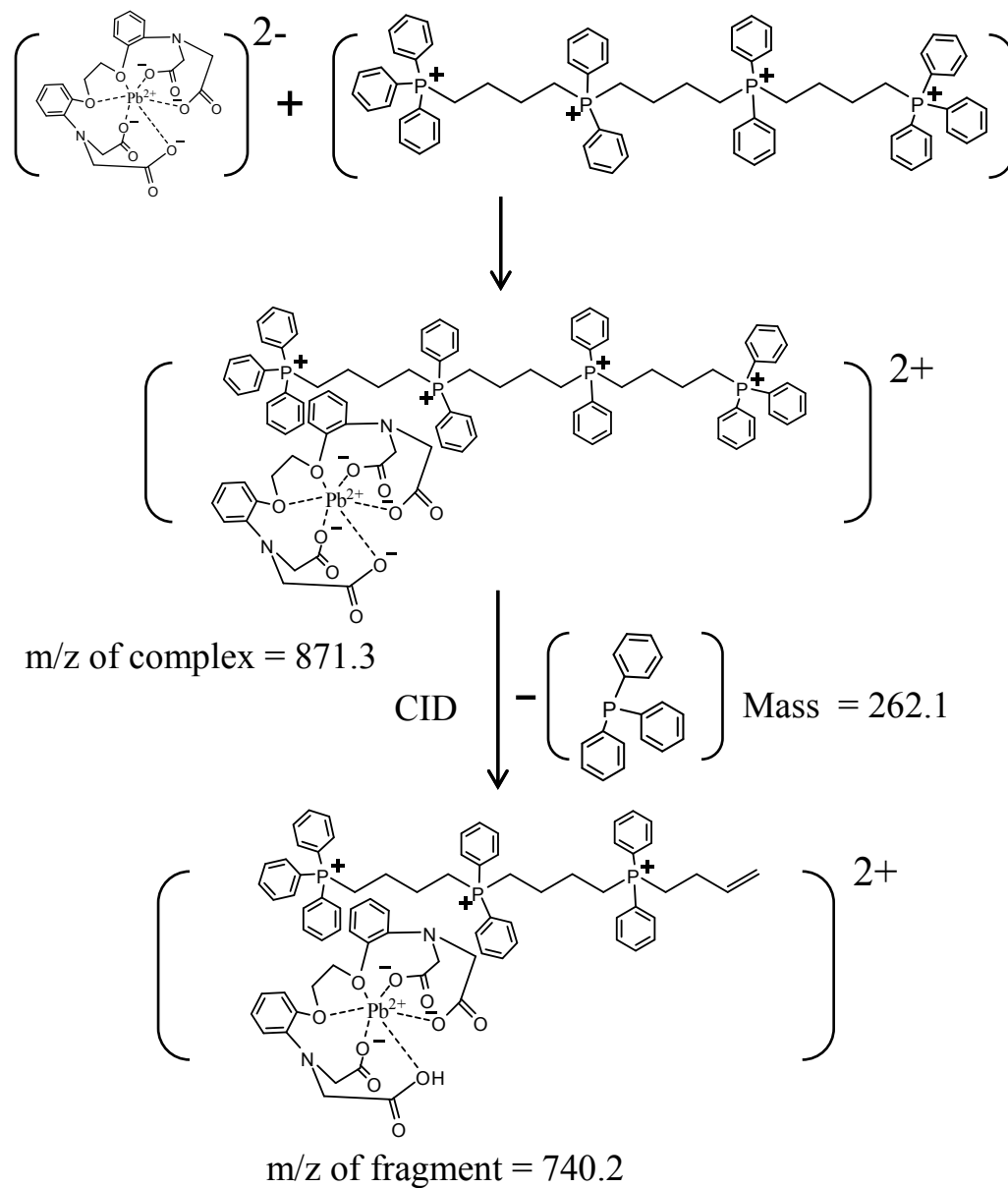


Figure 3-3 Proposed Fragmentation Pathway for the Metal Cation-Chelating Agent-Ion-Pairing Reagent Ternary Complex

3.3.5. A Comparison of the Best LODs Obtained in the Positive Ion Mode and in the Negative Ion Mode

Table 3-5 lists both the SIM and the SRM analysis in the negative ion mode, where the metal-chelates were monitored without adding ion-pairing reagent. The LODs determined in the SIM negative mode were on the ng to sub ng level. Furthermore, these LODs varied greatly for each metal when using different chelating agents. Generally speaking, Ca^{2+} was determined to be the most sensitive in the negative ion mode. It is interesting to find that an SRM transition could not be monitored for most metal-chelates in the negative ion mode. This is likely due to metal-chelate generated fragments falling below (or near) the low mass cut-off of the ion trap.

Compared to the LODs of metal cation chelates in the negative ion mode, improvements up to three orders of magnitude could be achieved by detecting them in the positive ion mode using both the ion-pairing agent together with the chelating agent. Table 3-6 compares the best results (in terms of LOD) for each metal in the positive ion mode versus the negative ion mode (when using the optimum chelating agent in each mode). Notably, using the ion-pairing reagent for detection in positive ion mode results in the most sensitive detection for all of these metal cation chelates by ESI-MS. For example, as shown in Table 3-6, the LOD for Pb^{2+} obtained in the positive SRM mode was more than 1100 times better than negative SIM mode.

Table 3-5 Limits of Detection of Metal Chelates in Negative Ion Mode ESI-MS.

Chelating agent	$^{120}\text{Sn}^{2+}$				$^{102}\text{Ru}^{3+}$			
	SIM LOD (ng)	Base peak	SRM LOD (ng)	SRM Mass	SIM LOD (ng)	Base peak	SRM LOD (ng)	SRM Mass
I	3.00×10^{-1}	409.1	—**	—	4.50×10^{-1}	391.1	—	—
II	1.50×10^0	204.0	—	—	—*	—	—	—
III	3.30×10^{-1}	395.1	—	—	1.53×10^0	377.1	—	—
IV	4.50×10^{-1}	254.6	—	—	9.18×10^{-2}	245.6	7.40×10^{-2}	140.8
V	1.20×10^0	231.1	—	—	1.28×10^0	445.1	5.10×10^{-1}	400.0
VI	1.50×10^{-1}	690.0	1.50×10^{-1}	680.8	1.53×10^{-1}	672.0	1.68×10^{-1}	652.8
VII	4.80×10^{-1}	296.1	—	—	5.10×10^{-1}	287.1	—	—
VIII	2.70×10^{-1}	394.1	—	—	3.06×10^{-1}	771.2	7.65×10^{-2}	748.0
IX	1.20×10^0	251.0	—	—	2.04×10^{-1}	485.0	2.04×10^{-1}	402.0
X	1.20×10^0	555.0	9.00×10^{-1}	511.1	1.28×10^0	537.0	—	—
XI	1.65×10^{-1}	475.0	—	—	—	—	—	—
XII	6.00×10^{-1}	556.0	—	—	—	—	—	—
XIII	6.00×10^{-1}	127.3	—	—	2.55×10^{-1}	182.5	—	—

Chelating agent	$^{40}\text{Ca}^{2+}$				$^{208}\text{Pb}^{2+}$			
	SIM LOD (ng)	Base peak	SRM LOD (ng)	SRM Mass	SIM LOD (ng)	Base peak	SRM LOD (ng)	SRM Mass
I	2.00×10^{-2}	329.1	—	—	5.20×10^{-1}	248.0	5.41×10^{-1}	203.8
II	—	—	—	—	1.04×10^{-1}	248.0	—	—
III	6.00×10^{-3}	315.1	6.00×10^{-3}	296.9	4.68×10^{-1}	483.1	4.68×10^{-1}	465.0
IV	9.40×10^{-2}	214.6	—	—	7.49×10^{-1}	298.6	—	—
V	5.00×10^{-3}	383.1	2.00×10^{-3}	364.9	4.16×10^{-1}	551.1	4.16×10^{-1}	532.8
VI	1.20×10^{-2}	304.5	—	—	4.68×10^{-1}	388.5	4.42×10^{-1}	371.0
VII	2.00×10^{-3}	513.1	2.00×10^{-3}	495.0	4.78×10^{-1}	340.1	—	—
VIII	1.00×10^{-1}	709.2	—	—	1.92×10^{-1}	291.7	—	—
IX	1.25×10^{-1}	423.0	—	—	6.76×10^{-1}	295.0	—	—
X	1.20×10^{-1}	475.0	8.60×10^{-2}	430.9	1.56×10^0	321.0	1.56×10^0	276.9
XI	1.04×10^{-1}	395.0	—	—	3.12×10^1	563.0	—	—
XII	2.00×10^{-1}	476.0	—	—	6.24×10^{-1}	644.0	2.60×10^{-1}	580.0
XIII	2.00×10^0	304.0	—	—	1.04×10^1	235.5	—	—

Table 3-5—Continued

Chelating agent	$^{114}\text{Cd}^{2+}$				$^{52}\text{Cr}^{3+}$			
	SIM LOD (ng)	Base peak	SRM LOD (ng)	SRM Mass	SIM LOD (ng)	Base peak	SRM LOD (ng)	SRM Mass
I	2.22×10^{-1}	201.0	—	—	5.72×10^{-1}	340.1	7.80×10^{-2}	295.9
II	4.96×10^{-2}	403.1	—	—	3.90×10^{-1}	340.1	—	—
III	3.42×10^{-1}	389.1	—	—	6.50×10^{-1}	326.1	6.50×10^{-1}	281.8
IV	7.07×10^{-1}	504.1	5.70×10^{-1}	485.8	2.34×10^{-1}	441.1	—	—
V	1.25×10^0	457.1	1.08×10^0	388.8	2.86×10^{-2}	394.1	1.95×10^{-2}	350.0
VI	2.00×10^{-1}	684.0	1.37×10^{-1}	665.9	6.24×10^{-2}	310.0	—	—
VII	3.71×10^{-1}	293.1	—	—	9.75×10^{-2}	524.1	4.68×10^{-2}	479.9
VIII	1.77×10^{-1}	391.1	—	—	1.82×10^{-1}	359.6	—	—
IX	2.57×10^{-1}	248.0	—	—	5.98×10^{-1}	216.5	—	—
X	1.43×10^{-1}	274.0	—	—	7.15×10^{-1}	486.0	4.42×10^{-1}	469.8
XI	1.14×10^0	469.0	—	—	—	—	—	—
XII	2.45×10^{-1}	550.0	4.90×10^{-2}	481.9	—	—	—	—
XIII	1.71×10^1	378.0	—	—	2.60×10^0	315.0	—	—

Table 3-6 Comparison of Detection Limits Obtained with the Optimum Chelating Agents for Each Metal Ion in Positive Ion Mode versus Negative Ion Mode ESI-MS.

Metal cation & chelating agent	Best LOD in negative ion mode (ng)	Metal cation & chelating agent	Best LOD in positive ion mode (ng)	Improvement
$^{120}\text{Sn}^{2+}$ + VI	1.50×10^{-1}	$^{120}\text{Sn}^{2+}$ + XI	8.40×10^{-4}	179
$^{102}\text{Ru}^{3+}$ + IV	7.40×10^{-2}	$^{102}\text{Ru}^{3+}$ + II	7.65×10^{-4}	97
$^{40}\text{Ca}^{2+}$ + VII	2.00×10^{-3}	$^{40}\text{Ca}^{2+}$ + IX	5.00×10^{-5}	40
$^{208}\text{Pb}^{2+}$ + II	1.04×10^{-1}	$^{208}\text{Pb}^{2+}$ + VII	9.36×10^{-5}	1111
$^{114}\text{Cd}^{2+}$ + XII	4.90×10^{-2}	$^{114}\text{Cd}^{2+}$ + IV	3.40×10^{-4}	144
$^{52}\text{Cr}^{3+}$ + V	1.95×10^{-2}	$^{52}\text{Cr}^{3+}$ + V	9.10×10^{-4}	21

Figure 3-4 illustrates the sensitivity enhancement that occurs when using the ion-pairing reagent for metal cation detection. A S/N = 3 was observed in the negative ion mode when 478 pg of Pb^{2+} was injected with BETA as the chelating agent (Figure 3-4a). When the same concentration of Pb^{2+} was detected through IPR/chelating agent complexation, S/N ratios of 142 and 1371 were obtained for the positive ion mode SIM and SRM respectively (Figure 3-4b, c). Thus, the positive ion mode SRM approach is approximately 450 times more sensitive.

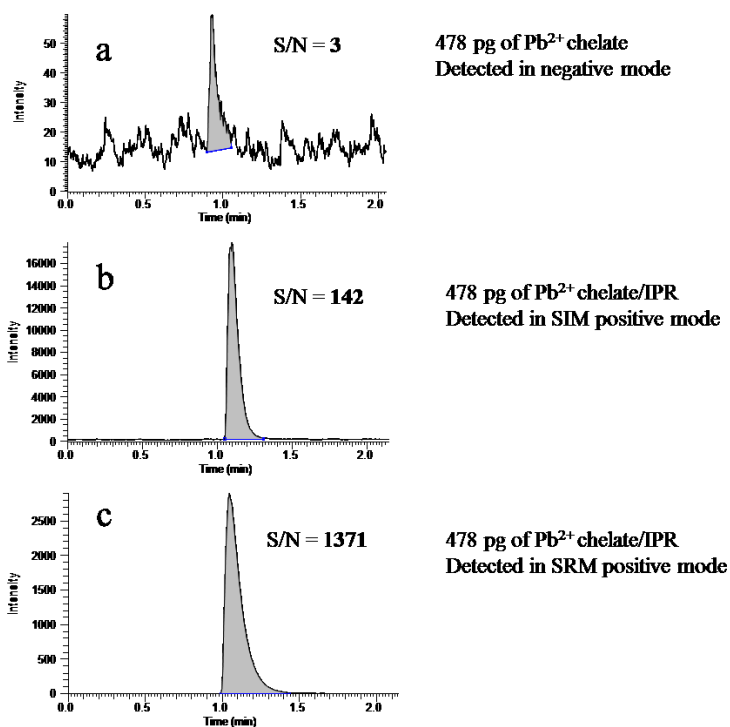


Figure 3-4 ESI-MS Signal-to-Noise Ratio Diagrams of Pb^{2+} Using BETA. (a) 478 pg of Pb^{2+} Injected, Analysis Performed in the Negative Ion Mode with BETA as Chelating Agent. (b) 478 pg of Pb^{2+} Injected, Analysis Performed in Positive Ion Mode (SIM) with BETA and IPR. (c) 478 pg of Pb^{2+} Injected, Analysis Performed in Positive Ion Mode (SRM) with BETA and IPR

3.3.6. Effect of Sample Solution pH on the Detection Sensitivity

It is anticipated that the limits of detection will be dependent on the solution pH.^{50,117,118} The sample solution pH will directly affect the formation and resultant relative concentrations of the metal chelate complexes. Therefore, a study of the influence of pH on the ESI-MS signal intensities was performed. The data generated in the pH study (Figure 3-5) illustrates that an optimum pH range to perform this analysis is between 5 and 7. All the four types of metal chelates tested showed very similar pH dependencies, however, the Cd-EDTA complex has maximum signal intensity at slightly more acidic conditions when compared with others. Also it was observed that the signal of the Sn-EDTA complex was lost at pH 4 while the other complexes could still be observed at pH values greater than 2.

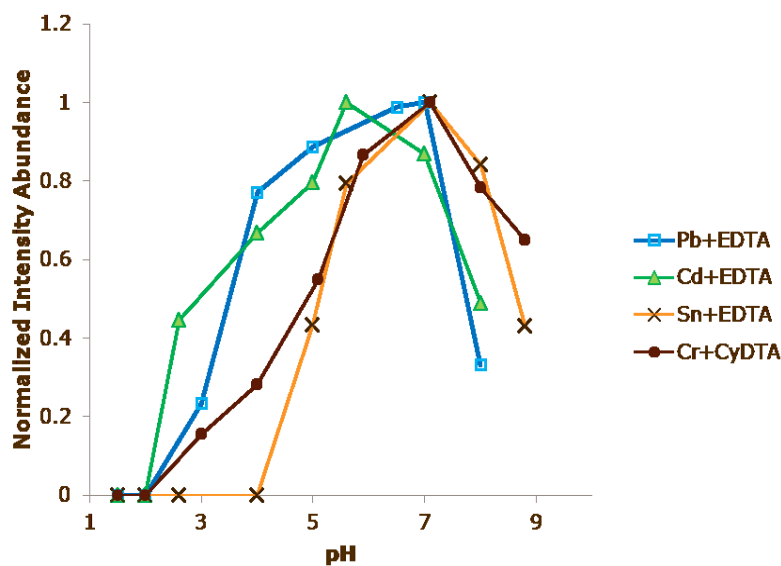


Figure 3-5 The pH Dependencies of the ESI-MS Signal Intensities of Metal Chelate Complexes

3.3.7. Quantitative Determination of Trace Lead (II) in CRM 3128e

Having demonstrated that using the combination of the IPR and chelating agents enables the sensitive detection of metal cations in positive ion mode ESI-MS, it was necessary to validate the method using certified reference materials (CRMs). The amount of lead (II) in CRM 3128e was determined by the present IPR method using external standard calibration (see the Experimental Section). The results showed that the relative standard deviation (RSD) of this method was 7.6% and the percent error was found to be 7.8% (n=5) (Table 3-7).

Table 3-7 Relative Standard Deviation (RSD) and Percent Error of the NIST Standard Measurement

Measured concentration	Linear equation	R ²	True value	RSD	Percent error
444.4 nM	y = 9.7455x + 11.484	0.9955	482.4 nM	7.6%	7.8%

It should be noted that NH₄NO₃ generated in the sample preparation can cause ionization suppression of the metal complexes. The effect of NH₄NO₃ at concentrations between 0 to 1 mM, on the signal intensities of [²⁰⁸Pb+EDTA+Tet]²⁺; [⁵²Cr+CyETA+Tet]³⁺ and [²⁰⁸Pb+BETA+Tet]²⁺ is shown in Figure 3-6. It was found that the signal intensities of the ternary complexes were dramatically decreased when the concentration of NH₄NO₃ in solution increased. The signal of [²⁰⁸Pb+EDTA+Tet]²⁺ was completely suppressed as the concentration of NH₄NO₃ reached 0.8 mM. Fortunately it was noted that dilution of the concentrated CRM to a level compatible with the linear dynamic range of this sensitive method, also diluted the NH₄NO₃ to a level where its effect was negligible (see the Experimental Section).

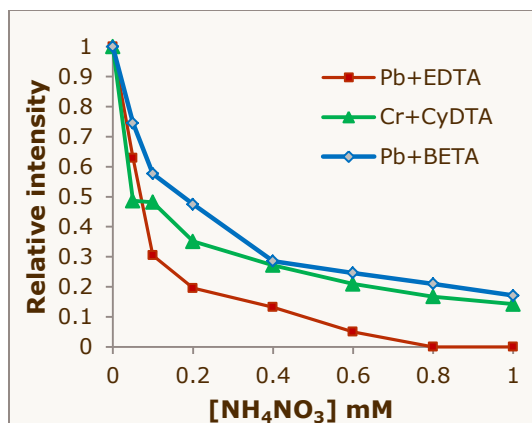


Figure 3-6 The Effect of NH₄NO₃ Concomitant (0–1 mM) on Signal Intensities of



Lastly, the linear range and linearity of this method were evaluated for three different metal chelate combinations (Pb-BETA, Pb-EDTA and Cd-BETA). The calibration curves for $[^{208}\text{Pb}+\text{EDTA}+\text{Tet}]^{2+}$, $[^{208}\text{Pb}+\text{BETA}+\text{Tet}]^{2+}$ and $[^{114}\text{Cd}+\text{EDTA}+\text{Tet}]^{2+}$ are shown in Figure 3-7. Figure 3-8 shows a typical ESI signal-to-noise ratio diagram for the direct injection of $[^{208}\text{Pb}+\text{EDTA}+\text{Tet}]^{2+}$ as an example of SIM mode quantitation. The calibration data of these three metal chelates showed qualified linearity ($R^2 > 0.99$) over a range of 2 orders of magnitude.

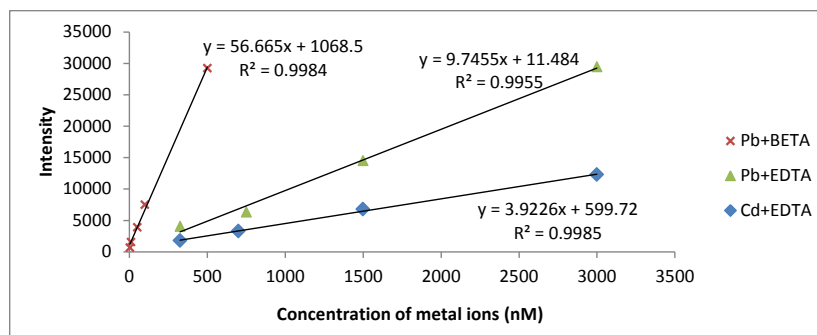


Figure 3-7 Calibration Curves for $[^{208}\text{Pb}+\text{EDTA}+\text{Tet}]^{2+}$ (Δ), $[^{208}\text{Pb}+\text{BETA}+\text{Tet}]^{2+}$ (\times) and $[^{114}\text{Cd}+\text{EDTA}+\text{Tet}]^{2+}$ (\diamond) Using External Standard Calibration Method.

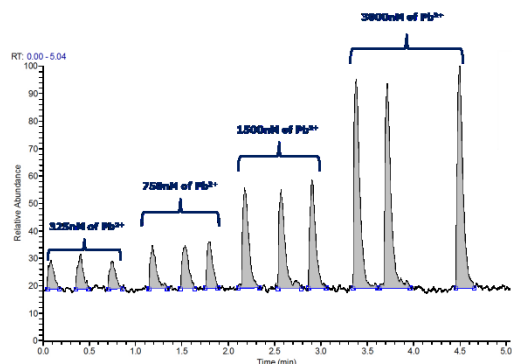


Figure 3-8 ESI S/N Ratio Diagram for the Direct Injection of $[^{208}\text{Pb}+\text{EDTA}+\text{Tet}]^{2+}$ in SIM Mode at m/z 779.3. Aliquots of 325, 750, 1500 and 3000 nM Injected in Triplicate

Table 3-8 and Table 3-9 show the relationship between the K_f values of metal complexes and the LODs of the metal cation of Pb obtained in the SIM positive mode. It was found that there was no direct correlation between K_f values of metal complexes and the corresponding LODs. This leads to the conclusion that formation of the metal chelate is necessary, but not sufficient to produce a low LOD. Reasonably, the LOD may be affected by other factors such as the association constant of the metal chelate with the IPR and most importantly, the ionization efficiency of the complex. Breitbach et. al. recently showed that the surface activity of the complex is a major contributing factor which leads to such low detection limits.²¹ In short, solution phase binding seems to be necessary for this technique, but does not directly equate to low LODs. The surface activity of the ternary complex likely plays a more dominant role.^{21,85,115}

Table 3-8 Formation Constant ($\log K_f$) of Metal Chelates^a

Metal	Chelating agent					
	I	II	III	IX	XI	XII
¹²⁰ Sn ²⁺	22.1	— ^b	—	—	—	—
⁴⁰ Ca ²⁺	11.0	8.4	12.3	—	6.1	5.4
²⁰⁸ Pb ²⁺	18.5	15.5	20.3	13.3	—	—
¹¹⁴ Cd ²⁺	16.4	13.0	19.9	8.1	—	—
⁵² Cr ³⁺	23.0	—	—	—	—	—

^a K_f values were obtained from Lange's Handbook of Chemistry, 15th edn., McGraw-Hill Inc., New York, 1999.

^bThe K_f values are not available in the current data source.

Table 3-9 SIM Mode LODs of the Metal Chelates and the IPR Complexes. Data Obtained from Table 3-2 of the Manuscript

Metal	Chelating agent					
	I	II	III	IX	XI	XII
¹²⁰ Sn ²⁺	1.50×10^{-2}	— ^a	—	—	—	—
⁴⁰ Ca ²⁺	4.00×10^{-4}	4.80×10^{-4}	6.60×10^{-3}	—	1.50×10^{-3}	2.00×10^{-1}
²⁰⁸ Pb ²⁺	3.22×10^{-1}	1.04×10^{-2}	6.76×10^{-2}	1.04×10^{-1}	—	—
¹¹⁴ Cd ²⁺	2.02×10^{-1}	1.14×10^{-1}	6.27×10^{-2}	5.70×10^{-2}	—	—
⁵² Cr ³⁺	2.60×10^{-1}	—	—	—	—	—

^a Data not shown in this table.

It should be noted that other types of mass analyzers such as a triple quadrupole could offer higher sensitivity than a linear ion trap (LIT), and therefore could further improve these results. Additionally, the optimization of a variety of instrumental

parameters can be carried out for each particular ternary complex to further improve the sensitivity.⁷⁷

3.4. Conclusions

The feasibility of sensitive metal cation detection by positive ion mode ESI-MS using an ion-pairing reagent and commercial chelating agents has been demonstrated. Thirteen chelating agents with diverse structures were evaluated for detection of metal cations with the optimal tetracationic ion-pairing reagent reported previously. Different chelating agents produced widely ranging LODs and the best chelating agents for each metal cation was determined. Sub pg level LODs were obtained using optimal chelating agents. Compared to negative ion mode, LODs improved one to three orders of magnitude in the positive ion mode. Both SIM and SRM analysis were performed using this method and the sensitivity for most metal cations was improved when tandem MS was performed on the ternary complex. The optimum solution pH to perform this analysis is between 5 and 7. The method was validated using CRM and the percent error was 7.8%. With this method, native metal cations are able to be rapidly detected in the positive ion mode ESI-MS with high sensitivity. Some aspects of the mechanism which contributes to this sensitivity enhancement are understood, but a more complete explanation will be the subject of future studies.

Chapter 4

Sensitive Analysis of Metal Cations in Positive Ion Mode Electrospray Ionization Mass Spectrometry Using Commercial Chelating Agents and Cationic Ion-Pairing Reagents

Abstract

Metals play a very important role in many scientific and environmental fields, and thus their detection and analysis is of great necessity. A simple and very sensitive method has been developed herein for the detection of metals in positive ion mode ESI-MS. Metal ions are positively charged, and as such they can potentially be detected in positive ion mode ESI-MS; however, their small mass-to-charge (m/z) ratio makes them fall in the low-mass region of the mass spectrum, which has the largest background noise. Therefore, their detection can become extremely difficult. A better and well-known way to detect metals by ESI-MS is by chelating them with complexation agents. In this study eleven different metals, Fe(II), Fe(III), Mg(II), Cu(II), Ru(III), Co(II), Ca(II), Ni(II), Mn(II), Sn(II), and Ag(I), were paired with two commercially available chelating agents: ethylenediaminetetraacetic acid (EDTA) and ethylenediaminedisuccinic acid (EDDS). Since negative ion mode ESI-MS has many disadvantages compared to positive ion mode ESI-MS, it would be very beneficial if these negatively charged complex ions could be detected in the positive mode. Such a method is described in this paper and it is shown to achieve much lower sensitivities. Each of the negatively charged metal complexes is paired with six cationic ion-pairing reagents. The new positively charged ternary complexes are then analyzed by ESI-MS in the positive single ion monitoring (SIM) and single reaction monitoring (SRM) modes. The results clearly revealed that the presence of the cationic reagents significantly improved the sensitivity for these analytes, often by several orders of magnitude. This novel method developed herein for the

detection of metals improved the limits of detection (LODs) significantly when compared to negative ion mode ESI-MS and shows great potential in future trace studies of these and many other species.

4.1. Introduction

Ionized metal species are present in many different biological, ecological and industrial environments; as such they play a very important role in our lives. In many instances metals are found associated with many different organic ligands. For example, about one-quarter of all existing proteins require a specific metal to help not only fulfill their precise functions in biochemical reactions, but also to maintain their stable state.¹¹⁹ Also, different oxidation states alter the specific role metal in a particular environment. For example, the oxide form of ruthenium (Ru), such as ruthenium(VIII) tetraoxide (RuO₄), is considered highly toxic, however ruthenium complexes containing Ru(II) and Ru(III) have been studied extensively and have shown great potential as anticancer agents when bound to certain ligands.¹²⁰ Knowing the correct oxidation state of Ru is also very important as Ru(II) is much more stable than Ru(III), and this does not only affect biological environments, but photochemical systems as well.¹²¹

The metals examined in this study can have different oxidation states and are crucial to many different ecological and industrial systems. They are cobalt (Co), calcium (Ca), nickel (Ni), manganese (Mn), tin (Sn), silver (Ag), iron (Fe), magnesium (Mg), and copper (Cu).

A number of methods have been developed for the accurate detection and quantification of these metals. Among the most used methods to detect metals are atomic absorption spectrometry (AAS), emission spectroscopies (ES), and inductively coupled plasma mass spectrometry (ICP-MS).^{122,123} Of course, due to the high

temperatures of these methods, speciation and the ability to determine oxidation state of the metals can be problematic.^{49,122,124-126} Another technique used to detect metals and their organic complexes is electrospray ionization mass spectrometry (ESI-MS) which is a softer ionization technique, and can further provide complete characterization of a metal-organic sample.^{49,50,125-129} The goal of this study is to detect anionic analytes (chelating agent + metal) in the positive ion mode at a higher sensitivity than the traditional negative ion mode ESI-MS, and to find the best ion-pairing reagent suitable for this task. In order to use this approach, the metal ions have to first associate with an anionic chelating agent.

Chelating agents are organic molecules that complex with metals with different coordination geometries and strengths. Currently, there is a large selection of commercially available chelating agents. These complexes have been studied extensively by ESI-MS.^{108,130,131}

In this study, two well-known chelating agents were chosen and used for metal analysis. They are: ethylenediamine-N,N,N',N'-tetraacetic acid (EDTA) and ethylenediamine-N,N'-disuccinic acid (EDDS). These multidentate ligands are aminocarboxylic acid compounds and as such they form negatively charged metal ion complexes.^{49,50,132,133} Thus, they are detected in negative ion mode ESI-MS. However, the negative ion mode tends to be unstable due to the fact that corona discharge is more prevalent, therefore creating chances for arcing, higher background noise and often resulting in an overall unstable Taylor cone and unstable signals.^{23,50} These phenomena can result in a higher overall limit of detection (LOD). These problems can be avoided if the positive ion mode is used.

In this study we have created a method in which we take these negatively charged metal complexes and associate them with multiply charged cationic pairing

reagents, creating an overall positive charged ternary complex that can be easily detected in positive ionmode ESI-MS. Many cationic ion-pairing reagents have been synthesized and evaluated previously.^{18,29,80,113,116,134-136} In this study six cationic ion-pairing reagents are examined as they were found to be effective (giving the lowest LODs) based on previous studies.^{18,21,29,81,134,137,138}

In addition to the very low LODs, other advantages of this method include great simplicity, very fast analysis times, and compatibility with high-performance liquid chromatography (HPLC) and capillary electrophoresis (CE).^{17,81,138} The large mass of these cationic ion-pairing reagents adds another major benefit to this technique which is the ability to bring small metal ions out of the low mass cutoff (LMCO) to a higher mass range where the background noise is lower. This study was performed in the selected ion monitoring (SIM) and selected reaction monitoring (SRM) mode.

4.2. Experimental

4.2.1. Chemicals

HPLC grade solvents were purchased from Honeywell Burdick and Jackson (Morristown, NJ). The metals and the chelating agents were purchased from Sigma-Aldrich (St. Louis, MO). The cationic ion pairing reagents were initially synthesized in the bromide form and then exchanged to the fluoride form prior to analysis. This ion-exchange method has been previously described by Soukup-Hein *et al.*¹⁷ The synthesis of the ion pairing reagents has been previously discussed.^{18,134,135} Each solution (metal and chelating agent) was prepared daily in situ and the serial dilutions started at 1 μ M. The ion pairing reagents are in aqueous solutions and their concentrations were maintained constant at 40 μ M.

4.2.2. ESI-MS Analyses

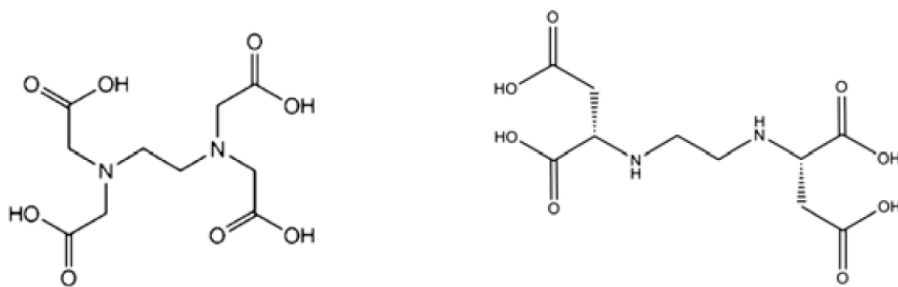
An external Shimadzu LC-6A pump (Shimadzu, Columbia, MD) was used to introduce the ion-pairing reagent to a Y-type mixing tee at a flow rate of 100 $\mu\text{L}/\text{min}$ (Figure 1-2). A 67:33 methanol/water mixture was also directed into the mixing tee at a flow rate of 300 $\mu\text{L}/\text{min}$, creating an overall flow of 50/50 water/methanol entering the mass spectrometer with a total flow rate of 400 $\mu\text{L}/\text{min}$. A Surveyor MS pump (Thermo Fisher Scientific, San Jose, CA) was used to pump the methanol/water mixture prior to entering the mass spectrometer. To introduce the sample, a six port injection valve with a 5 μL injection loop was used. Red PEEK tubing (i.d.0.005 in./125 μm) was used as solvent carrier for the ESI-MS analysis. In this study the LODs are reported as exact masses instead of concentrations to avoid confusion caused by different sample injection loops used in different studies.

The mass spectrometer used was a Thermo Finnigan LXQ (Thermo Fisher Scientific, San Jose, CA). The ESI-MS parameters were set as the following: spray voltage of 3 kV; capillary temperature of 350 $^{\circ}\text{C}$; capillary voltage of 11 kV; tube lens voltage of 105 V; sheath gas flow was set at 37 arbitrary units (AU), and the auxiliary gas flow at 6 AU. Necessary dilutions were prepared for each sample until five replicates of signal to noise (S/N) ratio of 3 was observed for each analyte. The data was analyzed using Xcalibur and Tune Plus software. The limits of detection in this analysis were determined based on Genesis Peak Detection Algorithm. The MS parameters were fixed to achieve a good sensitivity for the analyzed ternary and binary complexes. The parameters were kept the same in the negative and positive ion mode.

4.3. Results and Discussion

4.3.1. Metal Chelating Reagents and Ion-Pairing Reagents

In this study eleven metals of different oxidation states were paired individually with two commercially available chelating agents: ethylenediamine-tetraacetic acid (EDTA) and ethylenediamine-disuccinic acid (EDDS) (Figure 4-1). These negatively charged complexes were then analyzed sequentially by positive mode ESI-MS with six cationic ion pairing reagents (Figure 4-2). Thus, new and larger ternary complexes detected were all positively charged. A large pool of multiply charged cationic ion pairing reagents had been previously synthesized and evaluated.^{18,19,80,81,116,137} A recent study revealed that there are three main factors that contribute to the sensitivity these ion pairing agents achieve. They are: ionization efficiency, surface activity, and redox reactions occurring at the tip of the electrospray.²¹ 240 Based on these prior studies two linear tricationic and four tetracationic ion-pairing agents were selected for this study. Linear trication 1 has an imidazolium core with two C6 alkyl chains linking the imidazolium core to the terminal groups (LTC 1, Figure 4-2). The two end groups of this reagent are two tripropyl phosphonium groups. The second linear trication has an imidazolium core as well, and it contains C3 alkyl chain linkages and benzyl imidazolium terminal functional groups (LTC 2, Figure 4-2).



Ethylenediamine-*N,N,N',N'*-tetraacetic acid (EDTA)

Ethylenediamine-*N,N'*-disuccinic acid (EDDS)

Figure 4-1 Structures of the Two Metal Chelating Agents Used in this Analysis

The second set of reagents is the tetracationic ion pairing agents. Three of these are entirely phosphonium based salts (Tet 1, Tet 3, and Tet 4 in Figure 4-2) with a mixture of benzyl-, isopropyl and/or propyl functional groups. The alkyl linkages vary from C4 to C6. Tet 2 is the only ion pairing reagent containing a mixture of phosphonium, and imidazolium based moieties. The diphenyl phosphonium groups are positioned in the center of the structure separated by C4 linkages (Figure 4-2).

4.3.2. LODs of Metal Cations in the Positive SIM Mode with EDTA by Using Different Ion-Pairing Reagents

Table 4-1 shows the limits of detection (LOD) achieved for each $[M^{n+} + EDTA]^{-}$ complex in the SIM and SRM mode when paired with each of the ion pairing reagents (Figure 4-2).

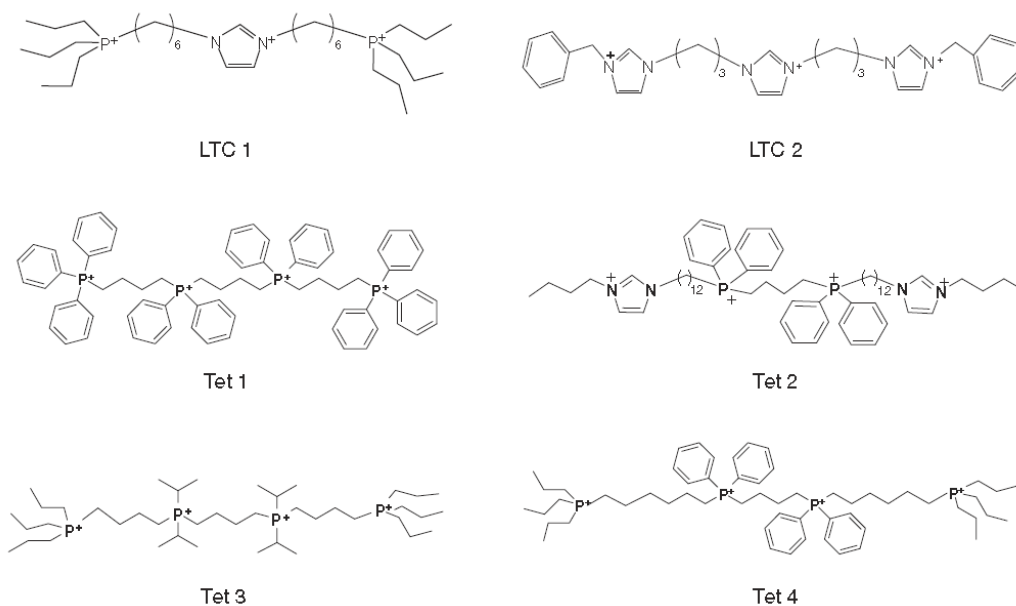


Figure 4-2 Structures of the Linear Tri- and Tetracationic Ion-Pairing Reagents Used in This Study

Table 4-1 Limits of Detection (ng) and the Corresponding Charge of Each Metal Complex in SIM and SRM Mode Using EDTA as the Chelating Reagent

	LTC 1		LTC 2		Tet 1		Tet 2		Tet 3		Tet 4	
	SIM LOD	SRM LOD	SIM LOD	SRM LOD	SIM LOD	SRM LOD	SIM LOD	SRM LOD	SIM LOD	SRM LOD	SIM LOD	SRM LOD
Cu 2+	2.3E-03/1+	1.5E-03/2+	4.7E-03/1+	1.4E-02/2+	2.2E-04/2+	5.3E-05/2+	3.1E-02/2+	9.4E-03/2+	1.5E-03/1+	5.3E-03/1+	3.1E-02/1+	3.7E-02/1+
Mg 2+	1.8E-02/1+	4.5E-03/3+	3.6E-03/1+	1.8E-03/3+	7.2E-04/2+	7.2E-04/2+	8.4E-03/3+	7.8E-03/3+	8.4E-03/2+	1.6E-03/2+	4.8E-02/2+	3.6E-02/2+
Ca 2+	1.9E-04/1+	1.8E-05/3+	1.0E-02/1+	4.0E-03/3+	4.0E-04/2+	6.0E-05/2+	1.6E-03/1+	4.0E-04/1+	2.0E-03/2+	1.5E-04/2+	5.0E-03/2+	2.0E-03/2+
Co 2+	1.0E-01/1+	1.3E-03/+2	1.4E-02/1+	N/D	1.7E-03/2+	2.9E-04/2+	9.4E-03/1+	N/D	3.6E-03/1+	3.6E-03/1+	5.9E-03/1+	1.4E-01/2+
Fe 2+	2.8E-02/2+	3.3E-04/2+	1.4E-02/2+	1.1E-02/2+	2.8E-03/2+	1.1E-03/2+	1.6E-01/1+	N/D	1.2E-02/2+	3.6E-04/2+	1.1E-02/3+	7.0E-03/2+
Fe 3+	2.8E-02/1+	2.5E-0/1+3	7.8E-02/1+	8.4E-03/3+	2.8E-03/2+	2.8E-04/2+	1.6E-01/1+	1.6E-01/1+	4.2E-03/2+	4.2E-03/2+	5.6E-02/4+	5.6E-02/1+
Ni 2+	2.9E-02/1+	8.7E-04/3+	8.1E-02/1+	1.7E-02/2+	7.2E-04/2+	2.9E-04/2+	6.9E-02/1+	1.8E-02/1+	1.1E-02/2+	1.1E-03/2+	1.4E-02/1+	2.3E-03/1+
Mn 2+	4.1E-02/1+	1.2E-03/3+	1.0E-01/1+	2.4E-02/2+	1.6E-03/2+	6.8E-05/2+	6.3E-02/2+	8.2E-03/2+	2.4E-02/2+	2.4E-02/2+	3.0E-02/2+	1.9E-03/1+
Ag +	5.3E-02/2+	5.3E-02/3+	2.6E-02/1+	N/D	4.0E-02/2+	9.6E-03/2+	2.6E-01/2+	N/D	2.4E-02/1+	2.4E-02/1+	1.6E-01/2+	1.2E-03/2+
Ru 3+	5.1E-01/4+	N/D ^a	1.9E-01/2+	N/D	7.6E-03/1+	1.2E-03/1+	1.7E-02/1+	2.0E-03/1+	2.0E-02/1+	5.1E-03/1+	1.0E-02/1+	7.6E-03/1+
Sn 2+	1.8E-01/1+	7.2E-02/1+	2.1E-01/1+	6.0E-01/2+	1.5E-02/2+	4.5E-03/1+	1.8E-01/2+	1.5E-02/2+	1.2E-02/1+	7.2E-02/1+	4.2E-01/2+	N/D

^aN/D – Indicates that a product ion was not detected. Bold and cursive typeface indicates the lowest limit of detection achieved for each analyzed anionic complex $[M^{n+}+EDTA]^-$.

Table 4-2 Limits of Detection (ng) and the Corresponding Charge of Each Metal Complex in SIM and SRM Mode Using EDDS as the Chelating Reagent

LOD	LTC 1		LTC 2		Tet 1		Tet 2		Tet 3		Tet 4	
	SIM	SRM LOD	SIM LOD	SRM LOD	SIM LOD	SRM LOD	SIM LOD	SRM LOD	SIM LOD	SRM LOD	SIM LOD	SRM LOD
Cu 2+	1.5E-02/1+	1.2E-02/2+	2.5E-02/1+	2.3E-02/2+	1.8E-04/2+	3.1E-05/2+	3.7E-03/1+	2.9E-04/1+	1.7E-03/2+	3.1E-04/2+	3.1E-01/1+	2.5E-03/1+
Mg 2+	1.8E-03/2+	4.9E-05/3+	1.2E-03/2+	1.4E-03/3+	2.1E-04/2+	1.8E-05/2+	9.6E-04/2+	3.0E-04/2+	2.4E-03/2+	2.6E-04/2+	4.8E-05/2+	7.5E-03/2+
Ca 2+	4.8E-04/2+	1.5E-03/3+	5.0E-03/2+	4.4E-03/3+	6.0E-03/3+	1.5E-04/3+	1.5E-01/2+	6.3E-03/2+	1.2E-02/2+	3.7E-03/2+	1.3E-02/2+	4.0E-03/2+
Co 2+	5.9E-03/2+	1.8E-03/3+	1.7E-01/1+	1.1E-01/1+	4.4E-04/2+	1.4E-04/2+	1.4E-01/1+	1.3E-02/1+	1.4E-03/1+	1.8E-03/2+	2.9E-01/1+	9.2E-02/2+
Fe 2+	1.4E-03/2+	7.4E-04/3+	2.8E-02/2+	4.2E-03/2+	8.4E-04/2+	8.8E-05/2+	8.4E-02/1+	2.1E-03/1+	8.4E-03/3+	1.2E-04/3+	2.5E-02/3+	9.2E-05/3+
Fe 3+	3.3E-03/2+	1.0E-02/2+	2.8E-01/1+	1.4E-01/3+	2.8E-03/2+	8.3E-05/2+	8.4E-03/1+	N/D	1.4E-03/3+	9.3E-03/1+	7.5E-03/3+	1.1E-03/3+
Ni 2+	2.3E-02/1+	2.9E-04/3+	5.8E-02/2+	5.8E-02/3+	1.1E-03/2+	2.9E-04/2+	1.4E-01/1+	7.2E-02/1+	8.7E-03/2+	5.8E-03/1+	6.9E-02/3+	1.4E-03/3+
Mn 2+	2.7E-02/2+	5.5E-02/3+	5.5E-02/2+	N/D	8.2E-03/2+	2.7E-03/2+	6.0E-02/1+	6.3E-02/1+	2.7E-02/2+	4.1E-03/2+	2.7E-02/3+	2.2E-02/3+
Ag +	1.0E-01/2+	N/D	1.0E-01/1+	1.0E-03/2+	5.3E-02/2+	1.0E-02/2+	6.4E-02/2+	N/D	2.9E-02/1+	3.7E-03/1+	2.1E-01/1+	N/D
Ru 3+	2.5E-01/4+	N/D ^a	N/D	N/D	6.1E-03/2+	7.6E-04/2+	3.0E-01/1+	8.1E-02/1+	5.1E-02/1+	N/D	2.5E-01/1+	1.0E-02/1+
Sn 2+	2.8E-01/1+	N/D	3.6E-01/1+	N/D	7.2E-02/2+	1.2E-02/2+	6.0E-01/2+	2.1E-02/2+	1.2E-01/1+	6.0E-02/1+	6.0E-01/1+	N/D

^aN/D – Indicates that a product ion was not detected. Bold and cursive typeface indicates the lowest limit of detection achieved for each analyzed anionic complex $[M^{n+}+EDDS]^-$.

All results are reported as exact masses (ng) of the metal, rather than concentrations to avoid any confusion caused by variations in the size of the sample injection loop which varies in different studies (a 5µL loop was used in this work, see *Experimental Section*). The bold-cursive typeface indicates the lowest limit of detection achieved for each metal. It is clear that the best ion-pairing reagent that resulted in the lowest LODs is Tet 1. In fact, for both SIM and SRM modes, Tet 1 produced the lowest LODs. It is also important to note that the limits of detection were further lowered, by varying degrees, for each metal when the analysis was carried out in the SRM mode. Indeed, Table 4-1 shows that the lowest limit of detection was achieved in the SRM mode for each metal complex (typically femtogram to picogram levels). Other ion pairing reagents that performed well were LTC 1 and Tet 3. The ion pairing reagents that produced poorer results were Tet 2, Tet 4, and LTC 2.

4.3.3. LODs of Metal Cations in the Positive SIM Mode with EDDS by Using Different Ion-Pairing Reagents

Table 4-2 shows the limits of detection when EDDS was used as a chelating agent. Similarly, every $[M_{n++} \text{ EDDS}]^-$ complex was individually paired with every ion pairing reagent. Again, the results show that, the lowest limits of detection were achieved when Tet 1 was used as the ion pairing reagent. Interestingly, in the case of EDDS the lowest limit of detection for each metal was achieved by Tet 1 in the SRM mode, except for one metal, Ag^+ . The lowest limit of detection for silver (Ag^+) was reached when LTC 2 was used as a pairing agent (10 x improvements when compared to Tet 1, Table 4-2). Also, the lowest LOD for nickel ($2.9\text{E-}04 \text{ ng, Ni}^{2+}$) was achieved by two pairing agents: LTC 1 and Tet 1 (see Table 4-2). As found for the EDTA metal complexes, both LTC 1 and Tet 3 produced good LODs as well. The worst LODs for each metal-EDDS complex

were again attained when LTC 2, Tet 2 and Tet 4 were used. One exception to this trend was LTC 2 and Tet 4 which produced the lowest LOD for only one metal (silver, Ag^+).

Upon examination of the data, it can be seen that the ion pairing reagent that produced the best LOD in the SIM mode for a specific metal, was not necessarily the same one that produced the lowest LOD in SRM experiments (Table 4-2). For example, the best LOD in the SIM mode for $[\text{Ag}^+ + \text{EDDS}]^-$ complex was achieved by Tet 3, however the best LOD in the SRM mode was produced by LTC 2. This held true for all metals except one. The same ion pairing reagents produced the lowest, average and highest LODs for both $[\text{Fe}^{2+} + \text{EDDS}]^-$ and $[\text{Fe}^{3+} + \text{EDDS}]^-$ complexes. For example the lowest LODs for both complexes were achieved by Tet 1, the second lowest were achieved by Tet 4, the third lowest limits of detection were achieved by Tet 3 and so on. This trend was unique only to Fe(II) and Fe(III) in the SRM mode and only with EDDS. Also, oxidation/reduction reactions were not observed when analyzing Fe (II) and Fe (III) standards.

4.3.4. A Comparison of the Best LODs Obtained in the Positive Ion Mode and in the Negative Ion Mode

Table 4-3 shows the summarized results of the best LODs achieved in the positive and negative ion mode ESI-MS. The data in this table also shows the best chelating agent and ion pairing reagents that were responsible in providing the lowest LODs. The final column of this table summarizes the improvements in sensitivity achieved in the positive mode. Based on these results it was concluded that the best overall ion-pairing reagent in detecting metals as ternary cationic complexes was Tet 1. These low limits of detection could be due to the presence of additional π interaction moieties present in Tet 1, which seems to be an important feature in some ion pairing reagents. Dicationic ion pairing reagents were attempted for this analysis, however the

LODs were significantly higher (data not shown). This was expected since a doubly charged ion pairing reagent could not make an overall positively charged complex because the chelating agents can carry multiple negative charges under normal conditions. Other factors that can contribute to the overall sensitivity of this method are the ability of the ions to ionize efficiently, and solution phase binding.²¹

Table 4-3 A Comparison of the Best LODs (pg) of the Metal Complexes Obtained in the Positive Ion Mode and in the Negative Ion Mode ESI-MS

	Negative Ion Mode LODs	Negative Ion Mode LODs	Chelater/Ion Pairing Reagents responsible for lowest LODs	Improvement
Cu 2+	9.4 /EDDS	0.031	EDDS /Tet 1	303x ^a
Mg 2+	14 /EDTA	0.018	EDDS /Tet 1	778x
Ca 2+	20 /EDTA	0.018	EDTA /LTC1	1111x
Co 2+	140 /EDDS	0.14	EDDS /Tet 1	1000x
Fe 2+	28 /EDTA	0.088	EDDS /Tet 1	318x
Fe 3+	28 /EDTA	0.083	EDDS /Tet 1	337x
Ni 2+	34 /EDDS	0.29	EDDS /Tet 1	117x
Mn 2+	24 /EDTA	0.068	EDTA /Tet 1	353x
Ag +	100 /EDDS	1	EDDS /LTC 2	100x
Ru 3+	450 /EDTA	0.76	EDDS /Tet 1	592x
Sn 2+	300 /EDTA	4.5	EDTA /Tet 1	67x

^aTimes of improvement

The goal of this study was to create a sensitive method in which anionic ions can be detected at a higher sensitivity in the positive ion mode rather than the traditional negative ionization mode ESI-MS. The sensitivity of the cationic pairing approach is even more apparent when compared to LODs achieved in the negative ion mode where no cationic ion pairing reagent is present. These results are shown in Table 4-4. Analysis of each complex was performed in both SIM and SRM modes. The SRM analysis was not successful for most complexes (Table 4-4). The limits of detection were significantly higher in the negative ion mode. For example, Mg²⁺ and Cu²⁺ showed an improved LOD of more than 5000x in the positive ion mode.

Table 4-4 Limits of Detection (pg) of All Metals When Complexed with Each of the Chelating Agents in Both SIM and SRM Analysis Without the Presence of Cationic Ion-Pairing Reagents

	EDTA SIM LOD (pg)	EDDS SRM LOD (pg)	EDTA SIM LOD (pg)	EDDS SRM LOD (pg)
Cu 2+	280	N/A	9.4	N/A ^a
Mg 2+	14	N/A	18	24
Ca 2+	20	N/A	N/A	N/A
Co 2+	290	N/A	590	140
Fe 2+	28	28	N/A	N/A
Fe 3+	28	N/A	30	N/A
Ni 2+	290	N/A	34	140
Mn 2+	24	N/A	30	140
Ag +	480	N/A	100	N/A
Ru 3+	450	N/A	N/A	N/A
Sn 2+	300	N/A	1500	N/A

^aNot determined

Other metals such as Ca^{2+} , Fe^{2+} , Ru^{3+} , were not detected at all in the negative ion mode at our starting concentration when using EDDS as the chelating agent. In the positive mode ESI-MS these three metals were easily detected at ppb/ppt levels. Other metals were detected with a few hundred to a thousand times greater sensitivity in the positive ion mode.

Comparisons of the MS flow injection profiles for Ca^{2+} in negative and positive ion mode ESI-MS are shown in Figure 4-3. Panel (A) of Figure 4-3 shows the lowest LOD (20 pg) of $[\text{Ca}^{2+} + \text{EDTA}]^-$ detected in the negative ion mode. Figure 4-3 (B) shows an injection of 400 fg of $[\text{Ca}^{2+} + \text{EDTA}]^-$ complex also in the SIM negative ion mode and a signal was not observed. Panel (C) of Figure 4-3 shows the same 400 fg sample now analyzed in the SIM positive ion mode ESI-MS (using Tet 1). This is a >50x improvement in LOD from negative to SIM positive ion mode. This limit of detection was further lowered in the SRM positive ion mode also using Tet 1 (Figure 4-3, D). The flow injection analysis displayed in (D) (Figure 4-3), represents $[\text{Ca}^{2+} + \text{EDTA}]^-$ complex in the SRM positive ion mode when the same ion-pairing reagent (Tet 1) was used. In this case, to achieve a S/N of 3 the concentration was lowered to 60 fg (~7x and 340x improvement in comparison to the SIM positive and SIM negative ion mode respectively). The low background noise contributes to the low LODs achieved in this mode. SRM analysis was not successful for this complex in the negative ion mode.

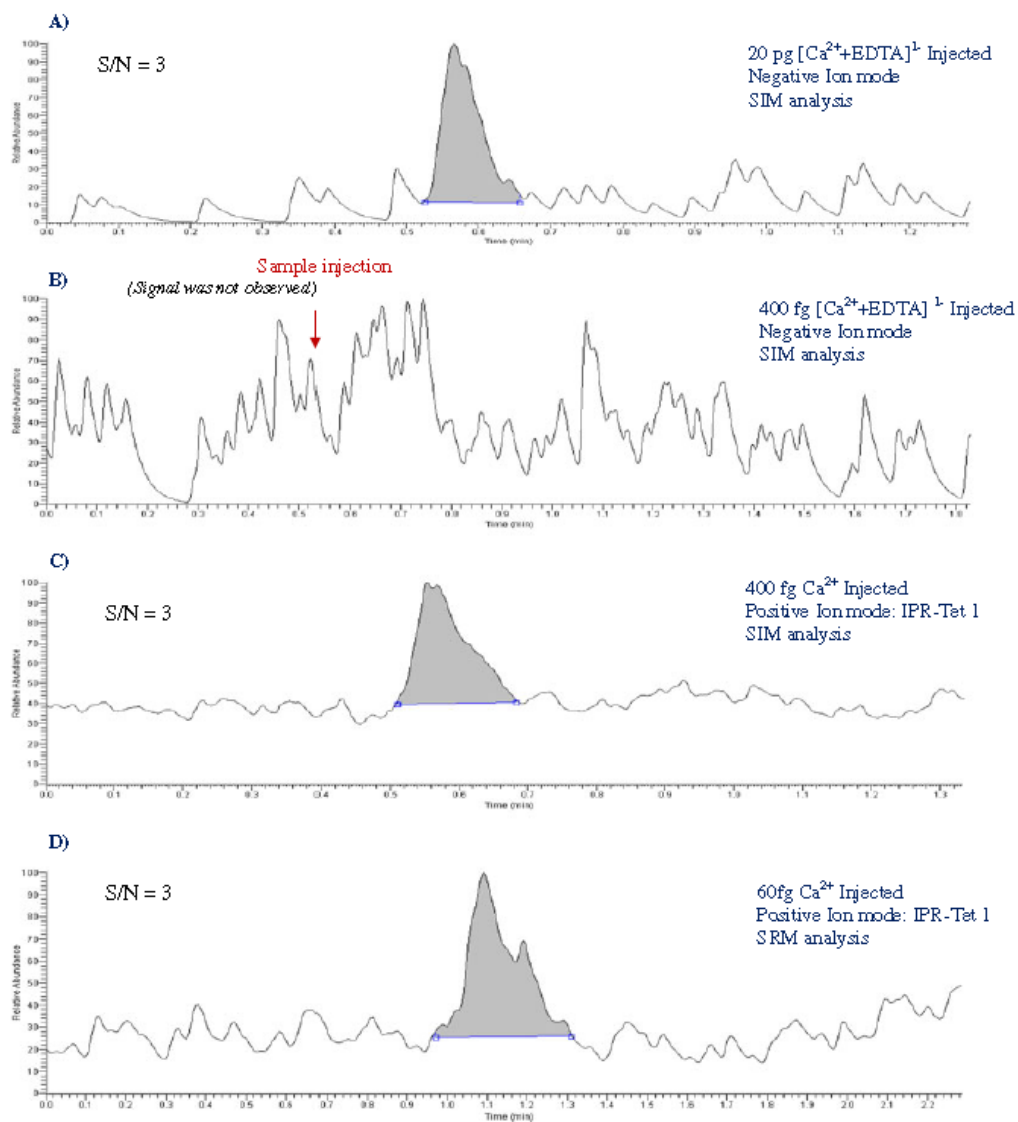


Figure 4-3 A Comparison of Limits of Detection of Ca^{2+} Achieved in Negative and Positive Ion Mode ESI-MS. (A) and (B) Demonstrate an Injection of the $[Ca^{2+}+EDTA]^{-}$ Complex Monitored in the SIM Negative Ion Mode at Two Different Concentrations. (C) and (D) Demonstrate the Results Achieved When the $[Ca^{2+}+EDTA]^{-}$ Complex was Monitored in the SIM and SRM Positive Ion Mode with the Addition of the Ion-Pairing Reagent Tet 1

When comparing the two chelating agents, EDTA complexes had better LODs for four out of the 11 metals analyzed in this study (Ca^{2+} , Mn^{2+} , Ag^+ , Sn^{2+}). These improvements varied from 3 times (Ag^+) to 40 times (Mn^{2+}) when compared to EDDS complexes. There was only one metal, Ni^{2+} , for which the lowest LOD ($2.9\text{E-}04$ ng) was achieved by both chelating agents. Currently, we are examining a much broader range of chelating agents to see if further improvements in the limits of detection can be achieved, and to better understand which chelating agents would be optimal for this type of analysis.

4.3.5. SRM Fragmentation Pathway

When analyzing the large ternary complexes in this study, all possible mass to charge (m/z) formations were monitored. In most cases, +1 and +2 complexes were observed in both SIM and SRM positive ion mode analysis. In the SRM experiments, these ions undergo collision-induced dissociation (CID), which causes the precursor ion (monitored in the SIM mode) to fragment into many product ions. Fragmentation patterns varied with the pairing reagents. In most cases, the new ions monitored in the SRM mode were just from the ion pairing reagents. For example, the ions monitored from LTC 2 resulted in a loss of one benzylimidazolium group or the loss of two hydrogen atoms from the imidazolium moieties. The main fragment monitored from LTC 1 was a loss of tripropyl-phosphonium terminal group.

In cases where the fragment represented the loss of a terminal charged group, the rest of the ion pairing reagent remained associated with the chelated metal. An example of this is shown in Figure 4-4, which represents a proposed fragmentation pathway for the tandem MS analysis of the $[\text{Mn}^{2+} + \text{EDTA}]^{2-}$ complex in the positive ion mode ESI-MS.

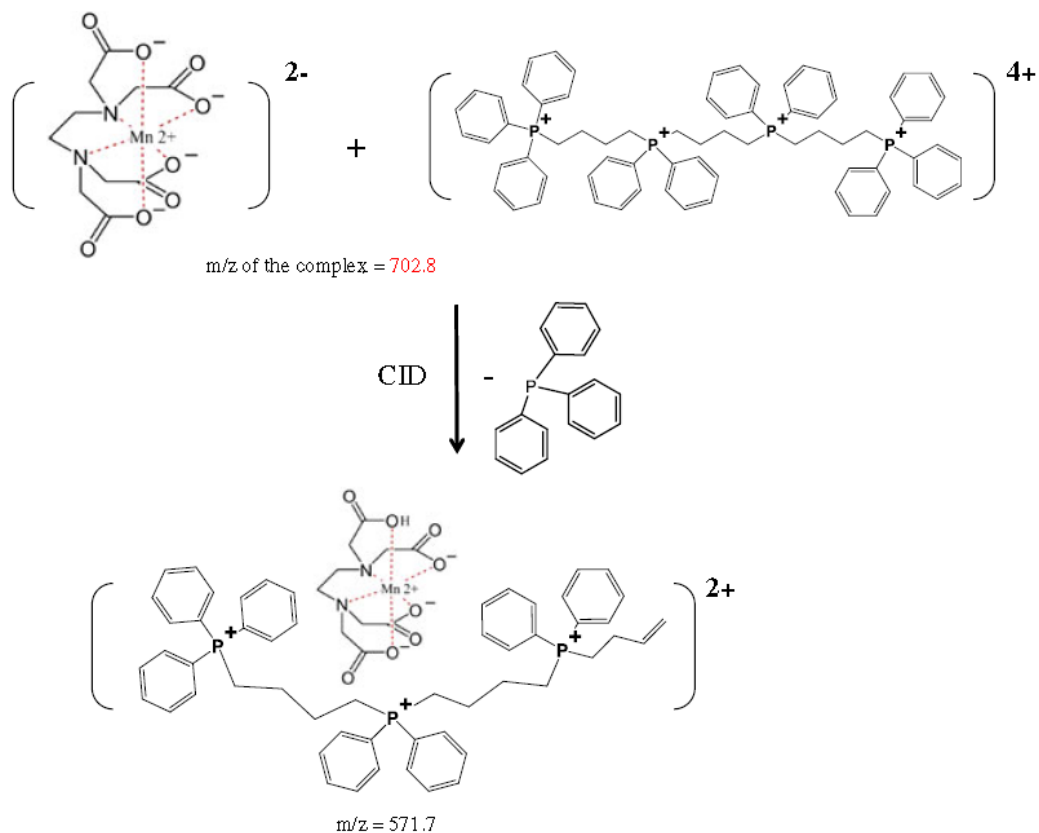


Figure 4-4 A Proposed Fragmentation Pathway for the Tandem Mass Spectrometric Analysis of Mn^{2+} When Complexed with EDTA as a Chelating Agent and Tet 1 Tetracationic Ion-Pairing Reagent in Positive Ion Mode ESI-MS

When Tet 1 is used as an ion pairing reagent, the overall complex monitored in the SIM positive ion mode has a m/z of 1405.6 (2+). In this mechanism (Figure 4-4) the new fragment monitored is a complex representing the tetracationic reagent (which loses one terminal end group, triphenyl phosphonium group, m/z 262 and becomes triply charged) associated in the gas phase with the $[Mn^{2+} + EDTA]^{-2}$ complex. During CID, $[Mn^{2+} + EDTA]^{-2}$ complex gains a proton becoming singly charged, thus forming an overall new complex with a mass to charge ratio of 571.7 (+2). A study on the effect of

pH and other important variables on these types of analytes and analysis has been published elsewhere.¹⁹ It was shown that the best detection limits were obtained when the analyzed solutions were at $5 \leq \text{pH} \leq 7$.

The method developed herein shows comparable results with other, widely and commonly used methods such as ICP-MS and AAS. A comparison of the reported LODs of the metals by more conventional techniques with the results of this study are given in Table 4-5.¹³⁹⁻¹⁴⁵

Table 4-5 Comparison of Detection Limits ($\mu\text{g/L}$) for Five Metals Measured by Three Different Instruments and Methodologies

Metals	ICP-MS	AAS	ESI-MS
Mn (II)	0.00026 ^a	0.13	0.0136
Cu ^b	0.002	0.05	0.0062
Fe	0.00117	1.06	0.0166
Ni (II)	0.02	1.9	0.058
Ag (I)	0.15	0.6	0.2

^aSince not all the references reported the amount of sample injected to find the LOD of these metals, for comparison purposes we converted our LODs to concentration units.

^bThe oxidation cannot be distinguished by ICP-MS and AAS, however it can by ESI-MS.

In this table Cu(II) and Fe (II) were monitored by ESI-MS

4.4 Conclusions

In this study two common chelating agents have been used to form anionic complexes with eleven different metals. These compounds were then paired with tri-, and

tetra-cationic ion pairing reagents, which were synthesized in our laboratories. These new ternary complexes were positively charged, and were monitored in the SIM and SRM positive ion mode ESI-MS, while the LODs were reported and compared to the ones achieved in the negative ion mode. The LODs in the positive mode were significantly better (often several orders of magnitude) than in the negative ion mode.

The best ion-pairing reagent for the detection of metals is the perphenylphosphonium tetracation Tet 1 (Figure 4-2) followed by LTC 1 and Tet 3. It appears that phosphonium based cationic reagents with aromatic moieties and short alkyl chain linkages are ideal ion pairing reagents for the detection of chelated metals. These limits of detection can be further improved with further optimization of ESI parameters.

Also, different, more sensitive mass analyzers such as a quadrupole mass analyzer would further lower the limits of detection especially in the SRM mode. The new detection method described herein was applied successfully to free metals in aqueous solution. Further investigations of the different uses of this method are under considerations. This experimental approach is very simple, with short analysis times, and most importantly, very low limits of detection. The flow rates used with this technique are compatible with HPLC and CE. Other advantages of this method include the detection of low mass cations at higher mass ranges where there is less background noise, sample preparation or pre-concentration step are often not needed and sample speciation is straight forward.

Chapter 5

Use of Ion Pairing Reagents for Sensitive Detection and Separation of Phospholipids in the Positive Ion Mode LC-ESI-MS

Abstract

Phospholipids make up one of the more important classes of biological molecules. Because of their amphipathic nature and their charge state (e. g., negatively charged or zwitterionic) detection of trace levels of these compounds can be problematic. Electrospray ionization mass spectrometry (ESI-MS) is used in this study to detect very small amounts of these analytes by using the positive ion mode and pairing them with fifteen different cationic ion pairing reagents. The phospholipids used in this analysis were phosphatidylethanolamine (PE), phosphatidylcholine (PC), phosphatidylglycerol (PG), phosphatidylserine (PS), phosphatidylinositol (PI), phosphatidic acid (PA), 1, 2-diheptanoyl-sn-glycero-3-phosphocholine (DHPC), cardiolipin (CA) and sphingosyl phosphoethanolamine (SPE). The analysis of these molecules was carried in the single ion monitoring (SIM) positive mode. In addition to their detection, a high performance liquid chromatography and mass spectrometry (HPLC-MS) method was developed in which the phospholipids were separated and detected simultaneously within a very short period of time. Separation of phospholipids was developed in the reverse phase mode and in the hydrophilic interaction liquid chromatography (HILIC) mode HPLC. Their differences and impact on the sensitivity of the analytes are compared and discussed further in the paper. With this technique, limits of detection (LOD) were very easily recorded at low ppt (ng/L) levels with many of the cationic ion pairing reagents used in this study.

5.1. Introduction

Phospholipids are well known and thoroughly studied molecules due to their seminal importance in biological organisms. They are mainly recognized as building blocks of cell membranes.^{146,147} However, they also play a very important role in many other, different cellular signaling events.¹⁴⁶⁻¹⁴⁸ Specifically, phospholipids play a crucial role as second messengers in signal transduction pathways, protein sorting, and apoptosis.¹⁴⁹⁻¹⁵² The basic structure of these molecules includes a hydrophilic head group to which two hydrophobic “tails” are attached. Having such a structure enables these molecules to form lipid bilayers, in which the nonpolar tails cluster together in the core of the bilayer.¹⁵³ Some common polar head groups found in phospholipids are inositol, glycerol, serine and ethanolamine.¹⁴⁶ These molecules are found as mixtures in biological matrices and are very diverse due to their different degrees of unsaturation, fatty acyl chain lengths and the different polar head groups. A combination of the wide variety of these compounds and the often small differences in their structures can make separating, identifying, and quantifying them challenging.^{148,154,155} Traditional and common methods of analysis of phospholipids include thin layer chromatography (TLC), high performance liquid chromatography (HPLC), gas chromatography (GC), and HPLC with evaporative light scattering detection (ELSD).^{148,149,155-163} However, these techniques have disadvantages, which can become problematic if accurate quantitation, and identification is needed. Some of these methods also require derivatization (GC), and large sample quantities.^{148,149,156-158} Nowadays, mass spectrometry has become one of the main techniques used to accurately detect and identify phospholipids. This technique is very often coupled with HPLC and/or capillary electrophoresis (CE).¹⁶⁰⁻¹⁶² For phospholipids, electrospray ionization mass spectrometry (ESI-MS) is the most used technique of mass

spectrometry due to its simplicity, soft ionization and capability to accurately identify analytes.^{148,163-165}

In this study, we present a new and simple way to detect phospholipids in the positive mode ESI-MS with the aid of multiply charged cationic ion pairing reagents. Previously, many of these analytes could only be detected in the negative ion mode ESI-MS as they mainly carry negative charges.^{155,164} However, it is well known that the negative ion mode ESI-MS has some disadvantages when compared to the positive ion mode. Some of these drawbacks include the formation of corona discharge, arcing, which then results in poor spray stability, thus affecting the sensitivity of the analytes.^{23,166} It has been shown that these drawbacks can be solved by using halogenated solvents or electron scavenging gases, however these types of solvents are not user friendly in liquid chromatography (LC) analysis in cases where such type of analysis is needed.^{25,26,79,167} The advantage of the technique used in this study is that it operates in the positive ion mode ESI-MS, therefore eliminating the problems mentioned above and further enhancing detection and the sensitivity of the analytes.^{17,113}

The method used herein involves the use of large cationic ion pairing reagents, which upon association with the anions of interest, form a new positively charged complex that can now be detected in the positive ion mode rather than the negative ion mode ESI-MS. This method was recently developed by our research group for the detection of the perchlorate ion.^{17,113} The successful results lead to an extensive study and the synthesis of many other cationic reagents.^{18,21,29,77,80,113,116} The major advantages of using this method involve high sensitivity, compatibility with HPLC, and ease of use. Additionally, because of the large positive complexes formed, this method has the advantage of detecting small anions that normally reside below or near the low mass cutoff (LMCO) at a higher mass range where the background noise is lower.^{20,22}

5.2. Experimental

5.2.1. Chemicals

The solvents used in this analysis were of HPLC-grade, purchased from Honeywell Burdick and Jackson (Morristown, NJ). The phospholipids were purchased in their sodium form from Avanti Polar Lipids (Alabaster, AL). The predominant species of these phospholipids were as follows: 18:2/16:0-PE (phosphatidylethanolamine), 18:2/16:0-PI (phosphatidylinositol), 18:2/16:0-PS (phosphatidylserine), 18:2/16:0-PA (phosphatidic acid), 7:0/7:0-DHPC (1, 2-diheptanoyl-sn-glycero-3-phosphocholine), 18:2/18:2-CA (cardiolipin), 18:2/16:0-PC (phosphatidylcholine), 18:1-SPE (sphingosyl phosphoethanolamine). Each cationic reagent was synthesized in the bromide form and prior to the analysis it was exchanged to the fluoride form using an ion-exchange method developed previously.¹⁷⁵

5.2.2. ESI-MS

ESI-MS analysis was performed on a Thermo Finnigan LXQ (Thermo Fisher Scientific, San Jose, CA) linear ion trap. A Surveyor MS pump (Thermo Fisher Scientific) was used to pump 100% methanol (MeOH) at 300 μ L/min. The different ion pairing reagents used in the analysis were introduced to the mass spectrometer from a Shimadzu LC-6A pump (Shimadzu, Columbia, MD) at a flow rate of 100 μ L/min. Prior to entering the MS, these two solutions, methanol and the ion pairing reagent, were directed to a Y-type mixing tee, resulting at a final flow rate of 400 μ L/min entering the MS.

The ESI-MS parameters were set as follows: spray voltage of 3 kV; capillary temperature of 350°C; capillary voltage of 11 kV; tube lens voltage of 105 V; sheath gas flow was set at 37 arbitrary units (AU), and the auxiliary gas flow at 6 AU. Red PEEK tubing (i.d.0.005 in.) was used as solvent carrier for the ESI-MS and LC-ESI-MS analysis. The sample analytes were introduced in the MS via a six port injection valve with a 5 μ L loop. The

concentration of the ion pairing reagent remained constant at 40 μ M throughout the study. The analytes were initially dissolved in acetonitrile/methanol (1:9) and necessary dilutions were performed only with methanol, until a S/N ratio of three was noted in five replicate injections of each sample. Initial concentration of the analytes was 10 μ g/mL.

5.2.3. *Reversed-Phase Mode HPLC-ESI-MS*

Reverse phase LC was performed on an AscentisTM C18 column (250 mm \times 2.1 mm) obtained from Supelco, Sigma-Aldrich Co (Bellefonte, PA). The mobile phase used was 60/25/15 isopropanol/acetonitrile/water with 0.1% formic acid. The flow rate was 0.2 mL min⁻¹.

5.2.4. *HILIC Mode HPLC-ESI-MS*

HILIC mode separation was performed on a silica-column (250mm \times 4.6mm) obtained from Advanced Separation Technologies (Whippany, NJ). The mobile phase used was 70/20/10 acetonitrile/methanol/water with a flow rate of 1mL min⁻¹. Phospholipids were detected, in both reverse and HILIC phase LC, at a wavelength of 210 nm. A flow splitter was used in the normal phase separation which it was adjusted so that 0.7 mL min⁻¹ was directed to the waste and 0.3 mL min⁻¹ was directed into a mixing tee. Similarly, the ion pairing reagent was directed towards the mixing tee as described earlier on the ESI-MS analysis. Thus, the final flow rate entering the MS remained 0.4 mL/min. The chromatographic separations for both modes were done by a Thermo Fisher Surveyor autosampler (10 μ L injections).

5.3. Results and Discussion

5.3.1. *Ion-Pairing Reagents and Analytes of Interest*

In this study nine phospholipids were detected individually with fifteen cationic ion pairing reagents in the positive ion mode ESI-MS. Five of the cationic reagents were

doubly charged (Figure 5-1) and contained different central cores such as imidazolium, phosphonium, and pyrrolidinium ones. The linear tricationic reagents contained imidazolium core moieties and different terminal functional groups. Their alkyl chain linkages varied from C3 to C12 (Figure 5-2). The last group of the pairing reagents, the tetracationic ion pairing reagents, were a little more diverse in their structural configurations when compared to the previous two groups. Four of these tetracationic reagents contained phosphonium based moieties and one consisted of an imidazolium core and phosphonium terminal groups (Figure 5-3). Among these, one ion pairing reagent is a cyclic phosphonium based reagent, while all the others are linear. The terminal groups consisted of propyl-, phenyl-, and butyl-functional groups. The alkyl chain linkages varied as well, from a C4 to a C12 linkage (Figure 5-3).

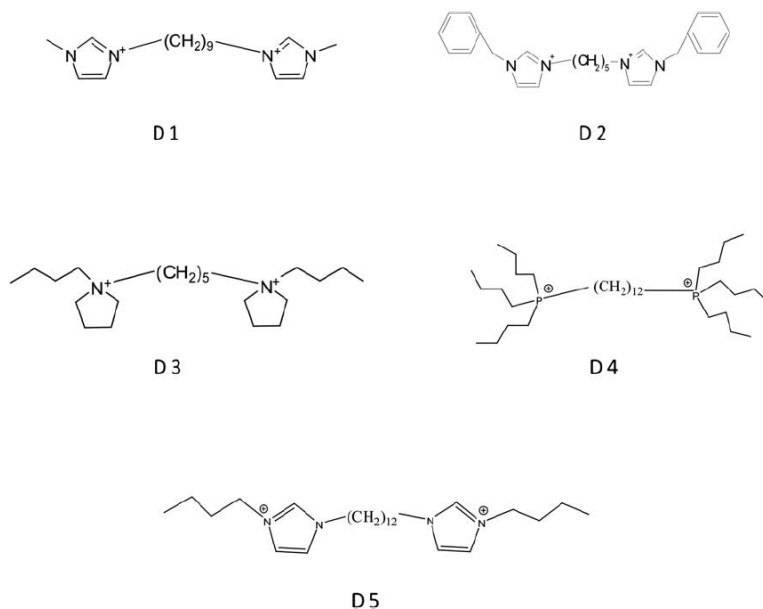


Figure 5-1 Structures of the Dicationic Ion Pairing Reagents with Their Corresponding Abbreviations Used in This Study

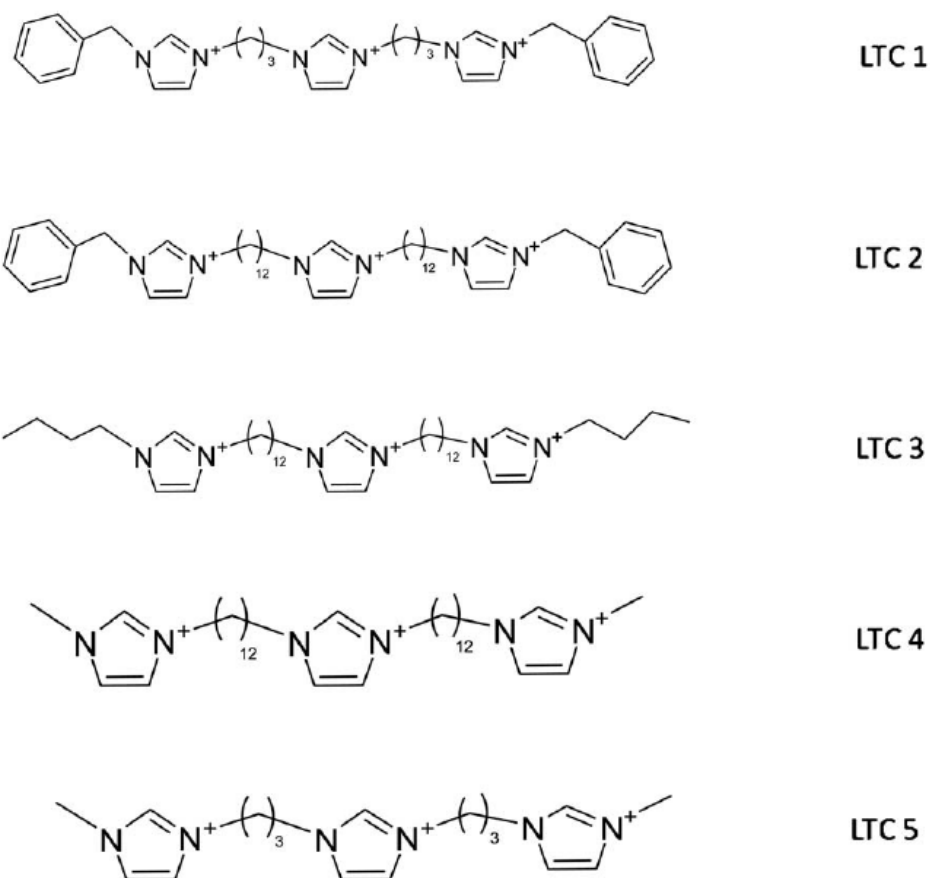


Figure 5-2 Structures of the Linear Tricationic Ion Pairing Reagents with Their Corresponding Abbreviations

The selection of some of these ion pairing reagents was based on our previous study on the ESI-MS mechanisms that produces the enhanced sensitivity of this ion pairing technique.²⁴⁰ In this study it was revealed that the association/binding of the anions and the ion pairing reagents is achieved in solution and further enhanced via ionization in the gas phase. Specific reagents with different alkyl chain linkages and different terminal groups were chosen for comparison purposes and to gain a better understanding of the behavior of these particular analytes.

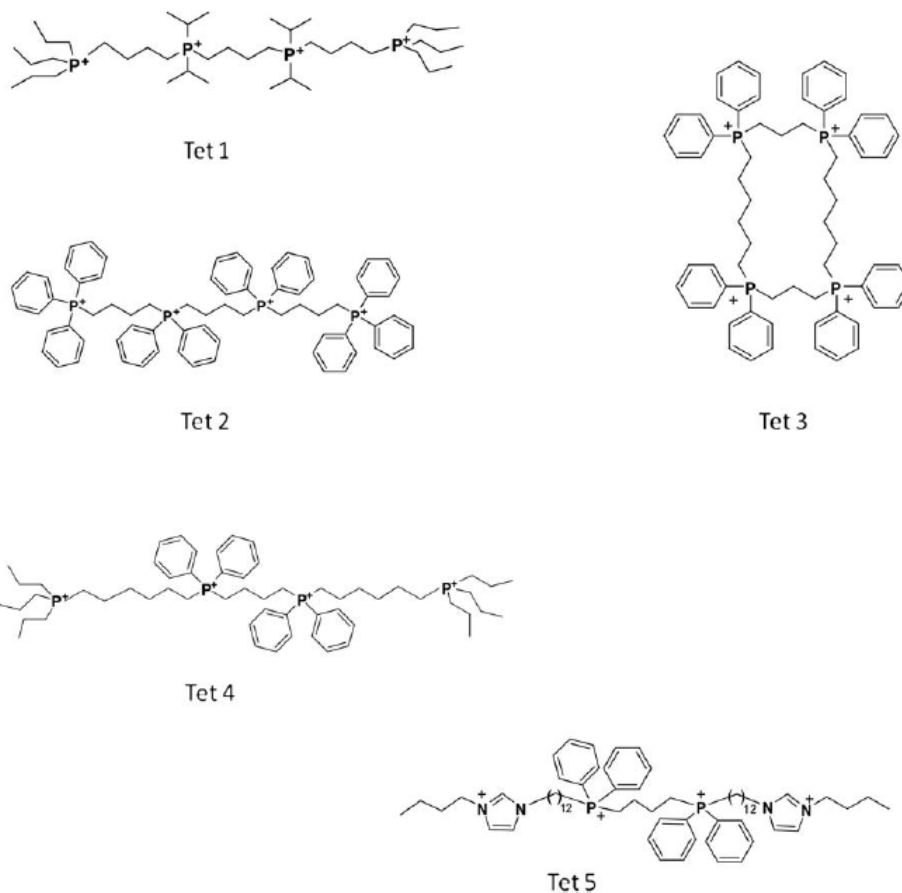


Figure 5-3 Structures of the Tetracationic Ion Pairing Reagents Used in This Study with Their Corresponding Abbreviations

5.3.2. Detection of Phospholipids Using IPRs in the Positive SIM Mode ESI-MS

Table 5-1 lists the limits of detection for the nine phospholipids in the positive ion mode ESI-MS. The table is set up so that the best pairing agent giving the best sensitivity for each analyte is placed at the top of the list. Conversely, the pairing agent producing the poorest sensitivity for each analyte is placed at the bottom of the list (Table 5-1).

Table 5-1 LODs for Phospholipids by PIESI with Fifteen Different Ion Pairing Reagents

PA			PG			PI		
IPR	Mass inj./ng	Charge	IPR	Mass inj./ng	Charge	IPR	Mass inj./ng	Charge
Tet 4	5.00×10^{-5}	3+	Tet 4	8.50×10^{-4}	3+	Tet 2	5.00×10^{-3}	3+
Tet 2	5.00×10^{-3}	2+	D1	1.00×10^{-2}	1+	Tet 4	1.00×10^{-2}	3+
D2	2.50×10^{-2}	1+	Tet 1	2.50×10^{-2}	3+	Tet 1	1.00×10^{-2}	2+
Tet 1	5.00×10^{-2}	2+	D2	6.50×10^{-2}	1+	D3	1.00×10^{-2}	1+
Tet 3	5.00×10^{-2}	2+	D3	1.00×10^{-1}	1+	LTC 1	1.00×10^{-2}	2+
LTC 2	7.50×10^{-2}	1+	LTC 2	1.00×10^{-1}	1+	D1	1.20×10^{-1}	1+
D1	1.00×10^{-1}	1+	LTC 1	1.00×10^{-1}	2+	LTC 5	1.50×10^{-2}	2+
D3	1.20×10^{-1}	1+	LTC 4	1.00×10^{-1}	2+	LTC 2	2.00×10^{-1}	1+
LTC 1	1.70×10^{-1}	1+	LTC 5	1.50×10^{-1}	2+	D4	2.50×10^{-1}	1+
LTC 5	2.00×10^{-1}	2+	Tet 2	1.50×10^{-1}	3+	Tet 5	3.00×10^{-1}	2+
LTC 3	3.00×10^{-1}	1+	LTC 3	2.00×10^{-1}	1+	LTC 3	3.50×10^{-1}	1+
LTC 4	5.00×10^{-1}	1+	D5	2.00×10^{-1}	1+	LTC 4	5.00×10^{-1}	1+
Tet 5	5.00×10^{-1}	1+	Tet 3	2.50×10^{-1}	2+	Tet 3	5.00×10^{-1}	1+
D5	5.00×10^{-1}	1+	D4	2.50×10^{-1}	1+	D2	5.00×10^{-1}	1+
D4	5.00×10^0	1+	Tet 5	5.00×10^{-1}	2+	D5	5.00×10^{-1}	1+

PS			PC			PE		
IPR	Mass inj./ng	Charge	IPR	Mass inj./ng	Charge	IPR	Mass inj./ng	Charge
Tet 2	1.00×10^{-5}	3+	Tet 2	1.50×10^{-5}	3+	LTC 1	3.50×10^{-3}	2+
Tet 4	1.00×10^{-3}	3+	D1	5.00×10^{-4}	1+	Tet 5	5.00×10^{-3}	1+
D1	1.00×10^{-3}	1+	Tet 4	7.50×10^{-4}	3+	D1	5.00×10^{-3}	1+
Tet 5	1.50×10^{-3}	3+	Tet 5	5.00×10^{-3}	3+	Tet 2	1.00×10^{-2}	2+
Tet 1	5.00×10^{-2}	3+	Tet 1	4.00×10^{-2}	3+	D3	1.50×10^{-2}	1+
LTC 2	1.00×10^{-1}	1+	D4	7.50×10^{-2}	1+	Tet 1	2.50×10^{-2}	3+
LTC 1	1.00×10^{-1}	2+	LTC 1	2.00×10^{-2}	2+	LTC 2	3.50×10^{-2}	1+
Tet 3	3.00×10^{-1}	2+	LTC 5	1.50×10^{-1}	2+	LTC 5	9.50×10^{-2}	2+
D2	3.50×10^{-1}	1+	LTC 2	3.00×10^{-1}	1+	Tet 4	1.00×10^{-1}	3+
D3	3.50×10^{-1}	1+	Tet 3	5.00×10^{-1}	2+	LTC 3	1.00×10^{-1}	1+
LTC 5	4.00×10^{-1}	2+	D3	5.00×10^{-1}	1+	LTC 4	1.00×10^{-1}	1+
D4	5.00×10^{-1}	1+	D2	8.50×10^{-1}	1+	Tet 3	1.50×10^{-1}	1+
LTC 4	5.00×10^{-1}	1+	LTC 3	1.50×10^0	2+	D4	3.00×10^{-1}	1+
LTC 3	5.50×10^{-1}	1+	LTC 4	1.50×10^0	1+	D2	5.00×10^{-1}	1+
D5	1.50×10^0	1+	D5	5.00×10^0	1+	D5	5.00×10^1	1+

CA			SPE			DHPC		
IPR	Mass inj./ng	Charge	IPR	Mass inj./ng	Charge	IPR	Mass inj./ng	Charge
Tet 2	5.00×10^{-4}	2+	Tet 1	5.00×10^{-6}	2+	D2	1.50×10^{-2}	1+
Tet 4	1.50×10^{-2}	2+	LTC 1	1.00×10^{-2}	1+	Tet 1	4.50×10^{-2}	2+
Tet 1	2.00×10^{-2}	2+	D2	1.90×10^{-2}	1+	Tet 5	5.00×10^{-2}	3+
LTC 1	1.20×10^{-1}	1+	Tet 2	2.50×10^{-2}	2+	LTC 2	7.50×10^{-2}	2+
LTC 4	1.20×10^{-1}	1+	LTC 4	7.50×10^{-2}	1+	LTC 3	1.00×10^{-1}	2+
LTC 5	3.00×10^{-1}	1+	D4	7.50×10^{-2}	1+	LTC 4	1.00×10^{-1}	2+
LTC 2	5.00×10^{-1}	2+	LTC 2	1.20×10^{-1}	1+	LTC 1	1.00×10^{-1}	2+
Tet 3	5.00×10^{-1}	2+	D5	1.50×10^{-1}	1+	D3	1.20×10^{-1}	1+
Tet 5	5.00×10^{-1}	2+	Tet 4	1.80×10^{-1}	1+	D5	1.50×10^{-1}	1+
D2	1.20×10^0	1+	LTC 5	1.90×10^{-1}	1+	Tet 2	1.50×10^{-1}	2+
D3	1.20×10^0	1+	LTC 3	3.70×10^{-1}	1+	Tet 4	2.50×10^{-1}	1+
D1	1.50×10^0	1+	Tet 3	4.00×10^{-1}	1+	LTC 5	3.00×10^{-1}	2+
D5	2.50×10^0	1+	Tet 5	5.00×10^{-1}	1+	Tet 3	5.00×10^{-1}	2+
LTC 3	2.00×10^1	2+	D1	7.50×10^{-1}	2+	D1	1.50×10^0	1+
D4	N/A	N/A	D3	1.00×10^0	1+	D4	1.50×10^1	1+

Based on this data, it is clearly observed that the tetracationic pairing agents consistently produce the best sensitivity for all phospholipids tested. In particular, it can be seen that **Tet 2**, a tetracationic reagent with phosphonium core moiety containing a total of ten phenyl functional groups and C4 alkyl linkages, shows the best sensitivity (ppq) for **PI, PS, PC** and **CA**. Out of these four phospholipids, **PI, PS**, and **CA** cannot be otherwise detected in the positive ion mode.^{155,164}

Under normal conditions they can only be detected in the negative ion mode. For comparison purposes the SIM limits of detection for these analytes were completed in the negative ion mode as well under the same conditions (Table 5-2). The LODs achieved in the negative ion mode were significantly higher than the ones found in the positive ion mode ESI-MS. For instance, the sensitivity for phosphatidylinositol (**PI**) was found to be 80 times better in the positive ion mode than the negative ion mode (Table 5-2). Also, cardiolipin (**CA**) has an improved LOD of 40,000 times in the positive ion mode, and even a higher LOD is observed for phosphatidylserine (**PS**) in which the sensitivity is improved by 400,000 times in the positive mode.

Table 5-2 LODs for Each Phospholipid Analyzed in the Negative Ion Mode ESI-MS.

Phospholipid	Anion Mass (g/mol)	SIM LOD (ng)
L-Phosphatidic Acid (PA)	671.89	1.50E+00
Phosphatidylglycerol (PG)	745.98	5.00E-01
Phosphatidylinositol (PI)	886.12	4.00E-01
Phosphatidylserine (PS)	758.97	4.00E+00
Phosphatidylcholine (PC)	758.06	ND ^a
Phosphatidylethanolamine (PE)	746.05	ND
Cardiolipin (CA)	1447.9	2.00E+01
Sphingosyl PE (SPE)	422.29	1.70E-01
Diheptanoyl-phosphocholine (DHPC)	481.28	ND

^aNot Detected at 10µg/mL

Another ion pairing reagent that also performed well in giving low limits of detection for phospholipids was **Tet 4**. This is a tetracationic reagent that is structurally very similar to **Tet 2**. Its structure contains phosphonium based moieties and a mixture of propyl-, and phenyl functional groups. This ion pairing reagent showed the lowest sensitivity for phosphatidylglycerol (**PG**) and phosphatidic acid (**PA**). These two phospholipids are usually detected in the negative ion mode as well (Table 5-2). Our analysis showed that **PA** and **PG** have an improvement in sensitivity of 30,000 times and 590 times respectively, when detected in the positive ion mode using the ion pairing method (versus the detection in the negative ion mode, Table 5-2).

Tet 4 also performed well as the second best pairing reagent for phosphatidylinositol (**PI**), phosphatidylserine (**PS**), and cardiolipin (**CA**). The rest of the tetracationic reagents that resulted in low sensitivities for our analytes were **Tet 1** followed by **Tet 3** and **Tet 5**. These phosphonium based tetracationic reagents, particularly the ones containing phenyl groups, previously have been shown to work very well at lowering the LODs of many anions.^{216, 241} This could possibly be due to the additional π - π interactions that are present within their structures. Furthermore, having a localized charge on the phosphonium functional group rather than a delocalized charge such as the imidazolium moiety, might affect the coulombic interactions between the ion pairing reagent and the analyte, therefore affecting overall sensitivity. Additional mechanistic studies are needed to further understand this behavior of these reagents.²¹

The second group of ion pairing reagents that performed well in detecting low levels of phospholipids were the dicationic reagents. In particular, **D 1** (Figure 5-1) produced the best sensitivity within this category. **D 1** is an imidazolium based reagent containing a C9 linkage chain. Following this reagent, were **D 2** and **D 3** dications that resulted in adequate sensitivities when coupled with the phospholipids. These cationic

reagents include imidazolium and pyrrolidinium moieties respectively. As seen from Table 5-1, the worst performing reagents in this category were **D 4** and **D 5**. The common feature of these two ions is the C12 alkyl linkage. The terminal end groups are tripropyl phosphonium and butyl imidazolium for **D 4** and **D 5** respectively. In this group of ion pairing reagents, it was observed that the length of the alkyl chain seems to be an important feature for sensitive detection of phospholipids. In this case, the chain length varied from C5 to C9 and C12, and it was noticed that the dicationic reagent containing C9 chain linkage resulted in the lowest LODs.

The last group of the ion pairing reagents tested were the linear tricationic ion pairing reagents. Overall, this group of reagents did not produce very good sensitivities for the nine phospholipids, as seen in Table 5-1. All of the tricationic pairing reagents used in this study were linear and contained imidazolium based cores in their structure. The differences among them included the different terminal charged groups and the length of the alkyl chain linkages. Based on our results from the other pairing agents, it was hypothesized that the phosphonium based linear ion pairing reagents might produce lower LODs for the analytes. Thus, a study was completed with a linear ion pairing reagent containing tripropyl phosphonium terminal groups, an imidazolium core, and C12 alkyl linkage. **PG** and **PI** were detected with this ion pairing reagent. However no further improvement was noticed in their LODs. To further understand these results, an extended study would be needed.

5.3.3. Detection of Phospholipids Using IPRs in the Positive SRM Mode ESI-MS

In addition to SIM analysis, single reaction monitoring (SRM) experiments were performed as well on these analytes. Previous studies have shown that in many cases SRM analysis further improves the LODs compared to the SIM analysis.^{240, 241}

However, this was not the case for the phospholipids. In this study it was observed that SRM analysis did not improve the sensitivity of the analytes except in a few instances.

For most of the phospholipids, SRM data were not able to be collected because of two main reasons: first, the background noise was very low therefore making it difficult to accurately identify the LODs, and secondly, in many cases a fragment from the parent ion was not observed when energy was applied to the mass of interest. In the instances in which a fragment was detected and enough background noise was available, the LODs monitored for the analytes did not improve when compared to the LODs in the SIM ion mode. Also, the fragments detected were mainly from the ion pairing reagents, in particular the tetracationic reagents.

During the SIM analysis, all possible combinations of ion pairing agents and the analyte were observed and tested. The complex that produced the highest signal was further analyzed and the lowest limit of detection was found for that complex until a signal to noise ratio of three is achieved. For the dicationic reagents the only type of complex formed is a singly charged complex (1+). However due to their multiple charged state, the tricationic and tetracationic reagents create more possibilities of charged complexes to be observed. It was noticed that linear tricationic agents that have short alkyl chain linkages (i.e., **LTC 1** and **LTC 5**, Figure 5-2) mainly formed doubly charged complexes (2+). On the contrary, the tricationic agents that contained long alkyl chain linkages within their structure (i. e., **LTC 2**, **LTC 3**, **LTC 4**, Figure 5-2) mainly formed singly charged complexes (1+).

The tetracationic ion pairing reagents mainly formed doubly charged complexes (2+). **Tet 2** formed an equal number of 2+ and 3+ complexes, whereas **Tet 4** was the only tetracationic reagent that mainly formed 3+ complexes. During the analysis with **Tet**

1 and **Tet 3**, in only a few instances there were singly charged (1+) complexes observed. In every case the complex charge that produced the best LODs is given in Table 5-1.

5.3.4. HPLC-ESI-MS Analysis of Phospholipids

LC analysis was coupled with this technique to further enhance the chromatographic detection of the analytes. Reverse phase LC was first used to separate two phospholipids, **PC** and **PE**. The total ion chromatogram which includes the separation of the analytes and the MS detection of these phospholipids is shown in chromatogram (A) of Figure 5-4. This separation was achieved on a C18 stationary phase. Chromatogram (B) of Figure 5-4 shows the extracted ion chromatogram in which the total mass of the phospholipids and the ion pairing reagent is monitored. In this chromatographic separation the ion pairing reagent was added post column at a flow rate of 100 $\mu\text{L}/\text{min}$. The other peaks observed on chromatogram (A) correspond to other homologous species of **PC** and **PE**. The HPLC chromatogram for the separation of these analytes does not show as many peaks as are seen in the total ion chromatogram (A) in Figure 5-4. This is one advantage that the mass spectrometer has over the ultraviolet (UV) detection often used in HPLC. Analytes that do not absorb at a certain wavelength, in this case 210 nm, cannot be detected by the UV detector, however they can easily be detected by the mass spectrometer as long as they can be ionized.

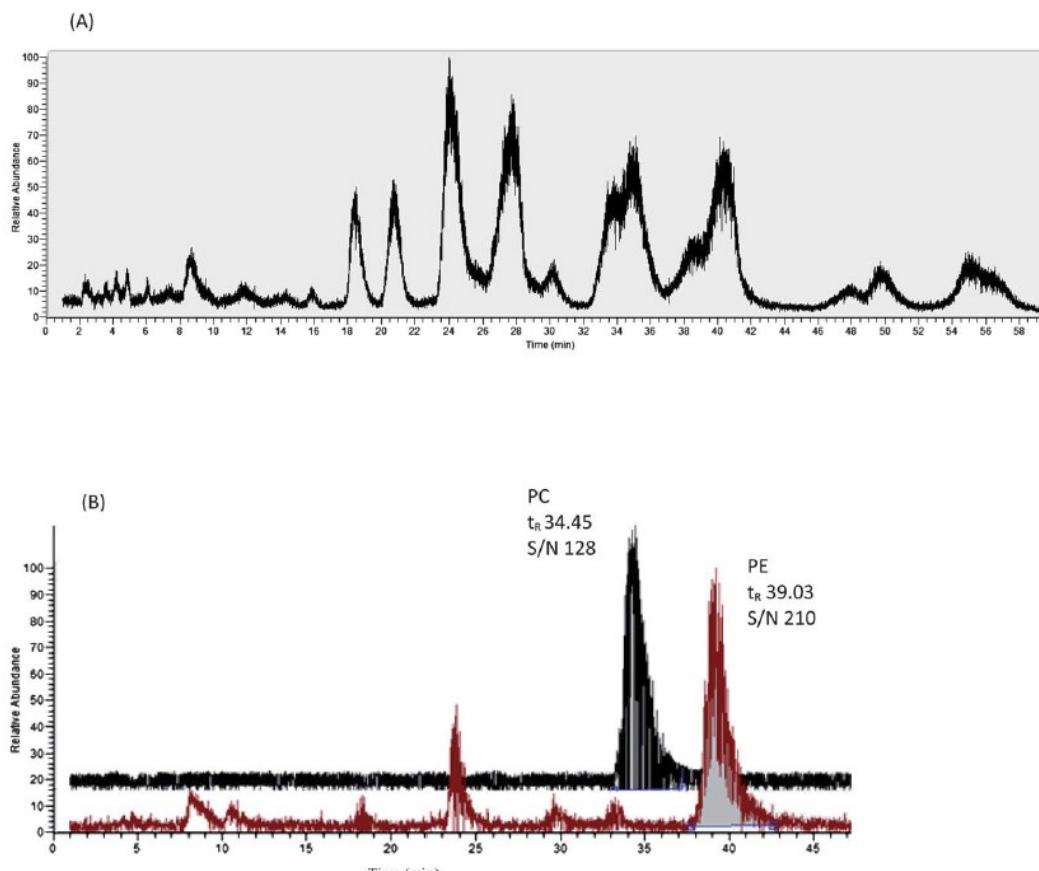


Figure 5-4 Chromatographic Separation and Detection of the PC and PE Mixture and Their Homologues in the SIM Positive Mode ESI-MS. (A) Total Ion Chromatogram of This Mixture and (B) Extracted Ion Chromatogram in Which the Major Species of the Phospholipids are Detected with Tetracation Ion Pairing Reagent Tet 5.

The extracted ion chromatogram (Figure 5-4, B) shows increased background noise and not a very high signal to noise (S/N) ratio for these analytes. This signal to noise ratio would result in a much higher LOD than the one reported in Table 5-1. This decrease in sensitivity is possibly due to the protonation of these analytes by the formic acid present in the mobile phase of this chromatographic separation (see Experimental). Also, another reason contributing to this decrease in sensitivity could be the mobile

phase used in the chromatographic separation, which is not composed of the same solvents that were used in the ESI-MS analysis for the detection of the phospholipids with the ion pairing reagents.

Since this type of LC analysis did not show very high sensitivity, another chromatographic method was developed in which formic acid was omitted and the solvents used were more similar to the ones chosen during the detection of the analytes with just the ion pairing reagent as described earlier. This separation was achieved on a silica column (Figure 5-5) with a mobile phase of 70/20/10 acetonitrile/methanol/water. Under these conditions there were three phospholipids that were detected, **PG**, **PC**, and **PE**, where **PG** is a phospholipid that is usually detected in the negative ion mode. The signal to noise ratio in this case remained high and very comparable to the previous results reported in Table 5-1. Another advantage of using the HILIC phase HPLC in this case is the shorter retention times (approximately 9 minutes).

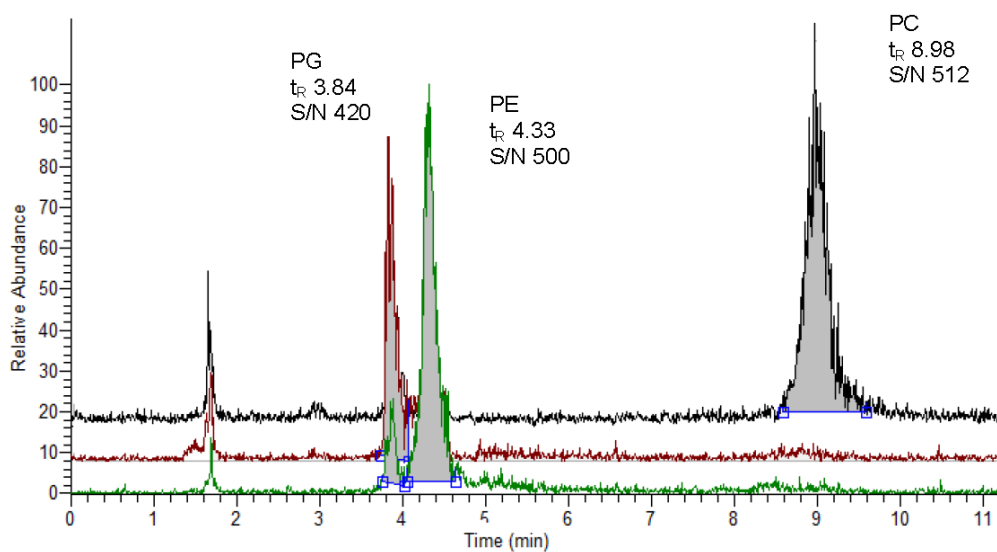


Figure 5-5 Extracted Ion Chromatogram Displaying the LC Separation of PC, PG, and PE on a Silica Column in the Positive Ion Mode ESI-MS.

5.4. Conclusions

Fifteen different cationic ion-pairing reagents were used in determining the limits of detection of nine phospholipids in the positive mode ESI-MS. The reagents that performed best were the tetracationic pairing reagents, followed by the dicationic and the linear tricationic ion pairing reagents. In particular it was **Tet 2** and **Tet 4**, phosphonium based reagents (Figure 5-3) that lowered the limits of detection for most of the phospholipids. The best dicationic reagent in this analysis was **D 1**, which also significantly increased the sensitivity of the analytes. The linear tricationic reagents performed equally when compared to each other, but gave poorer results when compared to the other groups of reagents. However as a whole group, based on previous studies, linear tricationic reagents did not perform as well as was expected.¹¹⁶ Thus, in detecting phospholipids tetracationic ion pairing reagents, with phosphonium moieties, and phenyl functional groups are recommended in achieving low limits of detection.

LC analysis was developed in both reverse and HILIC phase HPLC. It was also shown in this study that these chromatographic separations were successfully coupled to this ion pairing technique, and a separation and detection of three phospholipids (**PC**, **PG**, and **PE**) was achieved in the HILIC phase mode with satisfactory signal to noise ratios and very short retention times. Other advantages of this technique, besides low limits of detection, and compatibility with HPLC, are ease of use, simplicity, and fast analysis times.

Chapter 6

Separation and Sensitive Determination of Sphingolipids at Low Femtomole Level by Using HPLC-PIESI-MS/MS

Abstract

A highly sensitive paired ion electrospray ionization mass spectrometry (PIESI-MS) approach was developed for the trace determination of sphingolipids. Apart from their structure role, specific sphingolipids can play a role in cell signaling and as disease markers. With the optimal pairing reagents, detection limits ranged from low femtomole to picomole levels for 14 selected sphingolipids. This improved the detection sensitivity of ESI-MS for many of these analytes up to 4100 times.

6.1. Introduction

Sphingolipids (SLs) are a family of bioactive lipids with considerable functional and structural diversity. Beyond their role as a major class of structural lipids in the cellular membranes of eukaryotes,^{168,169} SLs and their metabolites also are involved in other important biological functions, such as signal transduction and the regulation of cell growth, differentiation, and apoptosis.¹⁷⁰⁻¹⁷² Both the levels of sphingolipids and the expression of their metabolizing enzymes has been shown to be altered in human diseases, such as Niemann-Pick disease^{173,174} and Alzheimer's disease¹⁷⁵. The biosynthetic pathways of sphingolipid metabolism begins with the condensation of palmitoyl CoA and serine to form 3-ketosphinganine, which is further reduced to produce the sphingoid base.¹⁷⁶ The sphingoid base backbone is subsequently acylated with a fatty acid, and the resulting ceramides produce sphingolipids via ester linkages to the hydrophilic headgroups. Of particular significance are phosphorycholine in case of

sphingomyelin and oligosaccharide residues in case of gangliosides.^{173,176-178} Various combinations of sphingoid bases, fatty acids, and hydrophilic headgroups result in numerous subspecies of sphingolipids.

Biological studies of sphingolipids require analytical approaches that can determine these entities with high specificity and sensitivity. Due to the structure similarity of many sphingolipid species, their often low concentrations, and the scarcity of their metabolites; both quantitative and qualitative analysis can be problematic. Mass spectrometry (MS) has been shown to be a useful analytical technique for sphingolipid analysis given its outstanding specificity, sensitivity, and speed.¹⁷⁹ Methodologies based on several types of mass spectrometry has been developed for sphingolipid analysis, including fast atom bombardment mass spectrometry (FAB-MS),^{180,181} matrix assisted laser desorption ionization mass spectrometry (MALDI-MS),¹⁸² atmospheric pressure chemical ionization (APCI),^{183,184} and electrospray ionization mass spectrometry (ESI-MS)^{168,184-186}. ESI-MS has unique advantages for sphingolipid determination, because it is easily coupled with chromatographic separation techniques, such as high-performance liquid chromatography (HPLC), and it is able to perform tandem MS for structure elucidation. In recent years, in-depth profiles of a large number of sphingolipids and their metabolites have been achieved with the use of HPLC-ESI-MS.^{179,187}

Paired ion electrospray ionization (PIESI) mass spectrometry was developed as a technique that provides ultrasensitive detection for anions.^{17-20,82} This technique involves introducing low concentrations of structurally optimized ion-pairing reagents (IPRs) into the sample stream, thereby allowing the anionic molecules and some zwitterions to be measured with high sensitivity in the positive ion mode ESI-MS as the anion/IPR associated complex. With the use of optimal IPRs, sub-picogram limits of detection (LOD) can be achieved for small organic anions and inorganic anions.^{20,77}

Further, it was shown that PIESI-MS is useful for both anions and zwitterions of moderate size molecules such as phospholipids.⁸¹ The mechanism for the great sensitivity enhancement obtained by PIESI was recently investigated.^{21,22} In the present study, methods for separation and ultrasensitive detection of sphingolipids utilizing HPLC-PIESI-MS are developed and discussed. The detection limits for 14 sphingolipids, including sphingomyelins, phosphosphingolipids, gangliosides, and sulfatides, were evaluated by using dicationic ion pairing reagents and tetracationic ion pairing reagents. The best ion pairing reagent for sphingolipid determinations were optimized. HPLC was used with PIESI-MS detection for sphingolipid sample mixtures.

6.2. Experimental

6.2.1. Chemicals

Dicationic ion-pairing reagents 1,5-pentanediy-bis(1-butylpyrrolidinium) difluoride (**Dicat I**) and 1,5-pentanediy-bis(3-benzylimidazolium) difluoride (**Dicat II**) were originally developed in our laboratory, and are now commercially available from Sigma-Aldrich (St. Louis, MO). The synthetic procedures of the tetracationic ion-pairing reagents (**Tetcat I** and **Tetcat II**) were described in our previous publications.²⁹

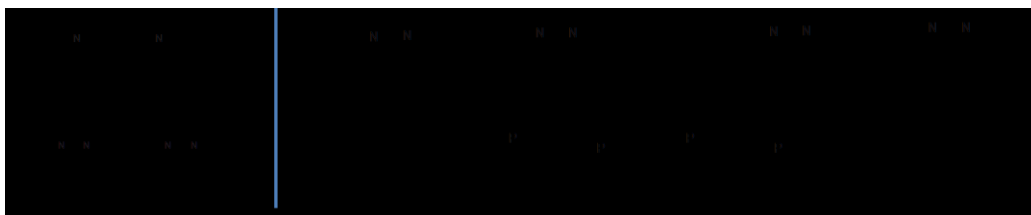


Figure 6-1 Structures and Abbreviations of the Dicationic Ion Pairing Reagents and Tetracationic Ion Pairing Reagents Used in this Study

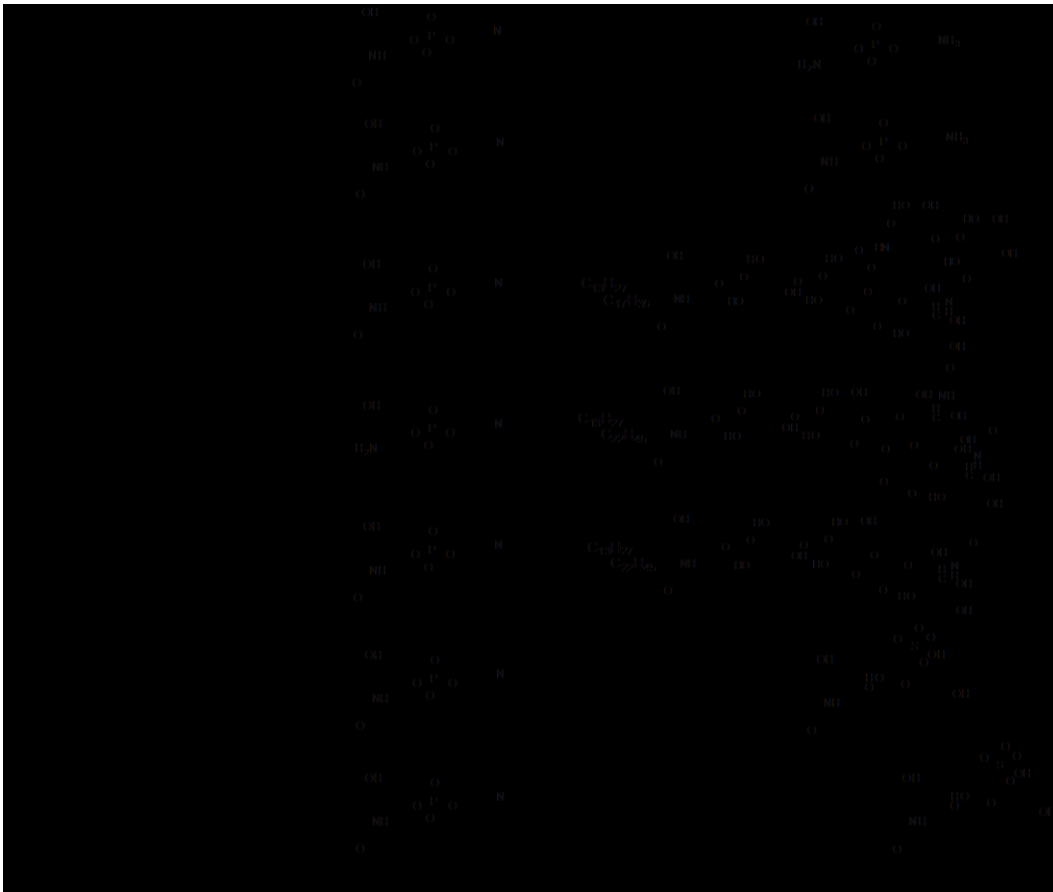


Figure 6-2 Structures and Abbreviations of the Sphingolipids

They were initially synthesized with the bromide ion as the counterion and converted to their fluoride salt form by using ion exchange resin prior to analysis. The structures of the four ion-pairing reagents are shown in Figure 6-1. Natural sphingomyelins standards (SM(d18:1/18:0), SM(d18:1/16:0), and SM(d18:1/23:0)), synthetic sphingomyelins standards (SM(d18:1/0:0), SM(d18:1/2:0), SM(d18:1/6:0), and SM(d18:1/12:0)), phosphosphingolipids (PE-Cer(d18:1/0:0) and PE-Cer(d17:1/12:0)), gangliosides (GM1, GM3, and GD3), and sulfatides (I3SO3-GalCer(d18:1/24:0) and I3SO3-GalCer(d18:1/12:0)) were purchased from Avanti Polar Lipids (Alabaster, AL) and

Matreya (Pleasant, PA). The structures of these sphingolipids are shown in Figure 6-2. The standard solutions used for LOD determination were prepared with methanol/water (50:50, v/v) mixture. HPLC-grade water, methanol, and acetonitrile were purchased from Honeywell Burdick and Jackson (Morristown, NJ).

6.2.2. Instrumentation

The PIESI-MS analyses were performed using a Finnigan LXQ mass spectrometer (Thermo Fisher Scientific, San Jose, CA). The mass spectrometry condition in the positive ion mode was set as follows: spray voltage, 3kV; capillary temperature, 350°C; capillary voltage, 11V; sheath gas flow, 37 arbitrary units (AU); and the auxiliary gas flow, 6 AU. For the analysis in the negative ion mode, an opposite polarity was used while other instrumental parameters were the same. In the selected reaction monitoring (SRM) acquisition mode, the normalized collision energy was set at 30, the activation time was set at 30 ms, and the Q value was set at 0.25. A description and a schematic diagram of the instrumental configuration of PIESI-MS have been given in our previous publications.^{20,82} The PIESI-MS instrumental configuration is similar to the operation principle of the flow injection analysis (FIA). Briefly, a continuous flow of a carrier solution (67% MeOH/33% H₂O, v/v) was provided by a Surveyor MS pump (Thermo Fisher Scientific, San Jose, CA) at a flow rate of 300 µL/min, and the ion-pairing reagent solution (40 µM IPR dissolved in H₂O) provided by a Shimadzu LC-6A pump (Shimadzu, Columbia, MD) was merged into the carrier solution at a flow rate of 100 µL/min through a Y-type mixing tee. This instrumental configuration results in a total flow rate of 400 µL/min and a final solvent composition of 50% MeOH/50% H₂O with 10 µM dicationic ion-pairing reagent flowing into the mass spectrometer. The sample was injected into the carrier solution through a six-port injection valve, and then reacted with the IPR in the mixing tee before reaching the mass spectrometer. For the HPLC-PIESI-MS analysis, a

column was installed between the injection valve and the mixing tee, so that the post-column addition of the ion-pairing reagent was achieved. The instrumental detection limits (LOD) were determined by serial dilutions of the standard solution until a signal-to-noise ratio of 3 was noted in 5 replicate injections of each sample. Mass-to-charge ratios of sphingolipids monitored in the SIM and SRM mode were listed Table 6-1 and Table 6-2. The HPLC separation was achieved by using a Supelco Ascentis™ C18 column (250 mm × 2.1 mm) with isocratic elution (40% MeOH/60% H₂O) in 15 min. A 5µL sample loop was used for both the LOD determination and the HPLC-PIESI-MS analysis. Xcalibur 2.0 software was used for the data analysis.

6.3. Results and Discussion

6.3.1. LODs of Sphingolipids by PIESI-MS in the Single Ion Monitoring Mode

The dicationic ion pairing reagents (**Dicat I** and **Dicat II**) and tetracationic ion pairing reagents (**Tetcat I** and **Tetcat II**) were selected as they provided the best performance for the singly charged anions and the zwitterions respectively in previously studies.^{20,81} The charged moieties and alkyl linkage chain lengths of the IPRs determine the binding affinity between IPR and sphingolipid and also the surface activity of the IPR/sphingolipid associated complex. These are the essential structural properties that affect the observed detection limits of PIESI analyses. Utilizing structurally optimized ion-pairing reagents, all the sphingolipids are sensitively detected by using PIESI-MS in the positive single ion monitoring mode (SIM) (Table 6-3). The LODs obtained cover a broad range from 2 fmol to 30 pmol. The LODs for two sphingolipids in the SIM mode reached low fmol levels (see SM (d18:1/2:0) (2 fmol by using **Dicat I**) and SM (d18:1/16:0) (8 fmol by using **Dicat II**) in Table 6-3).

Table 6-1 Mass-to-Charge Ratio of Sphingolipids Monitored in the Positive SIM Mode Using PIESI-MS

Analyte	Dicat I		Dicat II		Tetcat I		Tetcat II		Without IPR	
	m/z monitored	Charge state	m/z monitored	Charge state	m/z monitored	Charge state	m/z monitored	Charge state	m/z monitored	Charge state
d18:1, C18:0 SPM	527.5	2+	558.4	2+	496.4	3+	448.3	4+	731.6	1+
d18:1, C16:0 SPM	513.5	2+	544.4	2+	365.3	4+	441.3	4+	703.6	1+
d18:1, C23:0 SPM	562.5	2+	593.5	2+	519.4	3+	465.8	4+	801.7	1+
d18:1 SPM	394.4	2+	425.3	2+	610.5	2+	508.6	3+	465.3	1+
d18:1, C2:0 SPM	415.4	2+	446.3	2+	421.3	3+	522.6	3+	507.4	1+
d18:1, C6:0 SPM	443.4	2+	474.3	2+	330.3	4+	541.3	3+	563.4	1+
d18:1, C12:0 SPM	485.4	2+	516.4	2+	351.3	4+	569.3	3+	647.5	1+
d18:1 SPPE	373.3	2+	404.3	2+	589.5	2+	1481.8	1+	423.3	1+
d17:1, C12:0 SPPE	457.4	2+	488.4	2+	673.5	2+	825.5	2+	591.4	1+
GM1	1869.2	1+	1931.1	1+	767.8	3+	869.1	3+	1544.9	1-
GM3	1574.2	1+	1636.1	1+	669.5	3+	1155.7	2+	1249.8	1-
GD3	1865.3	1+	1927.2	1+	766.5	3+	867.8	3+	769.9	2-
d18:1, C24:0 GalCer	1130.9	1+	1192.8	1+	782.6	2+	934.5	2+	806.6	1-
d18:1, C12:0 GalCer	1046.8	1+	1108.7	1+	740.0	2+	892.0	2+	722.5	1-

Table 6-2 Mass-to-Charge Ratio Monitored During Collision Induced Dissociation (CID) in the Positive SRM Mode

Analyte	Dicat I		Dicat II		Tetcat I		Tetcat II	
	m/z precursor ion	m/z monitored	m/z precursor ion	m/z monitored	m/z precursor ion	m/z monitored	m/z precursor ion	m/z monitored
d18:1, C18:0 SPM	528.48	162.2	558.43	227.3	496.39	252.6	448.54	279.3
d18:1, C16:0 SPM	513.46	162.2	544.41	227.3	365.29	252.6	441.27	184.1
d18:1, C23:0 SPM	562.52	436.4	593.47	227.3	519.43	252.6	465.8	184.1
d18:1 SPM	394.35	162.2	425.3	227.3	610.47	385.7	508.61	406.3
d18:1, C2:0 SPM	415.35	162.3	446.3	227.3	421.32	252.6	522.62	353.9
d18:1, C6:0 SPM	443.38	162.3	474.33	193.3	330.25	252.6	541.3	353.9
d18:1, C12:0 SPM	485.43	162.2	516.38	193.3	351.28	252.6	569.33	353.9
d18:1 SPPE	373.32	162.2	404.27	193.3	589.45	378.3	1481.79	557.3
d17:1, C12:0 SPPE	457.4	162.3	488.35	193.3	673.52	594.4	825.47	694.5
GM1	1869.22	1742.1	— ^a	— ^a	767.81	671.2	869.12	503.3
GM3	1574.17	1447	— ^a	— ^a	669.47	252.3	1155.66	1025.1
GD3	— ^a	— ^a	— ^a	— ^a	766.5	669.5	867.8	821.9
d18:1, C24:0 GalCer	1130.9	923.9	— ^a	— ^a	782.56	427.3	934.61	803.7
d18:1, C12:0 GalCer	— ^a	— ^a	1108.7	385.3	— ^a	— ^a	891.98	761.5

^aNot detected.

Table 6-3 Limits of Detection of Sphingolipids Standard Solutions Obtained in the Positive SIM Mode Using PIESI-MS

Analyte	Dicat I	Dicat II	Tetcat I	Tetcat II	Best LOD	Best IPR ^a
	LOD (pmol)	LOD (pmol)	LOD (pmol)	LOD (pmol)	LOD (pmol)	
SM(d18:1/18:0)	0.2	1	1	5	0.2	Dicat I
SM(d18:1/16:0)	0.1	0.008	0.2	0.8	0.008	Dicat II
SM(d18:1/23:0)	30	2	1	30	1	Tetcat I
SM(d18:1/0:0)	1	0.2	0.6	2	0.2	Dicat II
SM(d18:1/2:0)	0.002	0.1	0.3	0.6	0.002	Dicat I
SM(d18:1/6:0)	0.08	0.09	0.2	0.4	0.08	Dicat I
SM(d18:1/12:0)	0.1	0.05	0.06	1	0.05	Dicat II
PE-Cer(d18:1/0:0)	1	0.4	0.01	0.1	0.01	Tetcat I
PE-Cer(d17:1/12:0)	0.2	2	0.03	0.4	0.03	Tetcat I
GM1	6	20	1	2	1	Tetcat I
GM3	20	10	0.4	3	0.4	Tetcat I
GD3	10	20	2	30	2	Tetcat I
I3SO3-GalCer(d18:1/24:0)	1	5	2	0.6	0.6	Tetcat II
I3SO3-GalCer(d18:1/12:0)	0.1	0.2	0.07	0.06	0.06	Tetcat II

^aSee Figure 6-1 for the IPR structures and abbreviations.

It was shown that the LODs for the same sphingolipids can be significantly different when using different IPRs. For example, the LOD of SM (d18:1/2:0) was 600 fmol when using **Tetcat II**, while it was 2 fmol with the use of **Dicat I**, indicating a 300 times difference in detection sensitivity. By using the optimal IPR, low fmol to pmol level LODs were obtained for all 14 sphingolipids. Interestingly, we found that the performances of the dication and tetracation IPRs on sphingolipid detection are complementary. Tetracationic IPRs show the best performance for phosphosphingolipids, gangliosides and sulfatides, while the dicationic IPRs were best for the determination of sphingomyelins (Table 6-3). Overall, **Tetcat I** was shown to be the best IPR for sphingolipid detection in the SIM mode. It was hypothesized that relatively higher detection sensitivity achieved by **Tetcat I** could be due to its longer alkyl linkage chain compared to other IPRs. This property may result in a higher affinity to the hydrophobic ceramide backbone of the sphingolipids, which would increase the presence of the IPR/sphingolipid associated complex, and consequently lead to a higher ESI response.

6.3.2. LODs of Sphingolipids by PIEESI-MS in the Selected Reaction Monitoring Mode

The LODs in the selected ion monitoring (SRM) mode were evaluated by using the IPR/sphingolipid complex ion as the precursor ion and the most abundant fragment as the daughter ion (Table 6-4). The SRM mode often provides better sensitivity than the SIM mode due to the enhancement in analyte specificity and background noise reduction. It was found that the LODs for most sphingolipids in the SRM mode were improved by 2 to 67 times compared to the SIM mode detection obtained using the same IPR. The LODs obtained for 13 out of 14 sphingolipids were below 1 pmol with the use of the optimal IPR in the SRM mode (Table 6-4). Compared to ESI-MS detection without using IPRs, PIEESI-MS approach improved the LODs by 10 to 4000 times for most of sphingolipids analyzed (Table 6-5).

Table 6-4 Limits of Detection of Sphingolipids Standard Solutions Obtained in the Positive SRM Mode Using PIESI-MS

Analyte	Dicat I	Dicat II	Tetcat I	Tetcat II	Best LOD	Best IPR ^a
	LOD (pmol)	LOD (pmol)	LOD (pmol)	LOD (pmol)	LOD (pmol)	
SM(d18:1/18:0)	0.05	1	0.1	7	0.05	Dicat I
SM(d18:1/16:0)	0.1	0.3	0.06	0.3	0.06	Tetcat I
SM(d18:1/23:0)	5	2	1	3	1	Tetcat I
SM(d18:1/0:0)	1	0.2	0.06	0.2	0.06	Tetcat I
SM(d18:1/2:0)	0.04	0.08	0.3	0.6	0.04	Dicat I
SM(d18:1/6:0)	0.06	0.05	0.07	0.4	0.05	Dicat II
SM(d18:1/12:0)	0.02	0.05	0.05	0.5	0.02	Dicat I
PE-Cer(d18:1/0:0)	0.2	2	0.004	0.1	0.004	Tetcat I
PE-Cer(d17:1/12:0)	0.2	0.03	0.02	0.08	0.02	Tetcat I
GM1	1	— ^b	0.6	2	0.6	Tetcat I
GM3	0.4	— ^b	0.4	0.2	0.2	Tetcat II
GD3	— ^b	— ^b	0.2	6	0.2	Tetcat I
I3SO3-GalCer(d18:1/24:0)	1	— ^b	2	0.2	0.2	Tetcat II
I3SO3-GalCer(d18:1/12:0)	— ^b	7	— ^b	0.009	0.009	Tetcat II

^aSee Figure 6-1 for the IPR structures and abbreviations.

^bNot detected.

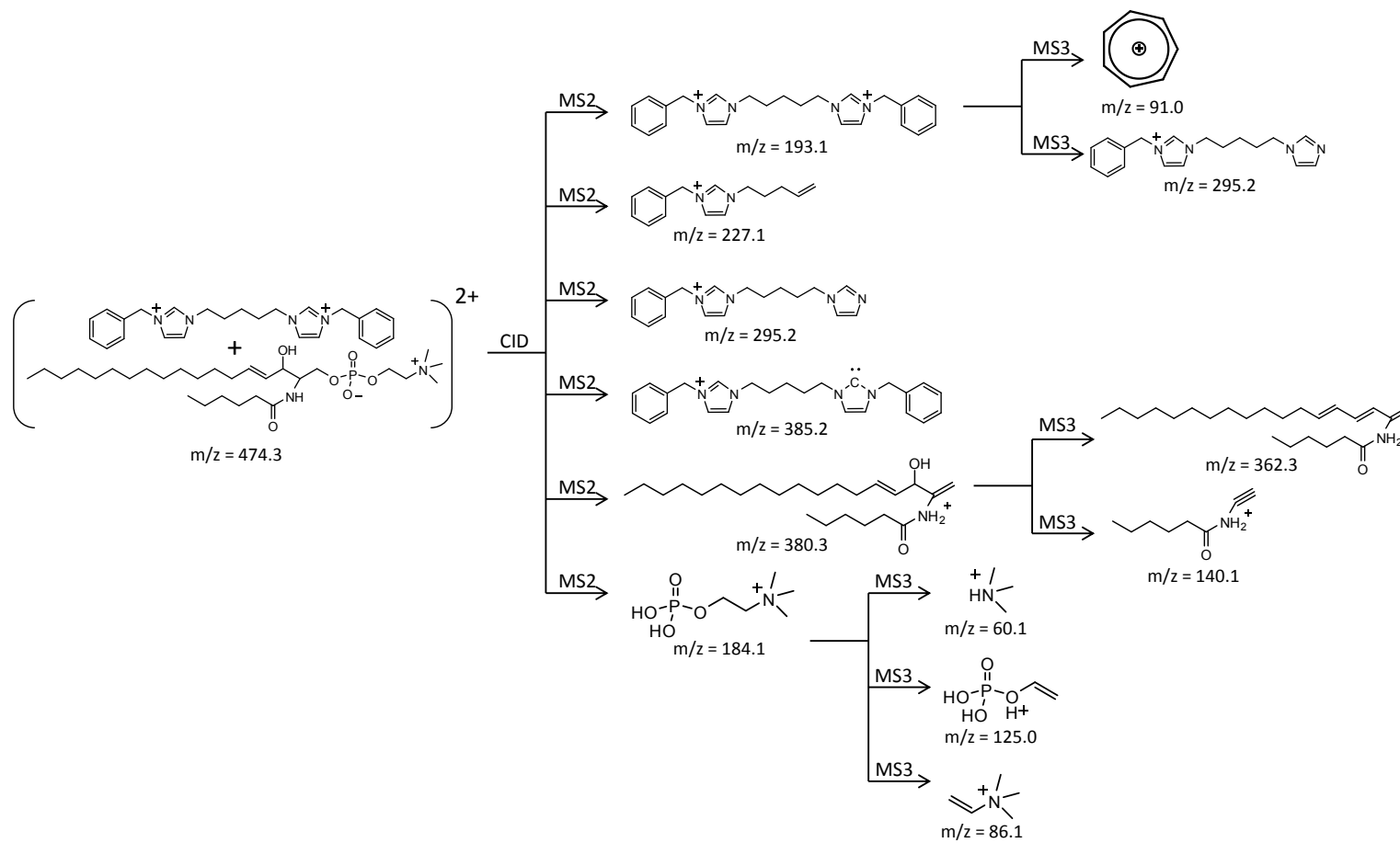


Figure 6-3 Proposed CID Fragmentation Pathways of Complex $[\text{SM}(\text{d}18:1/6:0) + \text{Dicat II}]^{2+}$ $m/z: 474.3$

Table 6-5 Comparison of Limits of Detection of Sphingolipids Standard Solutions Obtained by Using PIESI-MS and ESI-MS without Using IPR

Analyte	Best LOD by PIESI-MS	Without using IPR	Improvement factor ^a
	LOD (pmol)	LOD (pmol)	
SM(d18:1/18:0)	0.05 ^c	30 ^d	600
SM(d18:1/16:0)	0.008 ^b	30 ^d	4000
SM(d18:1/23:0)	1 ^{b, c}	40 ^d	40
SM(d18:1/0:0)	0.06 ^c	0.02 ^d	0.3
SM(d18:1/2:0)	0.002 ^b	0.8 ^d	400
SM(d18:1/6:0)	0.05 ^c	0.8 ^d	16
SM(d18:1/12:0)	0.02 ^c	4 ^d	200
PE-Cer(d18:1/0:0)	0.004 ^c	0.04 ^d	10
PE-Cer(d17:1/12:0)	0.02 ^c	6 ^d	300
GM1	0.6 ^c	10 ^e	17
GM3	0.2 ^c	2 ^e	10
GD3	0.2 ^c	2 ^e	10
13SO3-GalCer(d18:1/24:0)	0.2 ^c	0.3 ^c	1
13SO3-GalCer(d18:1/12:0)	0.009 ^c	0.01 ^e	1

^aTimes of improvement of LODs obtained using PIESI-MS vs. LODs obtained by ESI-MS without using IPR.

^bObtained in the SIM mode by PIESI-MS.

^cObtained in the SRM mode by PIESI-MS.

^dMeasured in the positive ion mode.

^eMeasured in the negative ion mode.

Table 6-6 Comparison of Limits of Detection of Sphingolipid Standards Obtained by Using PIESI-MS and Formic Acid (FA) and Trifluoroacetic Acid (TFA) as Mobile Phase Additives

Analyte	PIESI-MS ^a	0.1% FA ^b	0.1% TFA ^c
	LOD (pmol)	LOD (pmol)	LOD (pmol)
SM(d18:1/18:0)	0.05	10	2
SM(d18:1/16:0)	0.008	1	0.8
SM(d18:1/23:0)	1	10	6
SM(d18:1/0:0)	0.06	0.02	0.1
SM(d18:1/2:0)	0.002	0.06	0.1
SM(d18:1/6:0)	0.05	0.09	0.05
SM(d18:1/12:0)	0.02	0.1	0.2
PE-Cer(d18:1/0:0)	0.004	0.02	0.05
PE-Cer(d17:1/12:0)	0.02	0.1	0.03

^a Data obtained from Table 6-5.

^b LOD obtained using a mobile phase of methanol/water (50:50, v/v) mixture containing 0.1% formic acid.

^c LOD obtained using a mobile phase of methanol/water (50:50, v/v) mixture containing 0.1% trifluoroacetic acid.

It should be noted that the PIESI-MS detection of SM (d18:1/0:0) shows comparable sensitivity to the detection without using IPRs. The high detection sensitivity obtained when no IPR was present could be attributed to the primary amine group of SM (d18:1/0:0), which facilitates the ionization of the specific analyte in the positive ion mode ESI-MS. Hence, there was no apparent advantage in using pairing reagents for SM (d18:1/0:0).

6.3.3. Proposed SRM Fragmentation Pathways

Figure 6-3 shows proposed fragmentation pathways of complex [SM (d18:1/6:0) + **Dicat II**]²⁺ during the collision induced dissociation (CID). The secondary ions [$C_{25}H_{30}N_4^{2+}$ (m/z = 193.1), $C_{15}H_{19}N_2^+$ (m/z = 227.1), $C_{18}H_{23}N_4^+$ (m/z = 295.2), and $C_{25}H_{29}N_4^+$ (m/z = 385.2)] were determined to be **Dicat II** and its fragments; while $C_{24}H_{46}NO_2^+$ (m/z = 380.3) and $C_5H_{15}NO_4P^+$ (m/z = 184.1) were the fragments generated from SM (d18:1/6:0) (Figure 6-3). The formation of the **Dicat II** ion suggests that the non-covalent association between **Dicat II** and SM (d18:1/6:0) was disrupted during MS2. The generation of IPR as the major fragment ion in the CID process was found to be common in these SRM experiments while this is not the only transition pathway (Table 6-2).

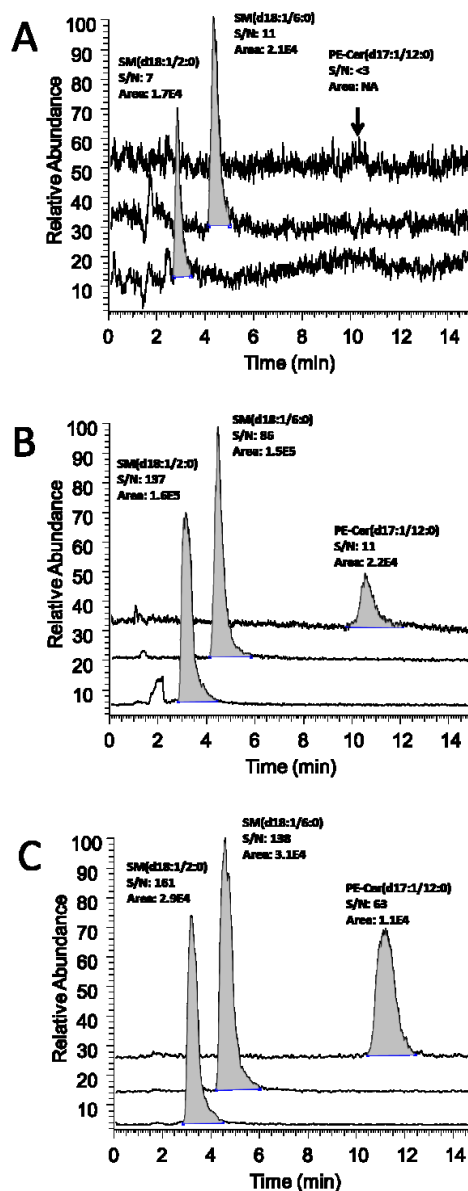


Figure 6-4 A Comparison of the HPLC-MS Separation and Sensitivity of Three Sphingolipids in the (A) Regular Positive SIM Mode HPLC-MS without Using IPR ($[\text{SM}(\text{d}18:1/2:0)]^+$ m/z : 507.4; $[\text{SM}(\text{d}18:1/6:0)]^+$ m/z : 563.4; $[\text{PE-Cer}(\text{d}17:1/12:0)]^+$ m/z : 591.4), (B) Positive SIM Mode by HPLC-PIESI-MS Using the Dicat I ($[\text{SM}(\text{d}18:1/2:0) + \text{Dicat I}]^{2+}$ m/z : 415.4; $[\text{SM}(\text{d}18:1/6:0) + \text{Dicat I}]^{2+}$ m/z : 443.4; $[\text{PE-Cer}(\text{d}17:1/12:0) + \text{Dicat I}]^{2+}$ m/z : 591.4), (C) Positive SIM Mode by HPLC-PIESI-MS Using the Dicat I² ($[\text{SM}(\text{d}18:1/2:0) + \text{Dicat I}^2]^{2+}$ m/z : 415.4; $[\text{SM}(\text{d}18:1/6:0) + \text{Dicat I}^2]^{2+}$ m/z : 443.4; $[\text{PE-Cer}(\text{d}17:1/12:0) + \text{Dicat I}^2]^{2+}$ m/z : 591.4).

$I]^{2+}$ m/z: 457.4), and (C) Positive SRM Mode by HPLC-PIESI-MS Using the Dicat I
([SM(d18:1/2:0) + Dicat $I]^{2+}$ SRM m/z: 415.4 \rightarrow 162.3; [SM(d18:1/6:0) + Dicat $I]^{2+}$ SRM
m/z: 443.4 \rightarrow 162.3; [PE-Cer(d17:1/12:0) + Dicat $I]^{2+}$ SRM m/z: 457.4 \rightarrow 162.3)

6.3.4. Analysis of Sphingolipids by HPLC-PIESI-MS/MS

Figure 6-4 is a comparison of the detection sensitivity of SM (d18:1/2:0), SM (d18:1/6:0), and PE-Cer (d17:1/12:0) by using HPLC-ESI-MS (Figure 6-4 (A)) and HPLC-PIESI-MS (Figure 6-4 (B) and (C)). It was shown in previous studies that the molecules processing phosphate moieties (i.e. sphingolipids) have inherently low ionization efficiencies in the positive ion mode ESI-MS, which results in relatively poor detection sensitivity.¹⁸⁸⁻¹⁹⁰ This is supported by the poor signal-to-noise ratio (S/N) of three sphingolipids observed in Figure 6-4 (A) (S/N = 7, 11, <3 for SM (d18:1/2:0), SM (d18:1/6:0), and PE-Cer (d17:1/12:0), respectively). When the same concentrations of sphingolipids were analyzed by HPLC-PIESI-MS, the S/N for SM (d18:1/2:0), SM (d18:1/6:0), and PE-Cer (d17:1/12:0) were increased to 137, 86, 11 in the SIM mode, and 161, 138, 63 in the SRM mode, respectively (Figure 6-4 (B) and (C)). Thus, the detection of these three sphingolipids by using HPLC-PIESI-MS approach was approximately 23 times more sensitive than HPLC-ESI-MS. Table 6-6 compares the detection of zwitterionic sphingolipids with the use of IPR, formic acid (FA) and trifluoroacetic acid (TFA) additives. As the most commonly used additives in the positive ion mode ESI-MS, FA and TFA provided decent sensitivity improvement in most cases when compared to the LODs obtained without using these acidic additives (improvement factor was 2 to 46 for FA and 8 to 170 for TFA, see Table 6-5). The IPR (PIESI) still produced better sensitivities compared to 0.1% FA and 0.1% TFA (Table 6-6). It was found that using the

optimal IPR further improves the LODs of sphingolipids by 2 to 270 times compared to using FA and TFA as mobile phase additives (Table 6-6).

6.4. Conclusions

A highly sensitive methodology based on HPLC-PIESI-MS was developed for the efficient separation and detection of sphingolipids. Utilizing the optimal IPR, detection limits from low fmol to pmol were achieved for all 14 sphingolipids analyzed, showing 10 to 4000 times sensitivity improvement compared to the ESI-MS without using IPR. The SRM experiment improved the LODs by 2 to 67 times compared to the SIM mode detection, resulting in LODs for 13 out of 14 sphingolipids below 1 pmol. While **Tetcat I** was found overall to be the best ion pairing reagent, the dications and the tetracations show complimentary performance for the determination of sphingolipids. Compared to most commonly used HPLC-ESI-MS additives, such as formic acid and trifluoroacetic acid, the PIESI approach produced better detection sensitivities of the sphingolipids. The PIESI-MS method is readily coupled with chromatographic separations (HPLC) to separate and sensitively determine the sphingolipids in a sample mixture. It can be anticipated that this method will be very useful for the sphingolipids profiling at low concentration levels.

Chapter 7

Mechanism and Sensitivity of Anion Detection Using Rationally Designed Unsymmetrical Dications in Paired Ion Electrospray Ionization Mass Spectrometry

Abstract

Paired ion electrospray ionization (PIESI) mass spectrometry was developed as a useful technique that provides sensitive detection for anions in the positive ion mode. The ion-pairing reagent (IPR) utilized plays an essential role affecting the detection limits. This work describes the design and synthesis of two novel dications with unsymmetrical structures and their utilization for anion detection and mechanistic insights. The performance of dications was evaluated for seven selected anions in both single ion monitoring (SIM) mode and selected reaction monitoring (SRM) mode. The unsymmetrical dications allowed sensitive detection for these anions with down to sub-picogram limits of detection (LOD), and an improved sensitivity from 1.5 to 12 times compared to the corresponding symmetrical dications. The enhanced sensitivity could be attributed to the surface activity of the unsymmetrical dications, which results in a concurrent strong partitioning of the anion to the aerosol droplet surface. Surface activity measurements of the anion/IPR complex were conducted and a correlation between the observed ESI responses and the surface activity of the complex was found. The mechanism was further explored and explained based on the concepts of the equilibrium partitioning model (EPM).

7.1. Introduction

The use of electrospray ionization (ESI), introduced by Fenn et al.^{14,45-47}, with mass spectrometry (MS) has grown tremendously in the last few decades. The power

and broad applicability of ESI-MS has been demonstrated in the analysis of different classes of molecules, ranging from extremely large molecules, such as proteins^{14,191,192}, polymers^{193,194}, and oligonucleotides³, to small molecules, such as lipids^{195,196} and amino acids^{197,198}. The majority of ESI-MS analyses are conducted in the positive ion mode, where the analyte cation produced from protonation/adduct formation is measured, whereas the detection of analyte anions is less preferable.²⁶ Anion detection by ESI-MS, which is not as extensively explored as the detection of cations, was primarily hampered by the low sensitivity and signal instability in the negative ion mode, resulting from the increased tendency toward electrical (corona) discharge and the inherent chemical noise.^{24,25,79}

Previously, we investigated the possibility of sensitive detection of anions in the positive ion mode by ESI-MS,^{17-20,77,81,82,113} and introduced an innovative approach named paired ion electrospray ionization (PIESI) mass spectrometry. This technique involves adding very low concentrations of multiple charged ion-pairing reagents (IPR) into the sample stream, thereby allowing the anionic molecules to be measured with extremely high sensitivity in the positive ion mode as the anion/IPR associated complexes. With the use of optimal IPRs, limits of detection (LOD) have been pushed down to sub-picogram for small organic anions,^{20,77} and to low picogram for inorganic anions.^{17,18} This technique was recently reviewed by Breitbach et al.¹⁹⁹ The advantages of PIESI were particularly notable when detecting inorganic ions (such as the halides), since they were previously hardly detectable in negative ion mode ESI-MS. Compared to the more common analytical anion detection techniques, such as ion selective electrodes, ion chromatography with conductivity detection, or atomic spectroscopy,²⁰⁰⁻²⁰⁴ PIESI-MS has shown superior performance in terms of both specificity and sensitivity. PIESI-MS also has been shown to be highly advantageous for the analysis of moderately

size lipophilic molecules such as anionic and zwitterionic phospholipids.⁸¹ The reported LODs were usually ranged from 2 to 3 orders of magnitude better than these of other known methods.

While these results have been impressive and of potential value, the use of polycationic ion-pairing agents is highly structurally dependant. For example, diquat difluoride (dication **XXII** in reference [20]) performed more than 500 times worse than structurally optimized dications used to detect singly charged anions.⁷⁷ Some common features of these “unsuccessful” IPRs usually include a relatively rigid structure and/or not containing any flexible linkage chain between the cationic moieties.^{21,77} This dichotomy of highly sensitive and insensitive detection by using structurally different dications indicates the need for a more comprehensive understanding of the characteristics of the IPR, as well as the formation and ionization mechanism of the IPR/anion complex, which could affect the observed sensitivity of this methodology.

Surface activity has been considered one of the important properties that affect all aerosol-based analytical methodologies including ESI-MS. Early on the role of surfactants and surface tension were noted for aerosol-based analytical techniques of atomic absorption and flame emission spectroscopy.⁸⁵ Subsequently similar effects were observed for ESI-MS.^{28,87,205-211} Tang and Kebarle observed that tetraalkylammonium ions, which are known to be surface active, give much higher ESI ion signals than alkali metal cations.²⁸ While the higher sensitivity of tetraalkylammonium ions can be attributed to their lower solvation energy (less solvated) and a consequent higher ion evaporation rate compared to alkali metal cations, they also suggested that the surface activity of the analytes may play an important role. The surface-active analyte ions, which are expected to be enriched on aerosol droplet surfaces, should leave the droplets and become gas-phase ions more readily and thus have a higher ESI response, according to the ion

evaporation model (IEM) proposed by Iribarne and Thomson.²¹²⁻²¹⁴ Subsequently the mechanistic interpretation was also extended to capillary electrophoresis (CE) with ESI-MS detection. Rundlett and Armstrong addressed a modified aerosol ionic redistribution (AIR) mode and qualitatively explained the analyte signal quenching when using modest concentrations of anionic surfactants in CE-ESI-MS.⁸⁷ Enke's equilibrium partitioning model (EPM) provided insight regarding the effect of analyte/solvent characteristics on the ESI response.²⁰⁵⁻²⁰⁷ They proposed that the ionic species in the ESI droplet partition between two phases: an interior phase which is solvated and electrically neutral and a surface phase which carries the excess charge determining the observed ion response. The higher response of the surface active ion species can be therefore quantitatively explained by their higher equilibrium partition coefficients (K), which allow them to favorably complete the excess charge sites on the droplet surface as was previously outlined by Rundlett and Armstrong.⁸⁷ Tang and Smith photographed the colored surfactant deposition on a grounded metal plate after electrospray, and observed both the satellite and the progeny droplets generated during the ESI fissioning process are significantly surfactant-enriched.²⁰⁸ This provided an experimental verification of the assumption that surface-active species preferentially reside on the droplet surface during the electrospray process. Brodbelt et al. extended the equilibrium partitioning model to host-guest complexation systems, and accurately modeled the ESI response to the host-guest complexation interactions.^{210,211} Recently, we investigated the mechanism for the greatly enhanced sensitivity obtained for anions by PIESI with consideration of both the binding behavior between anion and IPR and the surface activity of the anion/IPR complex.²¹ Since the system involves the process of anion/IPR complexation and the partitioning of ions in the aerosol droplets, both the binding constant of anion/IPR and the surface activity of the complex were considered. It was found that an appropriate binding

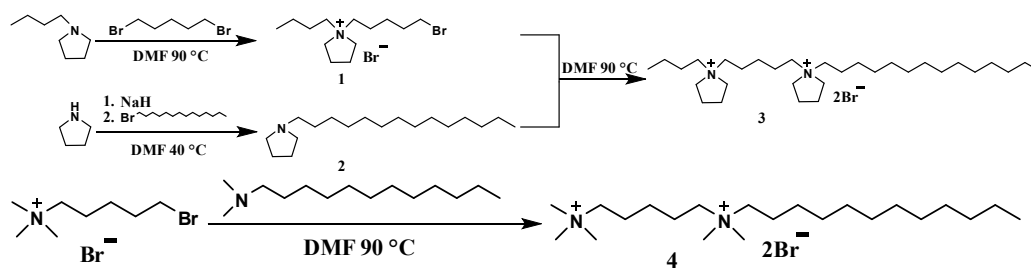
constant in both the solution phase and gas phase was necessary but not sufficient for high detection sensitivity. Interestingly, the surface activity of anion/IPR complex, which was greatly increased compared to either the anion or IPR alone, seems to be the most crucial factor leading to improved sensitivity.²¹

Based on the aforementioned proposed mechanism and model,²¹ we attempted, for the first time, to rationally design two novel dications with unsymmetrical structures, with the purpose of further improving the sensitivity for anion detection in the positive ion mode by PIESI-MS. The performances of the unsymmetrical dications were evaluated in terms of limits of detection, which were determined for seven selected anions in both single ion monitoring (SIM) mode and selected reaction monitoring (SRM) mode. A comparison of structurally related symmetrical and unsymmetrical dications was made. The surface activity of the anion/IPR complex and its correlation to the observed ESI responses were evaluated, which provides support for the proposed mechanism.²¹ The results from this work may also provide a basis for the design of future paired PIESI reagents.

7.2. Experimental

7.2.1. Dicationic Ion-Pairing Reagents

Names, abbreviations and structures of the dications are listed in Table 7-1. 1-butyl-1-[5-(1-butyl-1-pyrrolidiniumyl)pentyl]pyrrolidinium difluoride (**SDC I**) and N¹, N¹, N¹, N⁵, N⁵, N⁵-hexamethyl-1,5-pentanediaminium diiodide (**SDC II**) were commercially available from Sigma-Aldrich (St. Louis, MO). Synthetic procedures and elemental analysis data for 1-butyl-1-[5-(1-tetradecyl-1-pyrrolidiniumyl)pentyl]pyrrolidinium dibromide (**UDC I**) and N¹-dodecyl-N¹, N¹, N⁵, N⁵, N⁵-pentamethyl-1,5-pentanediaminium dibromide (**UDC II**) are described in the Scheme 7-1 and Table 7-2 respectively.



Scheme 7-1. Synthesis of *1-butyl-1-[5-(1-tetradecyl-1-pyrrolidiniumyl)pentyl]pyrrolidinium dibromide* (UDC I, 3) and *N¹-dodecyl-N¹,N¹,N⁵,N⁵,N⁵-pentamethyl-1,5-pentanediaminium dibromide* (UDC II, 4)

Table 7-1 Abbreviations and Structures of Dications and Anions Used in This Study

Dication Name (Abbreviation)	Structure
symmetrical dication I (SDC I)	
unsymmetrical dication I (UDC I) (Surfactant)	
symmetrical dication II (SDC II)	
unsymmetrical dication II (UDC II) (Surfactant)	
Analyte Anion Name (Abbreviation)	Structure
benzenesulfonate (BZSN ⁻)	
iodide (I ⁻)	I ⁻
benzoate (BZO ⁻)	
arsenate monobasic (ASN ⁻)	H ₂ AsO ₄ ⁻
monochloroacetate (MCA ⁻)	
thiocyanate (SCN ⁻)	⁻ S-C≡N
etidronate (HEDP ⁻)	

Table 7-2 Elemental Analysis Data of UDC I and UDC II.

Dication	Empirical formula	Calculated (%)				Found (%)			
		C	H	N	Br ⁻	C	H	N	Br ⁻
UDC I	C ₃₁ H ₆₄ Br ₂ N ₂	59.61	10.33	4.48	25.58	57.15	10.10	4.38	24.89
UDC II	C ₂₂ H ₅₀ Br ₂ N ₂	52.59	10.03	5.58	31.81	52.54	10.47	5.46	28.33

To maximize the production of dication/anion complex in the solution phase, the bromide and iodide dications were converted to fluoride form by using the anion-exchange resin. Anionic analytes were purchased as the sodium/potassium salt or as the free acid from Sigma-Aldrich (St. Louis, MO, USA). These structures are shown in Table 7-1.

7.2.2. PIESI-MS Analyses

Studies were performed using a Finnigan LXQ (Thermo Fisher Scientific, San Jose, CA) mass spectrometer in the positive ion mode with Xcalibur 2.0 as data analysis software. They were carried out at a spray voltage of 3 kV and a capillary voltage of 11 V. The temperature of the ion transfer capillary was held at 350 °C. Normalized collision energy in the selected reaction monitoring (SRM) mode was set at 30, the activation time was set at 30 ms, and the Q value was set at 0.25. PIESI-MS analysis was performed by using the above ESI-MS system and with an additional HPLC pump which was used for post-column reagent (PCR) addition of the cationic ion-pairing reagent. A schematic and description of the instrumental configuration of PIESI-MS has been given in detail in our previous publications.^{20,82} Except as otherwise noted, a Surveyor MS pump (Thermo Fisher Scientific, San Jose, CA) provided a 300 µL/min (33% H₂O/67% MeOH, by volume) carrier stream into the mass spectrometer, which was merged with a flow of 40 µM aqueous dicationic ion-pairing reagent solution delivered by a Shimadzu LC-6A pump

(Shimadzu, Columbia, MD) at rate of 100 $\mu\text{L}/\text{min}$. The sample was injected into the carrier stream through a six-port injection valve prior to the mixing tee. This setting results in an overall solvent composition of 50% $\text{H}_2\text{O}/50\%$ MeOH containing 10 μM of dicationic ion-pairing reagent flowing into the mass spectrometer (400 $\mu\text{L}/\text{min}$). Detection limits were taken to be a signal-to-noise ratio of 3 using a Genesis Peak Detection Algorithm with 5 replicate injections. Monoisotopic masses were used to monitor the dication/IPR complex ions in both SIM and SRM mode, which will result in the isotope of highest abundance being selected.

7.2.3. Surface Tension Measurements

The surface tensions were measured with a Fisher Model 20 tensiometer (Fisher Scientific, Fair Lawn, NJ) by the duNouy ring technique. The platinum ring used has a ring/wire radius ratio of 53.2113942 and a mean circumference of 5.940 cm. Measurements were taken at 23 ± 0.1 $^\circ\text{C}$. The surface tension measurement for the dication/IPR solution were performed through a titration experiment where the sodium thiocyanate was successively added into the bulk solution of **SDC I** and **UDC I** resulting in 0.1 M dication solutions containing a concentration of thiocyanate anion from 0.02 to 0.2 M being measured. Deionized water was titrated with thiocyanate anion as a blank. Each data point represents the average value of triplicate measurements.

7.3. Results and Discussion

7.3.1. Unsymmetrical Dicationic Ion-Pairing Reagents

Previous empirical observations have suggested that the performance of symmetrical dications could be greatly influenced both by the length of the alkyl linkage chain and the nature of the cationic moieties. In this study, identical, five carbon (methylene group) linkage chains were used for all of the dicationic agents (Table 7-1).

This spacing between cationic moieties avoided the formation of bolaform surfactants, which may spontaneously fold in solution and therefore result in an unpredictable surface activity.^{215,216} **SDC I** and **SDC II** have pyrrolidinium or ammonium charged moieties respectively (Table 7-1). The structures of the unsymmetrical dications were specifically designed to be surface active versions of the corresponding symmetrical dications, and thus a definitive comparison between the two types of dications can be made. The increased surface activity was achieved by attaching a long alkyl chain on one end of the symmetrical dication. The positively charged polar portion of these pairing agents was necessary to enable the association with the anion analytes of interest, while the hydrophobic portion was included to increase the fraction of the complex that preferably resides at the gas-solvent interface of the aerosol.

7.3.2. A Comparison of the LODs Obtained by Using Unsymmetrical Dications and Symmetrical Dications

The analytes selected represent a cross section of anion types that include both inorganic and small organic anions. The detection limits for the seven selected anions with the use of unsymmetrical dications and symmetrical dications in the single ion monitoring mode are given in Table 7-3. The results indicate that the LOD improved for six out of seven anions, using 1 μM **UDC I** (1.5 to 5 times) compared to using same concentration of **SDC I**. The LOD for six out of seven anions (using **UDC II**) improved 1.6 to 7.5 times. Note that the symmetrical dications are already known to improve the sensitivity of anion detection in the positive ion mode mass spectrometry (compared to the negative ion mode) often by orders of magnitude. However, the symmetrical dications are not surface active until paired with an appropriate anion.²¹ These observations (Table 7-3) tend to support the concept of the equilibrium partitioning model. Since the unsymmetrical dications are known to have greater surface activity than symmetrical

cations, the anion/IPR complex formed from unsymmetrical dications should also be more surface active, and thus the anion would partition to the droplet surface more efficiently resulting in a higher signal response. To investigate the effect of dication concentration on detection limit of anions, the LOD of seven anions were evaluated at a higher concentration level of dication (Table 7-3). It is shown that the LOD for five out of seven anions, using 10 μM **UDC I**, were 2.5 to 7.3 times better than using same concentration of **SDC I**. The LOD of four out of seven anions, using **UDC II**, were 2.5 to 12 times improved. Further increases in the concentration of the unsymmetrical pairing agent resulted in significant decreases in the LODs. For example, the LOD of BZSN^- , I^- , and SCN^- obtained when using 200 μM **UDC I** were found to be 320 pg, 60 pg, and 35 pg respectively, which were 27 times, 40 times, and 44 times worse compared to those obtained by using 1 μM **UDC I** respectively (Table 7-3). This observation also is in accordance with what would be expected with the equilibrium partitioning model, as will be explained in subsequent paragraphs.

Table 7-3 Comparison of Limits of Detection (LOD) of Anions Obtained with the Use of Unsymmetrical Dications (UDC I and UDC II) and Symmetrical Dications (SDC I and SDC II) in the SIM Mode by PIESI-MS.

Anion	1 μ M of Dication ^a								10 μ M of Dication ^a							
	UDC I		SDC I		UDC II		SDC II		UDC I		SDC I		UDC II		SDC II	
	LOD ^b (pg)	LOD ^b (pg)	Improvement ^c		LOD ^b (pg)	LOD ^b (pg)	Improvement ^c		LOD ^b (pg)	LOD ^b (pg)	Improvement ^c		LOD ^b (pg)	LOD ^b (pg)	Improvement ^c	
BZSN ⁻	12	24	2.0	+	12	30	2.5	+	8.0	20	2.5	+	6.0	28	4.7	+
I ⁻	1.5	6.5	4.3	+	4.0	5.0	1.3	○	15	110	7.3	+	50	45	0.9	○
BZO ⁻	40	200	5.0	+	60	450	7.5	+	30	18	0.6	○	33	84	2.5	+
ASN ⁻	2400	4000	1.7	+	4000	21000	5.3	+	480	1800	3.8	+	100	1200	12	+
MCA ⁻	16	24	1.5	+	9.0	40	4.4	+	7.2	20	2.8	+	9.0	12	1.3	○
SCN ⁻	0.80	1.6	2.0	+	5.0	8.0	1.6	+	4.0	12	3.0	+	200	160	0.8	○
HEDP ⁻	8000	4000	0.5	-	17000	35000	2.1	+	4000	4800	1.2	○	1600	13000	8.1	+

^aThe concentration refers to the final dication concentration that flowed in into the MS.

^bLOD was defined as the lowest analyte amount in picograms (pg) yielding a S/N = 3.

^cTimes of improvement of LOD of unsymmetrical dication vs. LOD of symmetrical dication. “+”: better; “-”: worse; “○”: similar.

In this study, it is clear that having the concentration of pairing reagents between 1 μM to 10 μM is an appropriate range for enhanced detection without causing significant suppression the analyte ion signal. Figure 7-1 shows the PIESI mass spectra of iodide by using **SDC I** and **UDC I**, where the ion signal observed for iodide by using the **UDC I** was approximately 3.6 times higher as compared to using **SDC I** indicating the improved performance of the unsymmetrical dications.

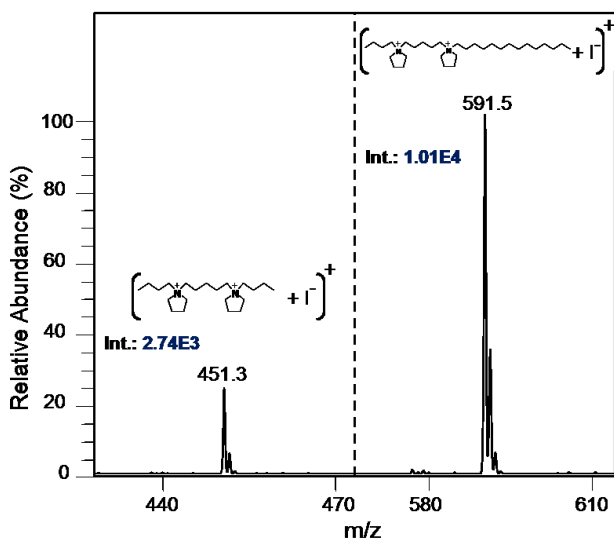


Figure 7-1 PIESI Mass Spectra of Iodide by Using SDC I and UDC I. Concentration of I^- Was 1 μM and the Molar ratio of Dication to I^- Was 20:1. $[\text{SDC I} + \text{I}]^+$ m/z: 451.3; $[\text{UDC I} + \text{I}]^+$ m/z: 591.5. The Spectra Were Recorded Separately in the Single Ion Monitoring Mode with a Width of 50

7.3.3. Surface Tension Measurements

To further investigate the surface activity of the anion/IPR complex and to better explain the aforementioned results, surface tension measurements of the anion/IPR

complex were performed (Figure 7-2). It was observed that the surface tension of neat water dropped only slightly (by a $\Delta\gamma$ less than 1.5 dynes/cm) upon addition of SCN^- , while the surface tension of the symmetrical dication solution dramatically decreased as SCN^- was added. This behavior was noted previously and formed the basis of the proposed mechanism of PIESI-MS signal enhancement.²¹

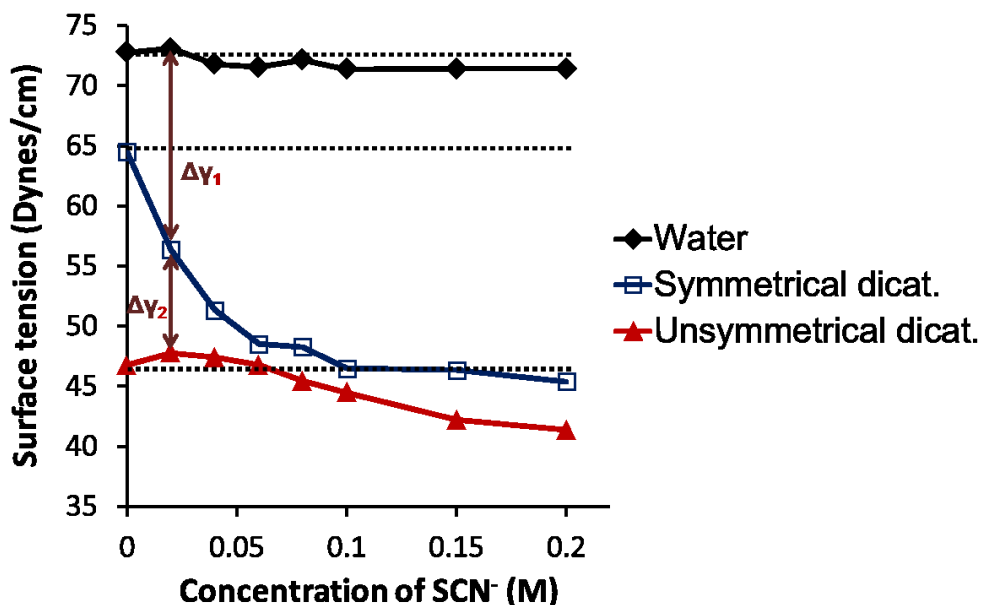


Figure 7-2 Surface Tension Measurements When Titrating SDC I and UDC I with SCN^- .

Concentration of SDC I and UDC I was 0.1 M. The Data Points at $[\text{SCN}^-] = 0$ M Represent Surface Tension of Neat Water (blank line), 0.1 M Aqueous Solution of SDC I (blue line) and 0.1 M Aqueous Solution of UDC I (red line), Respectively

As shown in Figure 7-2, at 0.02 M of SCN^- added (the molar ratio of the anion and IPR was 1:5), the surface tension for neat water was 73.1 dynes/cm while the surface tension for the symmetrical dication was 56.4 dynes/cm. This indicates that the presence of the symmetrical dication leads to a 16.7 dynes/cm surface tension decrease

($\Delta\gamma_1$) for the anion solutions. The increased surface activity achieved through complexation allows for an enhanced partitioning of the anion/dication complex to the aerosol droplet surface, which results in improved detection sensitivity. The surface tension of purely aqueous unsymmetrical solution of the dication (Figure 7-2 at $[\text{SCN}^-] = 0$ M) was observed to be lower than that of the symmetrical dication (by 17.7 dynes/cm between **SDC I** and **UDC I**) as expected. It is interesting that the addition of SCN^- did not cause a rapid decrease in the surface tension for the unsymmetrical dication as it did for the symmetrical dication (Figure 7-2). The surface tension of the unsymmetrical dication solution decreased by 5.4 dynes/cm over the entire titration range with SCN^- . Nonetheless, it is shown that the unsymmetrical dication still has a greater effect on lowering the surface tension of solution containing the anionic analyte (SCN^-). The surface tension of the solution containing both the unsymmetrical cation and 0.02 M SCN^- was 25.3 dynes/cm lower than neat water and was 8.6 dynes/cm ($\Delta\gamma_2$) lower compared to the comparable symmetrical dication solution (Figure 7-2). Consequently, it is expected that the presence of the unsymmetrical dication would lead to an increased concentration of the anion/dication complex at the aerosol droplet surface (Figure 7-3 (A)). This would lead to better detection sensitivity. It should be noted that another scenario is possible with this system. Since the unsymmetrical dication is an excellent surfactant even in the absence of an anionic analyte, it is initially enriched at the aerosol droplet surface. This is somewhat different from the case of the symmetrical dicationic reagent that is not surface active until it binds an anion.²¹ Only then does the symmetrical dication/anion complex partition to the aerosol surface. Therefore, in the case of the unsymmetrical dicationic reagent, there is a competition between the two highly surface active ionic species (i.e., one paired with the anionic analyte and the other unpaired). Once the surface of the aerosol droplet is saturated (monolayer) with the dicationic

surfactant, additional material can only be solubilized in the interior of the droplet (Figure 7-3 (B)). These “inner solution” dications will compete for any anionic analytes. Note that micelle formation in the inner solution would even more effectively compete for anions. In this case, some signal suppression could occur because of surface dilution of the anion/dication complex. Ultimately this limits the advantage of having increasingly surface active ion-pairing agents.

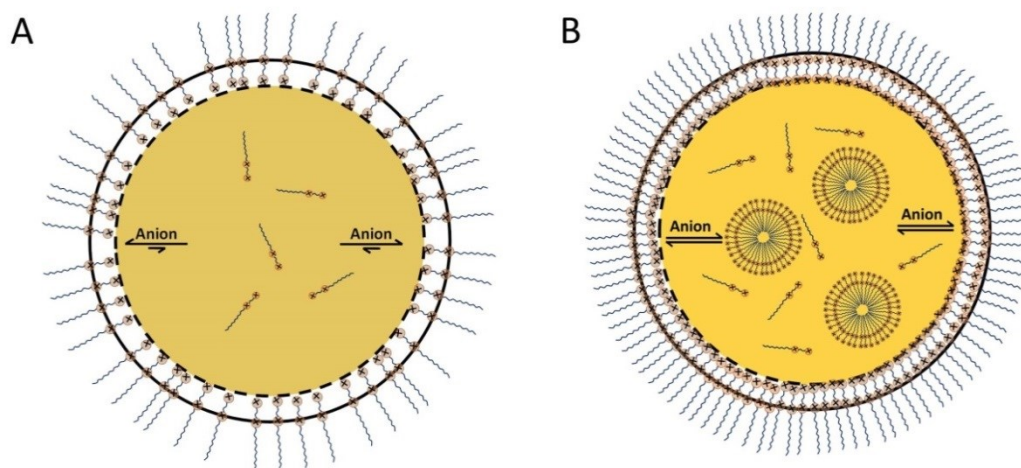


Figure 7-3 Schematic Showing the Partitioning of an Analyte Anion Between the Surface of an Aerosol Droplet and the Bulk Interior. When the Concentration of the Dicationic Surfactant Is Low (“A” above), It Resides Mainly at the Surface of the Droplet as will Any Associated Anions. When the Concentration of Surface of the Dicationic Surfactant is High (“B” above), Monolayer can be Formed and All Additional Surfactant Resides in the Interior Bulk Solution. Thus the Anionic Analyte Has Increased Partitions to the Interior Bulk Solution

7.3.4. Partitioning Behavior of the Species in the Aerosol Droplet

The partitioning behaviors of the dications and anion/IPR complexes were evaluated. In this experiment, the ESI responses of thiocyanate/**UDC I** complex were measured with increasing concentrations of solution containing **UDC I** and SCN^- (Figure 7-4, black line). It is shown that the response of the thiocyanate/**SDC I** complex initially increases linearly ($R^2 = 0.970$) as the concentration increases. However, signal saturation occurs when the concentration of the solution reaches approximately 5×10^{-5} M. This saturation behavior indicates the equilibrium for the ionic species partitioning between droplet surface and droplet interior is different at dication concentrations before and after 5×10^{-5} M. When the concentration of dication is greater than 5×10^{-5} M, where uncomplexed **UDC I** strongly competes with other paired ion species for the limited number of surface positions, the equilibrium for the thiocyanate/**UDC I** complex shifts to the droplet interior and consequently leads to a decrease in the amount of thiocyanate/**UDC I** complex that resides on the surface (a suppressed signal). This observation indicates that in the previous experiments, where $200 \mu\text{M}$ (2×10^{-4} M) IPR was used, surface saturation of the aerosol droplets by the surfactant had occurred. The methanol molecules in the solvent were easily protonated and initially carry the majority of charges.²¹⁷ The ESI response of the protonated methanol ions was shown to be suppressed when the concentrations of thiocyanate/**UDC I** solution exceeded 2×10^{-5} M, at approximately the same concentration when curvature and leveling off of the ESI responses of thiocyanate/**UDC I** complex occurs (Figure 7-4, red line). This signal suppression behavior is a result of the thiocyanate/**UDC I** complex ions outcompeting the solvent ions for limited numbers of excess charges on the droplet surface. According to Enke's equilibrium partitioning theory, the concentration of excess charge [Q] can be expressed as

$$[Q] = \frac{I}{F\Gamma} \quad (7-1)$$

in which [Q] is the excess charge in molar concentration, I is the total droplet current in amperes, F is the Faraday's constant (96,485 coulomb/mol), and Γ is the flow rate of sample solution in L/s. The value of [Q] determined by using Equation 7-1 was equal to 5.1×10^{-5} M, which means that the total charge ([Q]) will run out when the analyte concentration reaches 5.1×10^{-5} M. This suggests that there would be a charge limitation to the analyte response at higher concentration levels. Notably, the concentration at this charge limitation (5.1×10^{-5} M) is consistent with the concentration at which signal saturation of the thiocyanate/**UDC I** complex ion occurs (5×10^{-5} M). To prove that the leveling off of the ESI response observed is due to the lack of any more available surface area and/or the charges on ESI droplet rather than due to a saturation of detector response, a calibration curve of threonine, which is not a surface active species, was made (Figure 7-5). The ESI response of the ThrH⁺ was linear over a concentration range of 3×10^{-6} to 1×10^{-3} M. Since the discontinuity with our "ion-pairing surfactants" occurs at 5×10^{-5} M (well below that of the threonine saturation) this can only be due to the surface activity of the reagent causing it to saturate the droplet surface at the lower concentration.

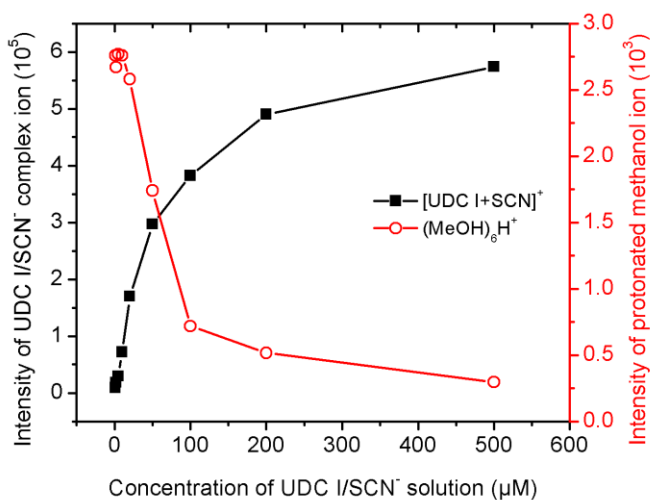


Figure 7-4 ESI-MS Response to the Dication/SCN⁻ Complex Ion (in Black) and ESI-MS Response to the Protonated Methanol Ion (in Red) for Solutions Containing UDC I and SCN⁻ (UDC I : SCN⁻ = 10 : 1) as the Dication Concentration Increased from 1×10^{-6} to 5×10^{-4} M

The competition behavior of the unsymmetrical and symmetrical dications also was evaluated by simultaneously measuring the ESI responses of **SDC I** and **UDC I** as a function of their concentrations (Figure 7-6 (A)). It is shown that the response curve was fairly linear at concentrations from 2×10^{-7} M to 10^{-4} M with $R^2 = 0.999$ for **UDC I** and $R^2 = 0.986$ for **SDC I**, and saturation behavior began to appear at a concentration of 10^{-4} M. Also, it was observed that the responses of the two dications were similar at the low concentration region from 2×10^{-7} M to 2×10^{-5} M. However, at higher concentrations the response of **UDC I** was significantly higher than that of **SDC I** (at concentrations greater than 2×10^{-5} M). This behavior could be explained by the competition between unsymmetrical and symmetrical dications for the limited number of charge positions on

the droplet surface at higher concentrations. Since the partitioning of **UDC I** (the surface active reagent) is more favorable, signal suppression occurs for **SDC I** leading to a gradually decreased response at its higher concentrations. These observations are in agreement with Enke's prediction using equilibrium partitioning model for analytes with different equilibrium partition coefficients²⁰⁵ as well as Kebarle and Tang's experimental data²⁸.

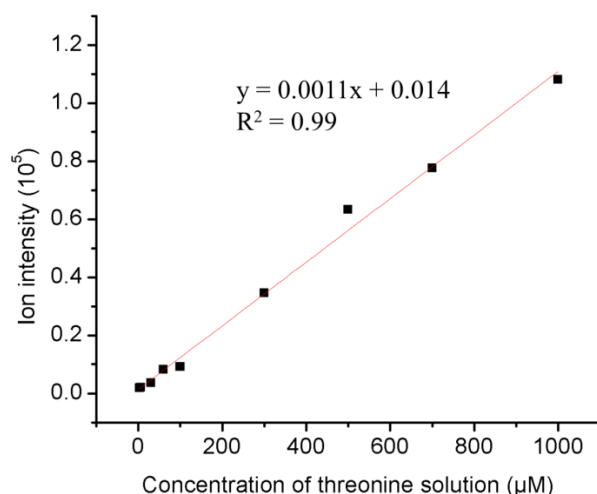


Figure 7-5 ESI-MS Response to the ThrH⁺ Ion as the Concentration of Threonine Solution Increased from 3×10^{-6} to 1×10^{-3} M. The Ion Intensity was Recorded by Monitoring the ThrH⁺ Ion (m/z: 120.1) in the SIM Mode

Ion responses of the anion/IPR complexes were examined for increasing concentrations of SCN⁻, in the presence of equimolar amounts of **UDC I** and **SDC I** (Figure 7-6 (B)). It was shown that increasing the concentration of SCN⁻ led to a concomitantly linear increase in ion response for both the thiocyanate/UDC I complex and thiocyanate/SDC I complex. This suggests that the addition of SCN⁻ has little effect on the relative partitioning of each complex to the droplet surface. The response of the

thiocyanate/UDC complex started to exhibit a saturation behavior when the concentration SCN^- reached 1×10^{-4} M, while the response of the thiocyanate/SDC complex did not. The early surface saturation of thiocyanate/UDC complex results in a smaller difference between response of the thiocyanate/UDC complex and the response of the thiocyanate/SDC complex at higher concentrations (difference in response is 6.3 times at $[\text{SCN}^-] = 10^{-6}$ M while 3.4 times at $[\text{SCN}^-] = 2 \times 10^{-4}$ M).

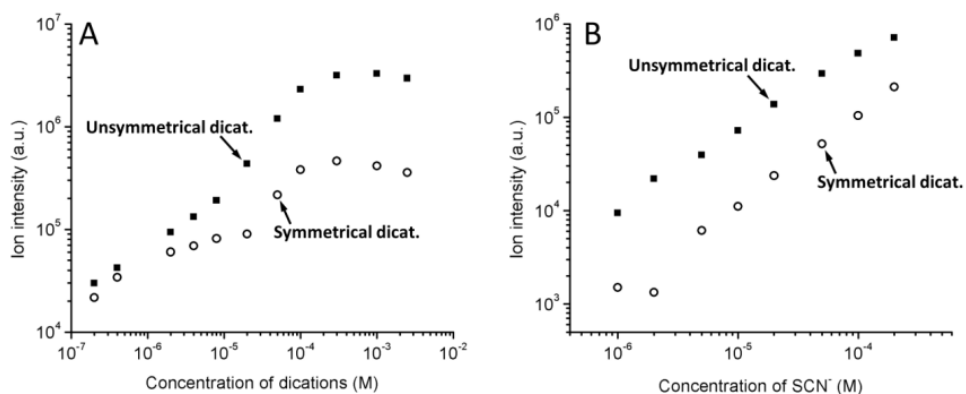


Figure 7-6 (A) ESI-MS Response to the Dications for Equimolar Solution of SDC I and UDC I as the Concentration Increase from 2×10^{-7} to 2.5×10^{-3} M. The Ion Intensity Were Recorded by Simultaneously Monitoring the +2 Charged Dications ($[\text{SDC I}]^{2+}$ m/z: 162.2; $[\text{UDC I}]^{2+}$ m/z: 232.2) in SIM Mode. (B) ESI-MS Response to the Dication/ SCN^- Complex Ion for Solutions Containing 10^{-4} M of SDC I and UDC I as the Concentration of SCN^- Added Increases from 1×10^{-6} M to 2×10^{-4} M. The Ion Intensity Were Recorded by Simultaneously Monitoring the +1 Charged Dication/ SCN^- Complex Ion ($[\text{SDC I} + \text{SCN}]^+$ m/z: 382.3; $[\text{UDC I} + \text{SCN}]^+$ m/z: 522.5) in SIM Mode

7.3.5. LODs Determined with the Use of Unsymmetrical Dications in the SRM Mode

SRM experiments were performed for the same anions with the use of the same unsymmetrical dications and symmetrical dications (Table 7-4). It was observed that the SRM mode usually provided somewhat better sensitivity (1.2 to 9 times) than the SIM mode. This is understandably due to the enhanced analytical specificity and reduction in the chemical noise. It should be noted that these SRM experiments utilized collision induced dissociation (CID) and monitored a fragment of the anion/IPR complex, and therefore the observed LODs are hardly correlated to the properties of the analytes without considering other factors involved, such as efficiency of fragmentation and ion transmission.

Table 7-4 Comparison of Limits of Detection (LOD) of Anions Obtained with the Use of Unsymmetrical Dications (UDC I and UDC II) and Symmetrical Dications (SDC I and SDC II) in the SRM Mode by PIESI-MS

Anion	UDC I	SDC I	Improvement ^b		UDC II	SDC II	Improvement	
	LOD ^a (pg)	LOD (pg)			LOD (pg)	LOD (pg)		
BZSN ⁻	2.3	3.5	1.5	○	10	28	2.8	+
I ⁻	3.2	0.72	0.2	-	1.2	3.4	2.8	+
BZO ⁻	1.5	3.2	2.1	+	2.0	4.0	2.0	+
ASN ⁻	100	320	3.2	+	16	600	38	+
MCA ⁻	0.16	3.2	20	+	1.8	2.4	1.3	+
SCN ⁻	— ^c	—			—	—		
HEDP ⁻	30000	660	0.02	-	500	2700	5.4	+

^aLOD was defined as the lowest analyte amount in picogram yielding a S/N = 3.

^bFactor of improvement of LOD of unsymmetrical dications vs. LOD of symmetrical dications. “+”: better; “-”: worse; “○”: similar.

^cNot detected.

7.4. Conclusions

Two unique unsymmetrical dications were synthesized and evaluated for the detection of seven anions by paired ion electrospray ionization mass spectrometry (PIESI-MS). It was shown that the unsymmetrical dications usually provided more sensitive detection (from 1.5 to 12 times) than symmetrical dications. They had an effective concentration range from 1 μM to 10 μM . SRM experiments were performed on the anion/dication complexes, which provided further improved detection limits for some of these anions by 1.2 to 9 times (compared to the LODs obtained in the SIM mode). It is proposed that the use of unsymmetrical dicationic ion-pairing reagents results in the formation of highly surface active anion/dication complex and thus an enhanced partitioning of the anion to the droplet surface. Therefore, both the effective binding with the anion and the high surface activity of the unsymmetrical dication were expected to be major factors that lead to the enhanced sensitivity. This assumption was further experimentally supported by the results of surface tension titration studies and the correlation between surface activity of the unsymmetrical dication and the ESI response of anion/dication complex, based on the concepts of the equilibrium partitioning model.

Chapter 8

General Summary

8.1. Part One (Chapters 2-6)

The development of methodologies based on PIESI-MS and the application of PIESI-MS for the ultrasensitive determination of anionic molecules were demonstrated. Small organic molecules, metal cations, and medium sized lipophilic molecules were detected using PIESI-MS, which was shown to have superior sensitivity (usually 2 to 3 orders of magnitudes more sensitive) compared to most reported methodologies. Chapter 2 describes the ultrasensitive determination of trace level of acidic pesticides with the use of HPLC-PIESI-MS methodology. With the use of an optimal IPR ($C_5(bpyr)_2$), LODs from 0.6 pg to 19 pg were obtained for nineteen acidic pesticides by using PIESI-MS in the SRM mode. This study demonstrated that the nature of both the IPR and the acidic pesticide analyte plays an important role on the observed LODs. The developed method was used to determine pesticides in river/pond water samples which were detection at low parts per trillion levels. Chapter 3 and Chapter 4 demonstrated the capability of PIESI-MS for the sensitive determination of chelated metal cations. With the use of a combination of IPR and metal chelating reagents, alkaline earth metals, transition metals, and post-transition metals were detected at down to the sub-picogram level by PIESI-MS. The method was validated in terms of accuracy with the determination of certified reference materials (CRMs). It was shown that both the structure properties of the chelating reagents and ion-pairing reagents played a vital role in the complex formation and detection sensitivity. The optimum solution pH to perform the analysis was found to be between 5 and 7. Chapter 5 and Chapter 6 demonstrated the application of HPLC-PIESI-MS on the ultrasensitive determination of lipids (phospholipids and

sphingolipids). It was found that the PIESI-MS method was particularly suitable for determination of the medium sized, zwitterionic charge state molecules. PIESI-MS method is readily coupled with separation techniques (e.g. HPLC) for the separation and sensitive determination of lipids in sample mixtures. The HPLC-PIESI-MS method can be very useful for lipid profiling at low concentration levels.

8.2. Part Two (Chapters 7)

This part of the dissertation describes the development of rationally designed unsymmetrical ion-pairing reagents (UDIs) and their performance on anion detection using PIESI-MS. It was found that the unsymmetrical dications provided more sensitive detection than symmetrical dications by 1.5 to 12 times in the single ion monitoring mode for the anions evaluated. The effective concentration range of UDI was optimized, which was from 1 μM to 10 μM . SRM experiments were conducted on the anion/UDI complexes, which provided further improvement of detection limits for the anions by 1.2 to 9 times than SIM mode. This study shed further light on the sensitivity enhancement mechanism of PIESI-MS. The correlation between the ESI response and the surface activity of the analytes emphasized the critical role of complex surface activity on the ionization efficiency. It is concluded that the use of unsymmetrical dicationic ion-pairing reagents results in the formation of highly surface active anion/UDI complex leading to an enhanced partitioning of the anion to the ESI droplet surface. Both effective binding with anion and the high surface activity of the unsymmetrical dication were shown to be essential for sensitive analyte detection by PIESI-MS. The results from this study provide a basis for the design of future PIESI-MS reagents.

Appendix A

Publication Information and Contributing Authors

Chapter 2: A manuscript published in *Analytica Chimica Acta*. Chengdong Xu, Daniel W. Armstrong, 2013, 792, 1-9. DOI: 10.1016/j.aca.2013.05.054. Copyright ©2013 with permission from Elsevier.

Chapter 3: A manuscript published in *Rapid Communications in Mass Spectrometry*. Chengdong Xu, Edra Dodbiba, Nilusha Padivitage, Zachary S. Breitbach, Daniel W. Armstrong, 2012, 26, 2885–2896. DOI: 10.1002/rcm.6413. Copyright ©2012 with permission from Wiley.

Chapter 4: A manuscript published in *Rapid Communications in Mass Spectrometry*. Edra Dodbiba, Chengdong Xu, Eranda Wanigasekara, and Daniel W. Armstrong, 2012, 26, 1005–1013. DOI: 10.1002/rcm.6185. Copyright ©2012 with permission from Wiley.

Chapter 5: A manuscript published in *Analyst*. Edra Dodbiba, Chengdong Xu, Tharanga Payagala, Eranda Wanigasekara, Myeong Hee Moon and Daniel W. Armstrong, 2011, 136, 1586-1593. DOI: 10.1039/C0AN00848F. Copyright ©2011 with permission from The Royal Society of Chemistry.

Chapter 6: A manuscript submitted to *Analyst*. Chengdong Xu, Eduardo Costa Pinto and Daniel W. Armstrong.

Chapter 7: A manuscript published in *Analytical Chemistry*. Chengdong Xu, Hongyue Guo, Zachary S. Breitbach, Daniel W. Armstrong, 2014, 86, 2665-2672. DOI: 10.1021/ac404005v. Copyright ©2014 with permission from American Chemical Society.

Appendix B
Copyrights and Permissions

ELSEVIER LICENSE TERMS AND CONDITIONS

Apr 30, 2014

This is a License Agreement between Chengdong Xu ("You") and Elsevier ("Elsevier") provided by Copyright Clearance Center ("CCC"). The license consists of your order details, the terms and conditions provided by Elsevier, and the payment terms and conditions.

All payments must be made in full to CCC. For payment instructions, please see information listed at the bottom of this form.

Supplier	Elsevier Limited The Boulevard, Langford Lane Kidlington, Oxford, OX5 1GB, UK
Registered Company Number	1982084
Customer name	Chengdong Xu
Customer address	700 Planetarium Place ARLINGTON, TX 76019
License number	3378961294033
License date	Apr 30, 2014
Licensed content publisher	Elsevier
Licensed content publication	Analytica Chimica Acta
Licensed content title	High-performance liquid chromatography with paired ion electrospray ionization (PIESI) tandem mass spectrometry for the highly sensitive determination of acidic pesticides in water
Licensed content author	Chengdong Xu, Daniel W. Armstrong
Licensed content date	20 August 2013
Licensed content volume number	792
Licensed content issue number	None
Number of pages	9
Start Page	1
End Page	9

Type of Use	reuse in a thesis/dissertation
Intended publisher of new work	other
Portion	full article
Format	both print and electronic
Are you the author of this Elsevier article?	Yes
Will you be translating?	No
Title of your thesis/dissertation	DEVELOPMENT OF PAIRED ION ELECTROSPRAY IONIZATION MASS SPECTROMETRY FOR ULTRASENSITIVE DETECTION OF ANIONS
Expected completion date	Aug 2014
Estimated size (number of pages)	100
Elsevier VAT number	GB 494 6272 12
Permissions price	0.00 USD
VAT/Local Sales Tax	0.00 USD / 0.00 GBP
Total	0.00 USD

JOHN WILEY AND SONS LICENSE TERMS AND CONDITIONS

Apr 30, 2014

This is a License Agreement between Chengdong Xu ("You") and John Wiley and Sons ("John Wiley and Sons") provided by Copyright Clearance Center ("CCC"). The license consists of your order details, the terms and conditions provided by John Wiley and Sons, and the payment terms and conditions.

All payments must be made in full to CCC. For payment instructions, please see information listed at the bottom of this form.

License Number	3378960214717
License date	Apr 30, 2014
Licensed content publisher	John Wiley and Sons
Licensed content publication	Rapid Communications in Mass Spectrometry
Licensed content title	Metal cation detection in positive ion mode electrospray ionization mass spectrometry using a tetracationic salt as a gas-phase ion-pairing agent: Evaluation of the effect of chelating agents on detection sensitivity
Licensed copyright line	Copyright © 2012 John Wiley & Sons, Ltd.
Licensed content author	Chengdong Xu,Edra Dodbiba,Nilusha L. T. Padivitage,Zachary S. Breitbach,Daniel W. Armstrong
Licensed content date	Nov 7, 2012
Start page	2885
End page	2896
Type of use	Dissertation/Thesis
Requestor type	Author of this Wiley article
Format	Print and electronic
Portion	Full article
Will you be translating?	No
Title of your thesis / dissertation	DEVELOPMENT OF PAIRED ION ELECTROSPRAY IONIZATION MASS SPECTROMETRY FOR ULTRASENSITIVE DETECTION OF ANIONS
Expected completion date	Aug 2014

**JOHN WILEY AND SONS LICENSE
TERMS AND CONDITIONS**

Apr 30, 2014

This is a License Agreement between Chengdong Xu ("You") and John Wiley and Sons ("John Wiley and Sons") provided by Copyright Clearance Center ("CCC"). The license consists of your order details, the terms and conditions provided by John Wiley and Sons, and the payment terms and conditions.

All payments must be made in full to CCC. For payment instructions, please see information listed at the bottom of this form.

License Number	3378961109225
License date	Apr 30, 2014
Licensed content publisher	John Wiley and Sons
Licensed content publication	Rapid Communications in Mass Spectrometry
Licensed content title	Sensitive analysis of metal cations in positive ion mode electrospray ionization mass spectrometry using commercial chelating agents and cationic ion-pairing reagents
Licensed copyright line	Copyright © 2012 John Wiley & Sons, Ltd.
Licensed content author	Edra Dodbiba, Chengdong Xu, Eranda Wanigasekara, Daniel W. Armstrong
Licensed content date	Mar 19, 2012
Start page	1005
End page	1013
Type of use	Dissertation/Thesis
Requestor type	Author of this Wiley article
Format	Print and electronic
Portion	Full article
Will you be translating?	No
Title of your thesis / dissertation	DEVELOPMENT OF PAIRED ION ELECTROSPRAY IONIZATION MASS SPECTROMETRY FOR ULTRASENSITIVE DETECTION OF ANIONS
Expected completion date	Aug 2014

Title: Mechanism and Sensitivity of
Anion Detection Using Rationally
Designed Unsymmetrical
Dications in Paired Ion
Electrospray Ionization Mass
Spectrometry

Author: Chengdong Xu, Hongyue Guo,
Zachary S. Breitbach, and Daniel
W. Armstrong

Publication: Analytical Chemistry

Publisher: American Chemical Society

Date: Mar 1, 2014

Copyright © 2014, American Chemical Society

PERMISSION/LICENSE IS GRANTED FOR YOUR ORDER AT NO CHARGE

This type of permission/license, instead of the standard Terms & Conditions, is sent to you because no fee is being charged for your order. Please note the following:

- Permission is granted for your request in both print and electronic formats, and translations.
- If figures and/or tables were requested, they may be adapted or used in part.
- Please print this page for your records and send a copy of it to your publisher/graduate school.
- Appropriate credit for the requested material should be given as follows: "Reprinted (adapted) with permission from (COMPLETE REFERENCE CITATION). Copyright (YEAR) American Chemical Society." Insert appropriate information in place of the capitalized words.
- One-time permission is granted only for the use specified in your request. No additional uses are granted (such as derivative works or other editions). For any other uses, please submit a new request.

References

- (1) Aebersold, R.; Mann, M. *Nature* **2003**, *422*, 198-207.
- (2) Griffiths, J. *Anal. Chem.* **2008**, *80*, 5678-5683.
- (3) Beck, J. L.; Colgrave, M. L.; Ralph, S. F.; Sheil, M. M. *Mass Spectrom. Rev.* **2001**, *20*, 61-87.
- (4) Bleakney, W. *Phys. Rev.* **1929**, *34*, 157-60.
- (5) Munson, M. S. B.; Field, F. H. *J. Am. Chem. Soc.* **1966**, *88*, 2621-30.
- (6) Macfarlane, R. D.; Torgerson, D. F. *Science* **1976**, *191*, 920-5.
- (7) Tanaka, K.; Waki, H.; Ido, Y.; Akita, S.; Yoshida, Y.; Yohida, T. *Rapid Commun. Mass Spectrom.* **1988**, *2*, 151-3.
- (8) Hutchens, T. W.; Yip, T. T. *Rapid Commun. Mass Spectrom.* **1993**, *7*, 576-80.
- (9) Wei, J.; Buriak, J. M.; Siuzdak, G. *Nature* **1999**, *399*, 243-246.
- (10) Barber, M.; Bordoli, R. S.; Sedgwick, R. D.; Tyler, A. N. *Nature* **1981**, *293*, 270-5.
- (11) Honig, R. E. *Int. J. Mass Spectrom. Ion Processes* **1985**, *66*, 31-54.
- (12) Gray, A. L. *Analyst* **1975**, *100*, 289-99.
- (13) Dzidic, I.; Carroll, D. I.; Stillwell, R. N.; Horning, E. C. *Anal. Chem.* **1975**, *47*, 1308-12.
- (14) Fenn, J. B.; Mann, M.; Meng, C. K.; Wong, S. F.; Whitehouse, C. M. *Science* **1989**, *246*, 64-71.
- (15) Cody, R. B.; Laramee, J. A.; Durst, H. D. *Anal. Chem.* **2005**, *77*, 2297-2302.
- (16) Takats, Z.; Wiseman, J. M.; Gologan, B.; Cooks, R. G. *Science* **2004**, *306*, 471-473.
- (17) Soukup-Hein, R. J.; Rensburg, J. W.; Dasgupta, P. K.; Armstrong, D. W. *Anal. Chem.* **2007**, *79*, 7346-7352.
- (18) Breitbach, Z. S.; Warnke, M. M.; Wanigasekara, E.; Zhang, X.; Armstrong, D. W. *Anal. Chem.* **2008**, *80*, 8828-8834.
- (19) Xu, C.; Dodbiba, E.; Padivitage, N. L. T.; Breitbach, Z. S.; Armstrong, D. W. *Rapid Commun. Mass Spectrom.* **2012**, *26*, 2885-2896, S2885/1-S2885/9.
- (20) Xu, C.; Armstrong, D. W. *Anal. Chim. Acta* **2013**, *792*, 1-9.
- (21) Breitbach, Z. S.; Wanigasekara, E.; Dodbiba, E.; Schug, K. A.; Armstrong, D. W. *Anal. Chem.* **2010**, *82*, 9066-9073.
- (22) Xu, C.; Guo, H.; Breitbach, Z. S.; Armstrong, D. W. *Anal. Chem.* **2014**, *86*, 2665-2672.
- (23) Cech, N. B.; Enke, C. G. *Mass Spectrom. Rev.* **2001**, *20*, 362-87.
- (24) Cole, R. B.; Harrata, A. K. *J. Am. Soc. Mass Spectrom.* **1993**, *4*, 546-56.
- (25) Cole, R. B.; Harrata, A. K. *Rapid Commun. Mass Spectrom.* **1992**, *6*, 536-9.
- (26) Cole, R. B.; Zhu, J. *Rapid Commun. Mass Spectrom.* **1999**, *13*, 607-611.
- (27) Cech, N. B.; Enke, C. G. *Mass Spectrom. Rev.* **2002**, *20*, 362-387.

- (28) Tang, L.; Kebarle, P. *Anal. Chem.* **1993**, *65*, 3654-68.
- (29) Zhang, X.; Wanigasekara, E.; Breitbach, Z. S.; Dodbibba, E.; Armstrong, D. W. *Rapid Commun. Mass Spectrom.* **2010**, *24*, 1113-1123.
- (30) Guan, C. L.; Ouyang, J.; Li, Q. L.; Liu, B. H.; Baeyens, W. R. G. *Talanta* **2000**, *50*, 1197-1203.
- (31) Rabin, S.; Stillian, J.; Barreto, V.; Friedman, K.; Toofan, M. *J. Chromatogr.* **1993**, *640*, 97-109.
- (32) Klein, H.; Leubolt, R. *J. Chromatogr.* **1993**, *640*, 259-70.
- (33) Ben Rayana, M. C.; Burnett, R. W.; Covington, A. K.; D'Orazio, P.; Fogh-Andersen, N.; Jacobs, E.; Katakya, R.; Kulpmann, W. R.; Kuwa, K.; Larsson, L.; Lewenstam, A.; Maas, A. H. J.; Mager, G.; Naskalski, J. W.; Okorodudu, A. O.; Ritter, C.; St John, A. *Clin. Chem. Lab. Med.* **2006**, *44*, 346-352.
- (34) Itai, K.; Tsunoda, H. *Clin. Chim. Acta* **2001**, *308*, 163-171.
- (35) Bastkowski, F.; Spitzer, P.; Eberhardt, R.; Adel, B.; Wunderli, S.; Berdat, D.; Andres, H.; Brunschwig, O.; Mariassy, M.; Feher, R.; Demuth, C.; Gonzaga, F. B.; Borges, P. P.; Silva, W. B., Jr.; Vospelova, A.; Vicarova, M.; Srithongtim, S. *Accredit. Qual. Assur.* **2013**, *18*, 469-479.
- (36) Malde, M. K.; Bjorvatn, K.; Julshamn, K. *Food Chem.* **2001**, *73*, 373-379.
- (37) Segui, M. J.; Lizondo-Sabater, J.; Martinez-Manez, R.; Sancenon, F.; Soto, J.; Garcia-Breijjo, E.; Gil, L. *Sensors* **2006**, *6*, 480-491.
- (38) Xu, R.; Bloor, D. M. *Langmuir* **2000**, *16*, 9555-9558.
- (39) Doble, P.; Haddad, P. R. *J. Chromatogr. A* **1999**, *834*, 189-212.
- (40) Buchberger, W. W.; Haddad, P. R. *J. Chromatogr. A* **1997**, *789*, 67-83.
- (41) Wang, E.; Liu, A. *Anal. Chim. Acta* **1991**, *252*, 53-7.
- (42) Barisci, J. N.; Wallace, G. G.; Clarke, A. *Electroanalysis* **1997**, *9*, 461-467.
- (43) Divjak, B.; Goessler, W. *J. Chromatogr. A* **1999**, *844*, 161-169.
- (44) Divjak, B.; Novic, M.; Goessler, W. *J. Chromatogr. A* **1999**, *862*, 39-47.
- (45) Yamashita, M.; Fenn, J. B. *J. Phys. Chem.* **1984**, *88*, 4451-9.
- (46) Yamashita, M.; Fenn, J. B. *J. Phys. Chem.* **1984**, *88*, 4671-5.
- (47) Whitehouse, C. M.; Dreyer, R. N.; Yamashita, M.; Fenn, J. B. *Anal. Chem.* **1985**, *57*, 675-9.
- (48) Ho, C. S.; Lam, C. W. K.; Chan, M. H. M.; Cheung, R. C. K.; Law, L. K.; Lit, L. C. W.; Ng, K. F.; Suen, M. W. M.; Tai, H. L. *Clin Biochem Rev* **2003**, *24*, 3-12.
- (49) Mollah, S.; Pris, A. D.; Johnson, S. K.; Gwizdala, A. B., III; Houk, R. S. *Anal. Chem.* **2000**, *72*, 985-991.
- (50) Hotta, H.; Mori, T.; Takahashi, A.; Kogure, Y.; Johno, K.; Umemura, T.; Tsunoda, K.-i. *Analytical Chemistry (Washington, DC, United States)* **2009**, *81*, 6357-6363.
- (51) Hu, J.-Y.; Aizawa, T.; Magara, Y. *Water Res.* **1998**, *33*, 417-425.
- (52) Liu, Y.; Liu, F.; Pan, X.; Li, J. *Environ. Sci. Technol.* **2012**, *46*, 5658-5659.

- (53) Bucheli, T. D.; Gruebler, F.; Mueller, S. R.; Schwarzenbach, R. P. *Anal. Chem.* **1997**, *69*, 1569-1576.
- (54) Famiglini, G.; Palma, P.; Termopoli, V.; Trufelli, H.; Cappiello, A. *Anal. Chem.* **2009**, *81*, 7373-8.
- (55) Munch, D. J.; Graves, R. L.; Maxey, R. A.; Engel, T. M. *Environ. Sci. Technol.* **1990**, *24*, 1446-51.
- (56) Wu, J.; Tragas, C.; Lord, H.; Pawliszyn, J. *Journal of Chromatography, A* **2002**, *976*, 357-367.
- (57) Moder, M.; Popp, P.; Eisert, R.; Pawliszyn, J. *Fresenius' J. Anal. Chem.* **1999**, *363*, 680-685.
- (58) Geerdink, R. B.; Niessen, W. M. A.; Brinkman, U. A. T. *Journal of Chromatography, A* **2002**, *970*, 65-93.
- (59) Rajski, L.; Lozano, A.; Belmonte-Valles, N.; Ucles, A.; Ucles, S.; Mezcua, M.; Fernandez-Alba, A. R. *Analyst (Cambridge, United Kingdom)* **2013**, *138*, 921-931.
- (60) Fernandes, V. C.; Vera, J. L.; Domingues, V. F.; Silva, L. M. S.; Mateus, N.; Delerue-Matos, C. *J. Am. Soc. Mass Spectrom.* **2012**, *23*, 2187-2197.
- (61) Walorczyk, S.; Drozdzyński, D.; Gnusowski, B. *Talanta* **2011**, *85*, 1856-1870.
- (62) Borrás, E.; Sanchez, P.; Muñoz, A.; Tortajada-Genaro, L. A. *Anal. Chim. Acta* **2011**, *699*, 57-65.
- (63) Catalina, M. I.; Dalluge, J.; Vreuls, R. J. J.; Brinkman, U. A. T. *Journal of Chromatography, A* **2000**, *877*, 153-166.
- (64) Leandro, C. C.; Bishop, D. A.; Fussell, R. J.; Smith, F. D.; Keely, B. J. *J. Agric. Food Chem.* **2006**, *54*, 645-649.
- (65) Yang, K.-W.; Eisert, R.; Lord, H.; Pawliszyn, J. *Applications of Solid Phase Microextraction* **1999**, 435-447.
- (66) Breitbach, Z. S.; Weatherly, C. A.; Woods, R. M.; Xu, C.; Vale, G.; Berthod, A.; Armstrong, D. W. *Journal of Separation Science* **2014**, *37*, 558-565.
- (67) Boston, D. J.; Xu, C.; Armstrong, D. W.; MacDonnell, F. M. *J. Am. Chem. Soc.* **2013**, *135*, 16252-16255.
- (68) Yu, J. T.; Bisceglia, K. J.; Bouwer, E. J.; Roberts, A. L.; Coelhan, M. *Anal. Bioanal. Chem.* **2012**, *403*, 583-591.
- (69) Field, J. A.; Field, T. M.; Poiger, T.; Giger, W. *Environ. Sci. Technol.* **1994**, *28*, 497-503.
- (70) Cappiello, A.; Famiglini, G.; Bruner, F. *Anal. Chem.* **1994**, *66*, 1416-23.
- (71) Santos, T. C. R.; Rocha, J. C.; Barcelo, D. *Journal of Chromatography, A* **2000**, *879*, 3-12.
- (72) Geerdink, R. B.; Kooistra-Sijpersma, A.; Tiesnitsch, J.; Kienhuis, P. G. M.; Brinkman, U. A. T. *Journal of Chromatography, A* **1999**, *863*, 147-155.

- (73) Crescenzi, C.; Di Corcia, A.; Marchese, S.; Samperi, R. *Anal. Chem.* **1995**, *67*, 1968-75.
- (74) Chiron, S.; Papilloud, S.; Haerdi, W.; Barcelo, D. *Anal. Chem.* **1995**, *67*, 1637-43.
- (75) Gervais, G.; Brosillon, S.; Laplanche, A.; Helen, C. *Journal of Chromatography, A* **2008**, *1202*, 163-172.
- (76) Koppen, B.; Spliid, N. H. *Journal of Chromatography, A* **1998**, *803*, 157-168.
- (77) Rensburg, J. W.; Soukup-Hein, R. J.; Crank, J. A.; Breitbach, Z. S.; Payagala, T.; Armstrong, D. W. *J. Am. Soc. Mass Spectrom.* **2008**, *19*, 261-269.
- (78) Cech, N. B.; Enke, C. G. *Mass Spectrom Rev* **2001**, *20*, 362-87.
- (79) Straub, R. F.; Voyksner, R. D. *J. Am. Soc. Mass Spectrom.* **1993**, *4*, 578-87.
- (80) Soukup-Hein, R. J.; Rensburg, J. W.; Breitbach, Z. S.; Sharma, P. S.; Payagala, T.; Wanigasekara, E.; Huang, J.; Armstrong, D. W. *Anal. Chem.* **2008**, *80*, 2612-2616.
- (81) Dodbiba, E.; Xu, C.; Payagala, T.; Wanigasekara, E.; Moon, M. H.; Armstrong, D. W. *Analyst* **2011**, *136*, 1586-1593.
- (82) Dodbiba, E.; Xu, C.; Wanigasekara, E.; Armstrong, D. W. *Rapid Commun. Mass Spectrom.* **2012**, *26*, 1005-1013.
- (83) Martinelango, P. K.; Anderson Jared, L.; Dasgupta Purnendu, K.; Armstrong Daniel, W.; Al-Horr Rida, S.; Slingsby Rosanne, W. *Anal Chem* **2005**, *77*, 4829-35.
- (84) Armstrong, D. W. *J. Liq. Chromatogr.* **1980**, *3*, 895-900.
- (85) Kornahrens, H.; Cook, K. D.; Armstrong, D. W. *Anal. Chem.* **1982**, *54*, 1325-9.
- (86) Armstrong, D. W.; Ward, T. J. *Anal. Chem.* **1986**, *58*, 579-82.
- (87) Rundlett, K. L.; Armstrong, D. W. *Anal. Chem.* **1996**, *68*, 3493-3497.
- (88) Anderson, J. L.; Ding, R.; Ellern, A.; Armstrong, D. W. *J. Am. Chem. Soc.* **2005**, *127*, 593-604.
- (89) Hopfgartner, G.; Varesio, E.; Tschaeppaet, V.; Grivet, C.; Bourgogne, E.; Leuthold, L. A. *J. Mass Spectrom.* **2004**, *39*, 845-855.
- (90) Mazzella, N.; Delmas, F.; Delest, B.; Mechin, B.; Madigou, C.; Allenou, J. P.; Gabellec, R.; Caquet, T. *J. Environ. Monit.* **2009**, *11*, 108-115.
- (91) Reemtsma, T. *TrAC, Trends Anal. Chem.* **2001**, *20*, 533-542.
- (92) Nicolai, M.; Rosin, C.; Tousset, N.; Nicolai, Y. *Talanta* **1999**, *50*, 433-444.
- (93) Begerow, J.; Turfeld, M.; Dunemann, L. *J. Anal. At. Spectrom.* **2000**, *15*, 347-352.
- (94) Long, X.; Hansen, E. H.; Miro, M. *Talanta* **2005**, *66*, 1326-1332.
- (95) Sarzanini, C.; Bruzzoniti, M. C. *TrAC, Trends Anal. Chem.* **2001**, *20*, 304-310.
- (96) Shaw, M. J.; Haddad, P. R. *Environ. Int.* **2004**, *30*, 403-431.

- (97) Arnold, R. J.; Arndt, B.; Blaser, E.; Blosser, C.; Caulton, D.; Chung, W. S.; Fiorenza, G.; Heath, W.; Jacobs, A.; Kahng, E.; Koh, E.; Le, T.; Mandla, K.; McCorry, C.; Newman, L.; Pithadia, A.; Reckelhoff, A.; Rheinhardt, J.; Skljarevski, S.; Stuart, J.; Taylor, C.; Thomas, S.; Tse, K.; Wall, R.; Warkentien, C. *Journal of Chemical Education* **2011**, *88*, 484-487.
- (98) Warnken, K. W.; Gill, G. A.; Wen, L.-S.; Griffin, L. L.; Santschi, P. H. *J. Anal. At. Spectrom.* **1999**, *14*, 247-252.
- (99) Plantz, M. R.; Fritz, J. S.; Smith, F. G.; Houk, R. S. *Anal. Chem.* **1989**, *61*, 149-53.
- (100) Vela, N. P.; Olson, L. K.; Caruso, J. A. *Anal. Chem.* **1993**, *65*, 585A-592A, 596A-597A.
- (101) Bloxham, M. J.; Hill, S. J.; Worsfold, P. J. *J. Anal. At. Spectrom.* **1994**, *9*, 935-8.
- (102) Ebdon, L.; Fisher, A. S.; Worsfold, P. J. *J. Anal. At. Spectrom.* **1994**, *9*, 611-14.
- (103) Munro, S.; Ebdon, L.; McWeeny, D. J. *J. Anal. At. Spectrom.* **1986**, *1*, 211-19.
- (104) Marin, B.; Valladon, M.; Polve, M.; Monaco, A. *Anal. Chim. Acta* **1997**, *342*, 91-112.
- (105) Ferguson, C. N.; Benchaar, S. A.; Miao, Z.; Loo, J. A.; Chen, H. *Analytical Chemistry (Washington, DC, United States)* **2011**, *83*, 6468-6473.
- (106) Yi, E. C.; Lee, H.; Aebersold, R.; Goodlett, D. R. *Rapid Commun. Mass Spectrom.* **2003**, *17*, 2093-2098.
- (107) Buchberger, W.; Czizsek, B.; Hann, S.; Stingeder, G. *J. Anal. At. Spectrom.* **2003**, *18*, 512-514.
- (108) Collins, R. N.; Onisko, B. C.; McLaughlin, M. J.; Merrington, G. *Environ. Sci. Technol.* **2001**, *35*, 2589-2593.
- (109) Minakata, K.; Suzuki, O. *Anal. Chim. Acta* **2005**, *554*, 202-206.
- (110) Tsierkezos, N. G.; Buchta, M.; Holy, P.; Schroeder, D. *Rapid Commun. Mass Spectrom.* **2009**, *23*, 1550-1556.
- (111) Kebarle, P.; Verkerk, U. H. *Mass Spectrom. Rev.* **2009**, *28*, 898-917.
- (112) Wang, G.; Cole, R. B. *Anal. Chem.* **1998**, *70*, 873-881.
- (113) Martinelango, P. K.; Anderson, J. L.; Dasgupta, P. K.; Armstrong, D. W.; Al-Horr, R. S.; Slingsby, R. W. *Anal. Chem.* **2005**, *77*, 4829-4835.
- (114) Warnke, M. M.; Breitbach, Z. S.; Dodbiba, E.; Crank, J. A.; Payagala, T.; Sharma, P.; Wanigasekara, E.; Zhang, X.; Armstrong, D. W. *Anal. Chim. Acta* **2009**, *633*, 232-237.
- (115) Rundlett, K. L.; Armstrong, D. W. *Anal. Chem.* **1996**, *68*, 3493-3497.
- (116) Warnke, M. M.; Breitbach, Z. S.; Dodbiba, E.; Wanigasekara, E.; Zhang, X.; Sharma, P.; Armstrong, D. W. *J. Am. Soc. Mass Spectrom.* **2009**, *20*, 529-538.

- (117) Gale, D. C.; Goodlett, D. R.; Light-Wahl, K. J.; Smith, R. D. *J. Am. Chem. Soc.* **1994**, *116*, 6027-8.
- (118) Soroka, K.; Vithanage, R. S.; Phillips, D. A.; Walker, B.; Dasgupta, P. K. *Anal. Chem.* **1987**, *59*, 629-36.
- (119) Waldron, K. J.; Robinson, N. J. *Nat. Rev. Microbiol.* **2009**, *7*, 25-35.
- (120) Travnicek, Z.; Matikova-Malarova, M.; Novotna, R.; Vanco, J.; Stepankova, K.; Suchy, P. *J. Inorg. Biochem.* **2011**, *105*, 937-948.
- (121) Campagna, S.; Puntoriero, F.; Nastasi, F.; Bergamini, G.; Balzani, V. *Top. Curr. Chem.* **2007**, *280*, 117-214.
- (122) Sabel, C. E.; Neureuther, J. M.; Siemann, S. *Anal. Biochem.* **2010**, *397*, 218-226.
- (123) Becker, J. S.; Jakubowski, N. *Chem. Soc. Rev.* **2009**, *38*, 1969-1983.
- (124) McCall, K. A.; Fierke, C. A. *Anal. Biochem.* **2000**, *284*, 307-315.
- (125) Rosenberg, E. *J. Chromatogr. A* **2003**, *1000*, 841-889.
- (126) Luo, M.; Hu, B.; Zhang, X.; Peng, D.; Chen, H.; Zhang, L.; Huan, Y. *Anal. Chem.* **2010**, *82*, 282-289.
- (127) Wuilloud, R. G.; Altamirano, J. C.; Smichowski, P. N.; Heitkemper, D. T. *J. Anal. At. Spectrom.* **2006**, *21*, 1214-1223.
- (128) Lobinski, R.; Szpunar, J. *Anal. Chim. Acta* **1999**, *400*, 321-332.
- (129) Stewart, I. I. *Spectrochim. Acta, Part B* **1999**, *54B*, 1649-1695.
- (130) Wang, H.; Agnes, G. R. *Anal. Chem.* **1999**, *71*, 4166-4172.
- (131) Baron, D.; Hering, J. G. *J. Environ. Qual.* **1998**, *27*, 844-850.
- (132) Ylivainio, K. *Environ. Pollut.* **2010**, *158*, 3194-3200.
- (133) Sharp, B. L.; Sulaiman, A. B.; Taylor, K. A.; Green, B. N. *J. Anal. At. Spectrom.* **1997**, *12*, 603-609.
- (134) Warnke, M.; Breitbach, Z.; Dodbiba, E.; Crank, J.; Payagala, T.; Sharma, P.; Wanigasekara, E.; Zhang, X.; Armstrong, D. *Anal. Chim. Acta* **2009**, *633*, 232-237.
- (135) Wanigasekara, E.; Zhang, X.; Nanayakkara, Y.; Payagala, T.; Moon, H.; Armstrong, D. W. *ACS Appl. Mater. Interfaces* **2009**, *1*, 2126-2133.
- (136) Dodbiba, E.; Breitbach, Z. S.; Wanigasekara, E.; Payagala, T.; Zhang, X.; Armstrong, D. W. *Anal. Bioanal. Chem.* **2010**, *398*, 367-376.
- (137) Dodbiba, E.; Breitbach Zachary, S.; Wanigasekara, E.; Payagala, T.; Zhang, X.; Armstrong Daniel, W. *Anal. Bioanal. Chem.* **2010**, *398*, 367-76.
- (138) Lin, X.; Gerardi, A. R.; Breitbach, Z. S.; Armstrong, D. W.; Colyer, C. L. *Electrophoresis* **2009**, *30*, 3918-3925.
- (139) Toscano, G.; Gambaro, A.; Capodaglio, G.; Cairns, W. R. L.; Cescon, P. *J. Environ. Monit.* **2009**, *11*, 193-199.
- (140) Milne, A.; Landing, W.; Bizimis, M.; Morton, P. *Anal. Chim. Acta* **2010**, *665*, 200-207.

- (141) Lewen, N.; Mathew, S.; Schenkenberger, M.; Raglione, T. *J. Pharm. Biomed. Anal.* **2004**, *35*, 739-752.
- (142) Shakerian, F.; Dadfarnia, S.; Shabani, A. M. H.; Rohani, M. *Talanta* **2008**, *77*, 551-555.
- (143) Tuzen, M.; Soylak, M.; Citak, D.; Ferreira, H. S.; Korn, M. G. A.; Bezerra, M. A. *J. Hazard. Mater.* **2009**, *162*, 1041-1045.
- (144) Bezerra, M. A.; Lemos, V. A.; Garcia, J. S.; Goncalves da Silva, D.; Araujo, A. S.; Arruda, M. A. Z. *Talanta* **2010**, *82*, 437-443.
- (145) Opoka, W.; Bas, B.; Reczynski, W.; Plonka, M.; Drozdowicz, D.; Sliwowski, Z.; Brzozowski, T. *Acta Pol. Pharm.* **2011**, *68*, 481-492.
- (146) Watson, A. D.; Leitinger, N.; Navab, M.; Faull, K. F.; Horkko, S.; Witztum, J. L.; Palinski, W.; Schwenke, D.; Salomon, R. G.; Sha, W.; Subbanagounder, G.; Fogelman, A. M.; Berliner, J. A. *J. Biol. Chem.* **1997**, *272*, 13597-13607.
- (147) Veatch, S. L.; Keller, S. L. *Biophys. J.* **2003**, *85*, 3074-3083.
- (148) Pulfer, M.; Murphy, R. C. *Mass Spectrom. Rev.* **2003**, *22*, 332-364.
- (149) Muthing, J.; Radloff, M. *Anal. Biochem.* **1998**, *257*, 67-70.
- (150) Singer, S. J.; Nicolson, G. L. *Science* **1972**, *175*, 720-31.
- (151) Martin, T. F. J. *Annu. Rev. Cell Dev. Biol.* **1998**, *14*, 231-264.
- (152) Bevers, E. M.; Comfurius, P.; Dekkers, D. W. C.; Zwaal, R. F. A. *Biochim. Biophys. Acta*, **1999**, *1439*, 317-330.
- (153) Roth, K. D. W.; Huang, Z.-H.; Sadagopan, N.; Watson, J. T. *Mass Spectrom. Rev.* **1999**, *17*, 255-274.
- (154) Petkovic, M.; Schiller, J.; Muller, M.; Benard, S.; Reichl, S.; Arnold, K.; Arnhold, J. *Anal. Biochem.* **2001**, *289*, 202-216.
- (155) Houjou, T.; Yamatani, K.; Imagawa, M.; Shimizu, T.; Taguchi, R. *Rapid Commun. Mass Spectrom.* **2005**, *19*, 654-666.
- (156) Descalzo, A. M.; Insani, E. M.; Pensel, N. A. *Lipids* **2003**, *38*, 999-1003.
- (157) Patton, G. M.; Fasulo, J. M.; Robins, S. J. *J. Lipid Res.* **1982**, *23*, 190-6.
- (158) Arvidson, G. A. E. *J. Lipid Res.* **1965**, *6*, 574-7.
- (159) Kim, H.-Y.; Wang, T.-C. L.; Ma, Y.-C. *Anal. Chem.* **1994**, *66*, 3977-82.
- (160) Kim, H.; Ahn, E.; Moon, M. H. *Analyst* **2008**, *133*, 1656-1663.
- (161) Wu, C.-Y.; Peng, Y.-N.; Chiu, J.-H.; Ho, Y.-L.; Chong, C.-P.; Yang, Y.-L.; Liu, M.-Y. *Journal of Chromatography B: Analytical Technologies in the Biomedical and Life Sciences* **2009**, *877*, 3495-3505.
- (162) Gao, F.; Zhang, Z.; Fu, X.; Li, W.; Wang, T.; Liu, H. *Electrophoresis* **2007**, *28*, 1418-1425.
- (163) Lytle, C. A.; Gan, Y. D.; White, D. C. *J. Microbiol. Methods* **2000**, *41*, 227-234.
- (164) Bang, D. Y.; Ahn, E. j.; Moon, M. H. *J. Chromatogr. B Anal. Technol. Biomed. Life Sci.* **2007**, *852*, 268-277.

- (165) Nakanishi, H.; Ogiso, H.; Taguchi, R. *Methods Mol. Biol.* **2009**, *579*, 287-313.
- (166) Kebarle, P.; Yeunghaw, H. *Electrospray Ionization Mass Spectrometry* **1997**, 3-63.
- (167) Apffel, A.; Chakel, J. A.; Fischer, S.; Lichtenwalter, K.; Hancock, W. S. *Anal. Chem.* **1997**, *69*, 1320-1325.
- (168) Shaner, R. L.; Allegood, J. C.; Park, H.; Wang, E.; Kelly, S.; Haynes, C. A.; Sullards, M. C.; Merrill, A. H., Jr. *J. Lipid Res.* **2009**, *50*, 1692-1707.
- (169) Pascher, I. *Biochim. Biophys. Acta*, **1976**, *455*, 433-51.
- (170) Spiegel, S.; Merrill, A. H., Jr. *FASEB J.* **1996**, *10*, 1388-1397.
- (171) Riboni, L.; Viani, P.; Bassi, R.; Prinetti, A.; Tettamanti, G. *Prog. Lipid Res.* **1997**, *36*, 153-195.
- (172) Hannun Yusuf, A.; Obeid Lina, M. *Nat. Rev. Mol. Cell Biol.* **2008**, *9*, 139-50.
- (173) Kolter, T. *Chem. Phys. Lipids* **2011**, *164*, 590-606.
- (174) Vanier, M. T. *Biochim. Biophys. Acta*, **1983**, *750*, 178-84.
- (175) van Echten-Deckert, G.; Walter, J. *Prog. Lipid Res.* **2012**, *51*, 378-393.
- (176) Lahiri, S.; Futerman, A. H. *Cell. Mol. Life Sci.* **2007**, *64*, 2270-2284.
- (177) Bui, H. H.; Leohr, J. K.; Kuo, M.-S. *Anal. Biochem.* **2012**, *423*, 187-194.
- (178) Sullards, M. C.; Liu, Y.; Chen, Y.; Merrill, A. H., Jr. *Biochim. Biophys. Acta*, **2011**, *1811*, 838-853.
- (179) Haynes, C. A.; Allegood, J. C.; Park, H.; Sullards, M. C. *Journal of Chromatography B: Analytical Technologies in the Biomedical and Life Sciences* **2009**, *877*, 2696-2708.
- (180) Adams, J.; Ann, Q. *Mass Spectrom. Rev.* **1993**, *12*, 51-85.
- (181) Hayashi, A.; Matsubara, T.; Morita, M.; Kinoshita, T.; Nakamura, T. *J. Biochem., Tokyo* **1989**, *106*, 264-9.
- (182) Fujiwaki, T.; Yamaguchi, S.; Sukegawa, K.; Taketomi, T. *J. Chromatogr. B Biomed. Sci. Appl.* **1999**, *731*, 45-52.
- (183) Farwanah, H.; Wohlrab, J.; Neubert, R. H. H.; Raith, K. *Anal. Bioanal. Chem.* **2005**, *383*, 632-637.
- (184) Farwanah, H.; Wirtz, J.; Kolter, T.; Raith, K.; Neubert, R. H. H.; Sandhoff, K. *J. Chromatogr. B Anal. Technol. Biomed. Life Sci.* **2009**, *877*, 2976-2982.
- (185) Merrill, A. H., Jr.; Sullards, M. C.; Allegood, J. C.; Kelly, S.; Wang, E. *Methods* **2005**, *36*, 207-224.
- (186) Bielawski, J.; Szulc, Z. M.; Hannun, Y. A.; Bielawska, A. *Methods* **2006**, *39*, 82-91.
- (187) Farwanah, H.; Kolter, T.; Sandhoff, K. *Biochim. Biophys. Acta*, **2011**, *1811*, 854-860.
- (188) Steen, H.; Kuester, B.; Fernandez, M.; Pandey, A.; Mann, M. *Anal. Chem.* **2001**, *73*, 1440-1448.

- (189) Steen, H.; Mann, M. *J. Am. Soc. Mass Spectrom.* **2002**, *13*, 996-1003.
- (190) Schmidt, A.; Csaszar, E.; Ammerer, G.; Mechtler, K. *Proteomics* **2008**, *8*, 4577-92.
- (191) Loo, J. A. *Mass Spectrom. Rev.* **1997**, *16*, 1-23.
- (192) Katta, V.; Chait, B. T. *J. Am. Chem. Soc.* **1993**, *115*, 6317-21.
- (193) McEwen, C. N.; Simonsick, W. J., Jr.; Larsen, B. S.; Ute, K.; Hatada, K. *J. Am. Soc. Mass Spectrom.* **1995**, *6*, 906-11.
- (194) Hop, C. E. C. A.; Bakhtiar, R. *J. Chem. Educ.* **1996**, *73*, A162, A164-A169.
- (195) Brugger, B.; Erben, G.; Sandhoff, R.; Wieland, F. T.; Lehmann, W. D. *Proc. Natl. Acad. Sci. U.S.A.* **1997**, *94*, 2339-44.
- (196) Hsu, F.-F.; Bohrer, A.; Turk, J. *J. Am. Soc. Mass Spectrom.* **1998**, *9*, 516-526.
- (197) Lu, W.; Yang, G.; Cole, R. B. *Electrophoresis* **1995**, *16*, 487-92.
- (198) Schultz, C. L.; Moini, M. *Anal. Chem.* **2003**, *75*, 1508-1513.
- (199) Breitbach, Z. S.; Berthod, A.; Huang, K.; Armstrong, D. W. *Submitted to Mass Spectrom. Rev.* **2013**.
- (200) Kappes, T.; Schnierle, P.; C. Hauser, P. *Anal. Chim. Acta* **1997**, *350*, 141-147.
- (201) Isildak, I.; Asan, A. *Talanta* **1999**, *48*, 967-978.
- (202) Gjerde, D. T.; Fritz, J. S.; Schmuckler, G. *J. Chromatogr.* **1979**, *186*, 509-19.
- (203) Kuban, P.; Hauser, P. C. *Anal. Chim. Acta* **2008**, *607*, 15-29.
- (204) Harwood, J. J.; Su, W. *J. Chromatogr. A* **1997**, *788*, 105-111.
- (205) Enke, C. G. *Anal. Chem.* **1997**, *69*, 4885-93.
- (206) Cech, N. B.; Enke, C. G. *Anal. Chem.* **2000**, *72*, 2717-2723.
- (207) Cech, N. B.; Enke, C. G. *Anal. Chem.* **2001**, *73*, 4632-4639.
- (208) Tang, K.; Smith, R. D. *J. Am. Soc. Mass Spectrom.* **2001**, *12*, 343-347.
- (209) Zhou, S.; Cook, K. D. *J. Am. Soc. Mass Spectrom.* **2001**, *12*, 206-214.
- (210) Sherman, C. L.; Brodbelt, J. S. *Anal. Chem.* **2003**, *75*, 1828-1836.
- (211) Sherman, C. L.; Brodbelt, J. S. *Anal. Chem.* **2005**, *77*, 2512-2523.
- (212) Iribarne, J. V.; Thomson, B. A. *J. Chem. Phys.* **1976**, *64*, 2287-94.
- (213) Thomson, B. A.; Iribarne, J. V. *Journal of Chemical Physics* **1979**, *71*, 4451-63.
- (214) Iribarne, J. V.; Dziedzic, P. J.; Thomson, B. A. *Int. J. Mass Spectrom. Ion Phys.* **1983**, *50*, 331-47.
- (215) Menger, F. M.; Littau, C. A. *J. Am. Chem. Soc.* **1993**, *115*, 10083-90.
- (216) Menger, F. M.; Bian, J.; Sizova, E.; Martinson, D. E.; Seredyuk, V. A. *Org. Lett.* **2004**, *6*, 261-264.
- (217) Tang, L.; Kebarle, P. *Anal. Chem.* **1991**, *63*, 2709-15.

Biographical Information

Chengdong Xu received his B.S. degree in Pharmaceutical Chemistry in 2009 from the Southwest University in China. He obtained his Ph.D in Analytical Chemistry at The University of Texas at Arlington under the supervision of Prof. Daniel W. Armstrong. His research areas focus on development of novel analytical methodologies based on paired ion electrospray ionization mass spectrometry (PIESI-MS) for ultrasensitive determination of anions. His research also involves in development of highly thermally stable ionic liquids as stationary phase for gas chromatography.